



universität
wien

DISSERTATION

Titel der Dissertation

Ecology of Riverine Particles: from Viruses to Aggregates

Ökologie von suspendierten Partikeln in Flußsystemen:
von Viren zu Aggregaten

angestrebter akademischer Grad

Doktorin der Naturwissenschaften (Dr. rer.nat.)

Verfasserin / Verfasser:	Mag. Birgit Luef
Matrikel-Nummer:	9505352
Dissertationsgebiet (lt. Studienblatt):	A 091 444 Ökologie
Betreuerin / Betreuer:	Ao. Univ.-Prof. Mag. Dr. Peter Peduzzi

Wien, am 16. November 2008

CONTENTS

GENERAL INTRODUCTION	7
Floating aquatic aggregates	7
Formation and occurrence	7
Structure and composition	7
Aquatic virus particles and their life cycle	8
Laser Scanning Microscopy (LSM)	9
Confocal Laser Scanning Microscopy (CLSM or 1Photon-LSM)	9
Application of the LSM technique	10
Objective lenses	11
Limitations of CLSM, its solutions and outlooks	12
Thesis outline	13
References	14
 FLUORESCENCE LECTIN-BINDING ANALYSIS IN RIVERINE AGGREGATES (RIVER SNOW): A CRITICAL EXAMINATION	 19
Abstract	20
Introduction	20
Material and Methods	21
Sampling and handling of aggregates	21
Staining procedure	22
Lectin specificity test	23
Laser Scanning Microscopy	23
Quantification, calculation and statistical analysis	24
Results	25
Inhibition test	25
Lectin screening and aggregate composition	25
Effect of season and type of lectin on glycoconjugate volume	26
Discussion	27
Lectin specificity	27
Structure and ecology of floating aggregates	29
Acknowledgements	31
References	32
Tables	32
Figure legends	32

THE POTENTIAL OF CONFOCAL LASER SCANNING MICROSCOPY IN COMBINATION WITH STATISTICAL AND IMAGE ANALYSIS TO INVESTIGATE VOLUME, STRUCTURE AND COMPOSITION OF RIVERINE AGGREGATES	49
Abstract	50
Introduction	50
Material and Methods	51
Study sites and sampling	51
Staining procedure	52
Confocal Laser Scanning Microscopy	53
Cryo-sections	53
Quantification & visualization	53
Calculations and statistics	54
Results	56
Abiotic and biotic parameters characterizing the two rivers Danube and Elbe	56
Scanning aggregates under in situ conditions	56
Distribution of aggregates' components based on the outer 20 µm	57
Cryo-sections	58
Discussion	59
Handling, staining and analyzing aggregates	59
Quantification of CLSM data sets	60
Visualization, calculation and quantification	61
Relationship between CNAS and EPS within aggregates	62
Ecological aspects of riverine aggregates	62
Summary	63
Acknowledgements	64
References	65
Tables	69
Figure legends	72
 IMAGING AND QUANTIFYING VIRUS FLUORESCENCE SIGNALS ON AQUATIC AGGREGATES: AN UNRESOLVED PROBLEM?	 81
Abstract	82
Introduction	82
Material and Methods	83
Sampling of aggregates	83
Extraction of viruses by sonication	83
Staining & CLSM	84
Cryo-embedding, Cryo-sections & CLSM	84
Quantification & Visualization	85
Results	85
Confocal laser scanning microscopy (CLSM) & visualization	85
CLSM & quantification	86
Discussion	86
CLSM, visualization & quantification	86

Comparison of different methods to quantify viruses and bacteria attached to riverine aggregates	88
Interactions of viruses and particulate material	89
Conclusions	91
Acknowledgements	91
References	92
Table	92
Figure legends	97
 ONLINE PROGRAM “VIPCAL” FOR CALCULATING LYTIC VIRAL PRODUCTION AND LYSOGENIC CELLS BASED ON A VIRAL REDUCTION APPROACH	 105
Abstract	106
Introduction	106
Materials and Methods	108
Study site	108
Virus production (VP) – experimental design of the virus reduction approach (VRA)	108
Abundance of viruses and bacteria	108
Bacterial secondary production (BSP)	109
Determination of the burst size	109
Results and Discussion	109
Computations of VP	109
Demonstration of the program VIPCAL	111
Conclusions	113
Acknowledgements	114
References	115
Table	115
Figure legends	115
 SUMMARY	 125
 ZUSAMMENFASSUNG	 127
 DANKSAGUNG	 129
 CURRICULUM VITAE	 133

General Introduction

Floating aquatic aggregates

Formation and occurrence

Suspended particulate material plays a significant role in biogeochemical cycles and for biological processes in natural aquatic environments (Simon, *et al.*, 2002; Azam & Malfatti, 2007). They represent an important source of energy. Primary particles are frequently and perhaps characteristically transported as larger flocculated aggregates (Droppo, *et al.*, 2005). Aggregating particles in the bulk water are heterogeneous and are composed of dissolved, colloidal and particulate materials of varying size and composition (Leppard & Droppo, 2005). Abiotic mechanisms such as physical coagulation, collision frequency and stickiness are involved in aggregation of particles (Droppo, *et al.*, 2005). Aggregates have different forms of size and generally, three size classes are distinguished: 1) submicron particles, 2) micro-aggregates and 3) macro-aggregates. Submicron particles are $< 1 \mu\text{m}$ (Koike, *et al.*, 1990; Kerner, *et al.*, 2003; Leppard & Droppo, 2005). In her review on aggregates in rivers, Zimmermann-Timm (2002) defined micro-aggregates $< 150 \mu\text{m}$ and macro-aggregates $> 150 \mu\text{m}$. Simon *et al.* (2002) classified organic micro-aggregates $< 500 \mu\text{m}$ and organic macro-aggregates $> 500 \mu\text{m}$, also known as marine and lake snow.

Aggregates harbor inorganic and organic, non-living components and are often densely colonized by various microbes and viruses (organic living matter). Aquatic aggregates and their microbial colonizers may interact in several ways (Kirchman, 1993). The availability of particulate material to microorganisms depends on the physical structure and on the biochemical composition of the organic matter (Azúa, *et al.*, 2007). But also microbial activity can influence e.g. size and chemical composition of the particles. Particle-associated microbial abundance and activity can contribute significantly to overall microbial processes depending on the quality of particles and the type of organisms involved (Kirchman, 1983; Luef, *et al.*, 2007).

Structure and composition

Aggregates are composed of a complex mixture of inorganic and organic components. They are often regarded as mobile biofilms and can be very heterogeneous in their composition. Up to 97% of the biofilm matrix is actually water (Sutherland, 2001). Apart of water, biofilms may consist of dissolved, colloidal and particulate materials of varying size and composition (Droppo, *et al.*, 2005). They are composed of a complex mixture of inorganic (minerals), non-

living organic (extracellular polymeric substances (EPS), allochthonous and autochthonous detritus, lignins, tannins, etc.) and living organic (bacteria, fungi, algae, protozoa and viruses) matter components from the specific aquatic habitat and its terrestrial environment (e.g. Simon, *et al.*, 2002). Cellular material within a biofilm can vary greatly. Measured organic carbon contents suggest that cellular material represents 2-15 % of the biofilm (Sutherland, 2001). Up to 95 % of the biofilms biomass is composed of EPS (Lawrence, *et al.*, 1991; Skillman, *et al.*, 1999; Flemming & Wingender, 2003). Many microorganisms, such as bacteria and algae, synthesize EPS, composed of different classes of organic macromolecules such as polysaccharides, proteins, nucleic acids, lipids/phospholipids and amphiphilic polymers (Flemming & Wingender, 2003). These EPS either remain attached to the cell surface or are present in the extracellular matrix! (Decho & Lopez, 1993). Many microorganisms live in aggregated forms such as biofilms, aggregates and sludge, where they are embedded in such an EPS matrix. The architecture as well as the structural and functional integrity of biofilms are determined by the presence of EPS, caused by the intermolecular interactions between many different macromolecules (Flemming & Wingender, 2003). Many additional functions are attributed to the EPS: The EPS matrix enables microorganisms to form stable aggregates of mixed populations, leading to synergistic micro-consortia. An important modern concept is the role of EPS in allowing microorganisms to live continuously at high cell densities in stable, mixed-population biofilm communities (Flemming & Wingender, 2003). The actual structure of the biofilm matrix varies greatly depending on the microbial cells present, their physiological status, the nutrients available and the prevailing physical conditions (Sutherland, 2001).

Aquatic virus particles and their life cycle

Viruses (mainly bacteriophages) are a highly abundant type of submicron particles in natural aquatic systems and they are thought to influence the activity, life strategy and diversity of their hosts and apparently influence organic matter fluxes (see review of Wommack & Colwell, 2000; Weinbauer, 2004; Peduzzi & Luef, in press). Estimates of bacterial mortality due to production of phages suggest that viruses can be responsible for up to 100 % of bacterial mortality (Hennes & Simon, 1995; Proctor, *et al.*, 1993; Noble & Fuhrman, 2000). Thus, viruses may have significant impacts upon natural bacterial abundance, productivity and community composition (Fuhrman & Schwalbach, 2003; Schwalbach, *et al.*, 2004; Weinbauer, 2004, Hewson & Fuhrman, 2006; Bouvier and del Giorgio, 2007). Therefore, information on viral survival mechanisms and viral life strategies is of considerable interest.

Viruses display different types of life cycles, the most common being lytic and lysogenic infections. In most aquatic environments, the lytic cycle is the dominant method of viral replication and results in the destruction of the infected cells. In the lysogenic cycle, the phage infects a host cell and the genome of the phage typically remains in the host in a dormant stage, called a prophage. The prophage replicates along with the host until environmental stimuli such as UV radiation, temperature etc. causes proliferation of new phages via the lytic cycle (see review of Weinbauer, 2004).

The viral reduction approach (VRA) provides rapid and reproducible estimates of viral production, which can be measured directly (Helton, *et al.*, 2005; Winget, *et al.*, 2005; Hewson & Fuhrman, 2007; Williamson, *et al.*, 2008). To induce the lytic cycle in lysogenized bacteria, mitomycin C and UV C radiation are the most powerful agents (Jiang & Paul, 1994; Wilcox & Fuhrman, 1994; Jiang & Paul, 1996; Weinbauer & Suttle, 1996; Tapper & Hicks, 1998). Lysogeny may be an important survival mechanism for viruses where host densities or resources are low (Wilson & Mann, 1997) or when the destruction rate of free phages is too high to allow lytic replication (Lenski, 1988). Temperate viruses may affect host assemblage composition, either by lysis or by other mechanisms, e.g., by resistance to lytic virus infection (Hewson & Fuhrman, 2007).

Laser Scanning Microscopy (LSM)

LSM is nowadays a widely used technique to investigate aquatic particles.

Confocal Laser Scanning Microscopy (CLSM or 1Photon-LSM)

In 1957 Marvin Minsky applied for a patent for a microscope that used a stage-scanning confocal optical system (Pawley, 2006). In 1960, Maiman announced the development of the first operating laser. In the next years, further development in laser and computer technology and verification of the theory of confocal imaging followed. A very good and comprehensive historic overview of confocal microscopy is given by Inoué (2006). The first CLSM became commercially available in 1987.

Nowadays, a CLSM is compiled out of a traditional epifluorescence microscope, lasers with different wave length and photomultiplier tubes (PMT) to detect the signals. The CLSM generates clear, thin optical section images, nearly totally free of out of focus fluorescence, from any biological specimen. These optically sectioned images can be obtained in seconds and can be rapidly captured and displayed on a monitor. A combination of a defined light source (laser beam), pinholes and a very sensitive detector makes this possible. Using the

appropriate filters and beam splitters in the emission path, fluorescence images can be obtained. A combination of the diameter of the pinhole, the wavelength and the numerical aperture of the objective determines the axial dimension of the optical section.

To record an image in the focal plane, the specimen is scanned with a point laser beam in the x- and y-directions. Spatial imaging is possible by moving the sample along the z-axis. xz-images lack the resolution of xy-images due to the nature of the corrections in standard objectives and the point spread function (describes the signal intensity distribution of a single point) of the lens.

The light which is emitted by the specimen is detected by PMTs. These detectors can be set to detect photons of a special wavelength (e.g. emission maximum of the used fluorochrome). Furthermore, the sensitivity of the detectors can be changed. Therefore, on the one hand low fluorescence signals can be detected by the PMTs easily. On the other hand over-exposure due to bright fluorochromes can be avoided. But it must be kept in mind, the more sensitive a detector is, the more background signals can be recorded.

Microscopical image data are now almost always recorded digitally. To accomplish this, the photons that form the final image must be divided into small geometrical subunits called pixels. Each pixel in the gray scale image corresponds to an integer between 0 and 255 reflecting the intensity of the light. Hence, each pixel is coded by one of the 256 gray values. The number 0 codes all pixels where no signal is recorded. The number 255 codes all pixels with maximum signal intensity. Generally, the human eye is significantly less sensitive to changes in grey levels than it is to changes in color. Hence, different color look up tables can be applied to grey-level images. All color images created by CLSM are pseudo-colors. Often, CLSM images are displayed in the colors in which the used fluorochromes are naturally emitted. To confirm the optimal settings of the microscopic parameters for analyzing a specimen, color look up tables, such as Glow Over Under (GOU), can be chosen.

Application of the LSM technique

A major goal of the use of the CLSM technique is to achieve minimum disturbance of a system under observation. Therefore, CLSM has become an indispensable tool to study interfacial microbial communities (Tab. 1; e.g. Holloway & Cowen, 1997; Neu & Lawrence, 1999; Neu, 2000; Neu, *et al.*, 2001).

Table 1: Advantages of confocal laser scanning microscopy for biological specimens.

1. examination of fully hydrated, living samples (several 100 µm thick, dependent from density and scattering properties)
2. virtually no light of out of focus regions
3. optical sections in xy, xz and xt (temporal) dimensions
4. reduction of scattering by point illumination
5. availability of numerous fluorescent and non-fluorescent probes
6. simultaneous application of multiple probes (up to 5 channels)
7. digital signals – visualisation and quantitative analyses

For example, in this study, CLSM was used to obtain more information on the 3-dimensional structure, composition and heterogeneity of riverine aggregates and the spatial distribution of associated microorganisms. CLSM allowed optical sectioning, creating images with enhanced resolution of fully hydrated aggregates.

Another reason for the use of CLSM may be the increasing number of probes and fluorescent stains suitable to study biological specimens. In general, fluorescent stains are very stable and show narrow emission bands and high extinction coefficients. By applications of different stains, fluorochromes should be chosen in a way, that excitation and emission wavelengths do not overlap.

The availability of computer hardware and software for digital image acquisition and analysis provides the basis for quantitative analysis and presentation of images obtained by CLSM and fluorescent stains.

Objective lenses

On the one hand, scanning riverine aggregates in their whole dimension, and on the other hand the determination of small objects such as bacteria and virus like particles are important issues in aquatic microbial ecology. Therefore, advantages of objective lenses for analyzing aquatic aggregates are a long working distance, a high numerical aperture (NA) and superior brightness (Lawrence, *et al.*, 2002). The perfect match of lens, resolution and magnification depends on 1) the type of specimen to be analyzed, 2) how the sample is prepared and 3) the type of information which is required. The major limitation of all objective lenses, especially when applying to CLSM, is that the axial resolution is poor compared to the lateral resolution. It is important that the resolution is dependent upon the numerical aperture of the lens according to the following relationship: $d = 0.61 \times \lambda / NA$, where λ is the light source

wavelength and d represents the minimum distance between two dots which can be identified as separate. Usually a combination of high magnification (60x and 100x) and high numerical aperture (NA of 1.2 - 1.4) is desirable for microscopic analysis of cellular and subcellular details.

Hence, when gross morphological structures of the aggregates were of interest, different lenses (50x and lower and $NA < 1.0$; water and oil immersion lenses, water immersible lenses) were used. For scanning aggregates in their whole dimensions and also for imaging bacteria a water immersible lens with a relatively high NA, such as a 0.90 NA 63x that also has a working distance of several millimeters, was employed. For investigating viruses associated to aggregates, the highest magnification and NA was needed. Therefore, a 1.4 NA 100x oil immersion objective, which offers high resolution, but a relative short working distance (approx. 0.10 mm) was used.

Limitations of CLSM, its solutions and outlooks

Despite all of its advantages, CLSM has several limitations. Photosensitivity, fading, scattering, laser penetration and background fluorescence can cause challenges using CLSM. They may be overcome by using a two photon laser microscope (2P-LSM; Neu, *et al.*, 2002; Neu & Lawrence, 2004; Neu, *et al.*, 2004). Here an infrared laser with an extremely short pulse is used to produce a high photon density. Two or more photons interact simultaneously with a fluorescent dye molecule. The coherently interfering photons can excite molecules at half the wavelength of the long wavelength laser and do so selectively in the focused spot. Therefore, no pinhole is required. As a consequence, no out of focus bleaching, no cell damage in out-of focus areas and no background fluorescence are possible. In addition, the infrared laser penetrates deeper into scattering media. But still, not much has been published in microbiology using 2P-LSM. The reasons maybe that 2P-LSM is too expensive and it does not present a solution to every 1-photon problem, e.g. thick environmental samples require sectioning anyway.

Axial resolution has improved substantially in 3-dimensional imaging by a technique called 4Pi microscopy (Bewersdorf, *et al.*, 2006). 4Pi microscopy coherently illuminates through two opposing lenses focusing a pulsed infrared laser beam into the same spot. With the current 4Pi microscopes it is possible to record 3-dimensional data sets from living cells with an axial resolution of 100 nm.

Another technique called stimulated emission depletion (STED) microscopy dramatically improves the lateral resolution and to a certain degree the axial resolution (Hell, *et al.*, 2006;

Hell, 2007). STED microscopy uses a focused excitation beam and a red-shifted, doughnut-shaped “STED beam” for quenching excited fluorophores to the zero of the doughnut. STED initially attained an axial resolution of 100 nm with a single lens. The combination of 4Pi and STED microscopy has already been demonstrated to attain an axial resolution of 33nm. Combinations of STED with 4Pi will probably push the z resolution to < 10 nm.

Thesis outline

This thesis focuses on particulate matter in riverine systems. On the one hand, the structure and composition of riverine aggregates and the colonization with microorganisms (including viruses) were investigated. A variety of strategies for examination of aggregates and their microbial (bacteria and viruses) colonizers, collected from the Danube and Elbe River, are presented. On the other hand, viruses (bacteriophages), organic colloids in the size range of 20 to 200 nm, were investigated. The thesis also focuses on the significance of the lytic and lysogenic viral life strategies based on the fact, that viruses may have significant impacts upon natural bacterial abundance, productivity and community composition. Therefore, an elaborate calculation procedure for quantifying lytic and lysogenic viral production in environmental samples was developed.

Chapter 1 (pages 19 – 48) describes the lectin-binding pattern in aquatic aggregates from the Danube River (Vienna, Austria) and the Elbe River (Magdeburg, Germany). The purpose of this study was to determine whether these two large European rivers harbor a distinct particle quality and whether the glycoconjugate composition changes over time. By employing different carbohydrate-specific probes in combination with CLSM, the fully hydrated riverine aggregates were analyzed with respect to the distribution of glycoconjugates.

In *Chapter 2* (pages 49 – 80) aggregates from the Danube and Elbe River were analyzed by collecting nucleic acid, glycoconjugate and negative stain signals using CLSM. Challenges and solutions, which may occur when scanning and quantifying riverine aggregates, are discussed on the basis of environmental samples.

Chapter 3 (pages 81 – 104) focuses on the use of CLSM to resolve for the first time fluorescence signals of single viruses and bacterial cells in a complex three-dimensional matrix of riverine aggregates. In addition, the CLSM data sets of virus signals in fully hydrated riverine aggregates were quantified. Different methods for quantifying viruses

associated with aquatic aggregates in combination with advanced imaging techniques are discussed.

In *Chapter 4* (pages 105 – 124) an on-line tool, called **Viral Production calculator (VIPCAL)**, for the estimation of lytically and lysogenically produced viruses during a virus reduction approach, is presented. The application of the program for the assessment of lytic viral production and of the proportion of lysogenic cells in environmental samples is shown. Other viral parameters, such as the percentage of lytically infected cells, lysis rate of bacteria, percentage of bacterial production lysed, proportion of bacterial loss per day, viral turnover time and dissolved organic carbon and nitrogen release during host lysis can be calculated with this on-line tool.

References

- Azam F, Malfatti F, (2007) Microbial structuring of marine ecosystems. *Nature Rev Microbiol* **5**: 782-791.
- Azúa I, Unanue M, Ayo B, Artolozaga I & Iriberry J (2007) Influence of age of aggregates and prokaryotic abundance on glucose and leucine uptake by heterotrophic marine prokaryotes. *International Microbiology* **10**: 13-18.
- Bewersdorf J, Egner A & Hell S (2006) 4Pi Microscopy. *Handbook of biological confocal microscopy, third edition*, (Pawely JB, ed.), p. 561-570. Springer Science+Business Media, LLC, New York, USA.
- Decho AW & Lopez GR (1993) Exopolymer microenvironments of microbial flora: multiple and interactive effects on trophic relationships. *Limnol Oceanogr* **38**(8): 1633-1645.
- Droppo IG, Leppard GG, Liss SN & Milligan TG (2005) *Flocculation in natural and engineered environmental systems*. CRC Press, Boca Raton, Florida.
- Flemming H-C & Wingender J (2003) The crucial role of extracellular polymeric substances in biofilms. *Biofilms in wastewater treatment*, (Wuertz S, Bishop PL & Wilderer PA, eds.), p. 178-210. IWA Publishing.
- Fuhrman JA & Schwalbach M (2003) Viral influence on aquatic bacterial communities. *Biol Bull* **204**: 192-195.
- Hell S, Willig K, Dyba M, Jakobs S, Kastrup L & Westphal V (2006) Nanoscale resolution with focused light: stimulated emission depletion and other reversible saturable optical fluorescence transitions microscopy concepts. *Handbook of biological confocal microscopy*,

third edition, (Pawley J, ed.), p.571-579. Springer Science+Business Media, LLC, New York, USA.

Hell SW (2007) Far-field optical nanoscopy. *Science* **316**: 1153-1158.

Helton RR, Cottrell MT, Kirchman DL & Wommack KE (2005) Evaluation of incubation-based methods for estimating virioplankton production in estuaries. *Aquat Microb Ecol* **41**: 209-219.

Hennes KP & Simon M (1995) Significance of bacteriophages for controlling bacterioplankton growth in a mesotrophic lake. *Appl Environ Microbiol* **61**: 333-340.

Hewson I & Fuhrman J (2006) Viral impacts upon marine bacterioplankton assemblage structure. *J Mar Biol Ass U.K.* **86**: 577-589.

Hewson I & Fuhrman J (2007) Covariation of viral parameters with bacterial assemblage richness and diversity in the water column and sediments. *Deep-Sea Res I* **54**: 811-830.

Hewson I & Fuhrman J (2007) Characterization of lysogens in bacterioplankton assemblages of the Southern California Borderland. *Microb Ecol* **53**: 631-638.

Holloway CF & Cowen JP (1997) Development of a scanning confocal laser microscopic technique to examine the structure and composition of marine snow. *Limnol Oceanogr* **42**: 1340-1352.

Inoué S (2006) Foundations of confocal scanned imaging in light microscopy. *Handbook of biological confocal microscopy, third edition*, (Pawley JB, ed.), p. 1-19. Springer Science+Business Media, LLC, New York, USA.

Jiang SC & Paul JH (1994) Seasonal and diel abundance of viruses and occurrence of lysogeny/bacteriocinogeny in the marine environment. *Mar Ecol Prog Ser* **104**: 163-172.

Jiang SC & Paul JH (1996) Occurrence of lysogenic bacteria in marine microbial communities as determined by prophage induction. *Mar Ecol Prog Ser* **142**: 27-38.

Kerner M, Hohenberg H, Ertl S, Reckermann M & Spitzzy A (2003) Self-organization of dissolved organic matter to micelle-like microparticles in river water. *Nature* **422**: 150-154.

Kirchman D (1983) The production of bacteria attached to particles suspended in a freshwater pond. *Limnol Oceanogr* **28**: 858-872.

Kirchman DL (1993) Particulate detritus and bacteria in marine environments. *Aquatic Microbiology. An Ecological Approach.*, (Ford TE, ed.), p. 321-341. Blackwell Scientific Publications, Boston.

Koike I, Hara S, Terauchi K & Kogure K (1990) Role of sub-micrometre particles in the ocean. *Nature* **345**: 242-244.

- Lawrence JR, Korber DR, Hoyle BD, Costerton JW & Caldwell DE (1991) Optical sectioning of microbial biofilms. *J Bacteriol* **173**: 6558-6567.
- Lawrence JR, Korber DR, Wolfaardt GM, Caldwell DE & Neu TR (2002) Analytical imaging and microscopy techniques. *Manual of environmental microbiology, second edition*, (Hurst CJ, Crawford RL, Knudsen GR, McInerney MJ & Stetzenbach LD, eds.), p. 39-61. ASM Press, Washington D.C.
- Lenski RE (1988) Dynamics of interactions between bacteria and virulent phage. *Advances in Microbial Ecology*, Vol. 10 (Marshall KC, ed.), p. 1-44. Plenum Publishing Corporation.
- Leppard G & Droppo I (2005) Overview of flocculation processes in freshwater ecosystems. *Flocculation in natural and engineered environmental systems*, (IG Droppo GL, ST Liss, T.G. Milligan, eds.), p. 25-46. CRC Press, Boca Raton, Florida.
- Luef B, Aspetsberger F, T. Hein, Huber F & Peduzzi P (2007) Impact of hydrology on free-living and particle-associated microorganisms in a river floodplain system (Danube, Austria). *Freshwater Biol* **52**: 1043 - 1057.
- Neu T & Lawrence J (2004) One-photon versus two-photon laser scanning microscopy and digital image analysis of microbial biofilms. *Methods Enzymol* **34**: 87-134.
- Neu T, Kuhlicke U & Lawrence J (2002) Assessment of fluorochromes for two-photon laser scanning microscopy of biofilms. *Appl Environ Microbiol* **68**: 901-908.
- Neu T, Walczysko P & Lawrence J (2004) Two-photon imaging for studying the microbial ecology of biofilm systems. *Microbes Environ* **19**: 1-6.
- Neu TR (2000) *In situ* cell and glycoconjugate distribution in river snow studied by confocal laser scanning microscopy. *Aquat Microb Ecol* **21**: 85-95.
- Neu TR & Lawrence JR (1999) Lectin-binding analysis in biofilm systems. *Methods Enzymol* **310**: 145-152.
- Neu TR, Swerhone GDW & Lawrence JR (2001) Assessment of lectin-binding analysis for *in situ* detection of glycoconjugates in biofilm systems. *Microbiol* **147**: 299-313.
- Noble RT & Fuhrman JA (2000) Rapid virus production and removal as measured with fluorescently labeled viruses as tracers. *Appl Environ Microbiol* **66**: 3790-3797.
- Pawley JBe (2006) *Handbook of biological confocal microscopy, third edition*. Springer Science+Business Media, LLC, New York, USA.
- Peduzzi P & Luef B (in press) Viruses. *Encyclopedia of Inland Waters*, (Likens GE, ed.), Elsevier, Oxford.

- Proctor LM, Okubo A & Fuhrman JA (1993) Calibrating estimates of phage-induced mortality in marine bacteria: ultrastructural studies of marine bacteriophage development from one-step growth experiments. *Microb Ecol* **25**: 161-182.
- Schwalbach M, Hewson I & Fuhrman J (2004) Viral effects on bacterial community composition in marine plankton microcosms. *Aquat Microb Ecol* **34**: 117-127.
- Simon M, Grossart H-P, Schweitzer B & Ploug H (2002) Microbial ecology of organic aggregates in aquatic ecosystems. *Aquat Microb Ecol* **28**: 175-211.
- Skillman LC, Sutherland IW & Jones MV (1999) The role of exopolysaccharides in dual species biofilm development. *J Appl Microbiol Sym Suppl* **85**: 13S-18S.
- Sutherland IW (2001) The biofilm matrix - an immobilized but dynamic microbial environment. *TIM* **9**: 222-227.
- Tapper MA & Hicks RE (1998) Temperate viruses and lysogeny in Lake Superior bacterioplankton. *Limnol Oceanogr* **43**: 95-103.
- Weinbauer MG (2004) Ecology of prokaryotic viruses. *FEMS Microbiol Rev* **28**: 127-181.
- Weinbauer MG & Suttle CA (1996) Potential significance of lysogeny to bacteriophage production and bacterial mortality in coastal waters of the Gulf of Mexico. *Appl Environ Microbiol* **62**: 4374-4380.
- Wilcox RM & Fuhrman JA (1994) Bacterial viruses in coastal seawater: lytic rather than lysogenic production. *Mar Ecol Prog Ser* **114**: 35-45.
- Williamson K, Schnitker J, Radosevich M, Smith D & Wommak K (2008) Cultivation-based assessment of lysogeny among soil bacteria. *Microb Ecol* **56**: 437-447.
- Wilson WH & Mann NH (1997) Lysogenic and lytic viral production in marine microbial communities. *Aquat Microb Ecol* **13**: 95-100.
- Winget DM, Williamson KE, Helton RR & Wommack KE (2005) Tangential flow diafiltration: an improved technique for estimation of virioplankton production. *Aquat Microb Ecol* **41**: 221-232.
- Wommack KE & Colwell RR (2000) Virioplankton: viruses in aquatic ecosystem. *Microbiol Mol Biol Rev* **64**: 69-114.
- Zimmermann-Timm H (2002) Characteristics, dynamics and importance of aggregates in rivers - an invited review. *Internat Rev Hydrobiol* **87**: 197-240.

Chapter 1

Fluorescence Lectin-Binding Analysis in Riverine Aggregates (River Snow): a Critical Examination

Birgit Luef, Peter Peduzzi and Thomas R. Neu
(submitted to FEMS Microbiology Ecology)

Abstract

This study examines the lectin-binding pattern in aquatic aggregates from the Danube River (Vienna, Austria) and the Elbe River (Magdeburg, Germany). The aggregate structure was assessed by Confocal Laser Scanning Microscopy. River aggregates were examined in the reflection and fluorescence modes in order to record mineral content, autofluorescence and fluorochrome signals. Glycoconjugates of extracellular polymeric substances (EPS) were examined with up to 74 different commercially available lectins. Almost all of the lectins tested on riverine aggregates exhibited some kind of binding pattern to the polymeric matrix. However, only few lectins showed strong and clear binding to the specific glycoconjugates of the aggregates. These two large European rivers appeared to harbor different particle qualities. For example Danube and Elbe aggregates differed in their glycoconjugate composition when compared at the same season. Furthermore, the binding patterns of most lectins to the glycoconjugates of the riverine aggregates changed over time. This necessitates lectin screening to find the most suitable lectin or panel of lectins for aggregate analyses. This elaborate technique may have a significant potential for *in situ* studies on particle-related aspects and biogeochemical cycling in freshwater ecosystems.

Introduction

Many microorganisms, such as bacteria and algae, synthesize extracellular polymeric substances (EPS), composed of different classes of organic macromolecules such as polysaccharides, proteins, nucleic acids, lipids/phospholipids and amphiphilic polymers (Flemming & Wingender, 2003). These EPS either remain attached to the cell surface or are present in the extracellular matrix (Decho & Lopez, 1993). Many microorganisms live in aggregated forms such as biofilms, flocs and sludge, where they are embedded in such an EPS matrix. The architecture as well as the structural and functional integrity of biofilms are determined by the presence of EPS, caused by the intermolecular interactions between many different macromolecules (Flemming & Wingender, 2003). Many additional functions are attributed to the EPS: The EPS matrix enables microorganisms to form stable aggregates of mixed populations, leading to synergistic micro-consortia. An important modern concept is the role of EPS in allowing microorganisms to live continuously at high cell densities in stable, mixed-population biofilm communities (Flemming & Wingender, 2003).

EPS in microbial structures have been traditionally quantitatively estimated using extraction and chemical methods (Bura, *et al.*, 1998; John & Nielsen, 1995; McSwain, *et al.*, 2005). Chemical approaches, however, are limited to pure culture and chemically defined systems.

Moreover, chemical analyses of EPS eliminate information on the spatial distribution, relations and structures of all the constituents. To analyze carbohydrate structures of the EPS matrix *in situ*, lectin staining is the method of choice (Neu & Lawrence, 1999). Lectins are a diverse group of proteins and glycoproteins that exhibit specific binding for certain carbohydrate moieties (e.g. see Brooks, *et al.*, 1997; Sharon & Lis, 2003). Most lectins recognize just a few of the hundreds of monosaccharides found in nature, primarily mannose, glucose, galactose, fucose, N-acetylglucosamine, N-acetylgalactosamine and N-acetylneuraminic acid. They typically recognize hetero-oligosaccharides composed of these monosaccharides. Lectins bind with their ligands primarily by a network of hydrogen bonds and hydrophobic interactions; in rare cases, electrostatic interactions (or ion pairing) and coordination with metal ions also play a role.

Recently, the use of fluorescently labeled lectins in combination with Confocal Laser Scanning Microscopy (CLSM) has become an indispensable technique to estimate extracellular polysaccharides of the EPS matrix in lotic biofilms (Battin, *et al.*, 2003; Neu, *et al.*, 2001; Staudt, *et al.*, 2003). The actual structure of the biofilm matrix can vary greatly depending on the microbial cells present, their physiological status, the nutrients available and the prevailing physical conditions (Sutherland, 2001). As mentioned above, the architecture, composition etc. of biofilms is well investigated, but only few studies have analyzed floating freshwater aggregates (Böckelmann, *et al.*, 2000; Böckelmann, *et al.*, 2002; Neu, 2000). Here, we examine the architecture of aquatic aggregates from the Danube (Vienna, Austria) and the Elbe (Magdeburg, Germany) during different seasons by lectin-binding-analysis. One purpose of this study was to determine whether these two large European rivers harbor a distinct particle quality and whether the glycoconjugate composition changes over time. Moreover, to optimally characterize the EPS of riverine aggregates, a panel of lectins was tested. By employing different carbohydrate-specific probes in combination with CLSM, the fully hydrated riverine aggregates were analyzed with respect to the distribution of glycoconjugates.

Material and Methods

Sampling and handling of aggregates

For lectin screening samples were taken from the Danube River (Wildungsmauer, Austria, stream kilometer 1894) and Elbe River (Magdeburg, Germany, stream kilometer 318) in fall 2004 and summer 2005. To test the effect of season and the type of lectin on glycoconjugate volume, additional water samples from the Danube River were taken in spring (05/03/2005),

summer (07/20/2005), fall (10/13/2005) and winter (01/08/2006). Sampling depth was approximately 30 cm at all stations. Lotic aggregates were sampled in 1L plexiglass bottles. The samples were always kept at +4 °C until analysis, which was completed within 24 h (Bura, *et al.*, 1998). The aggregates were carefully transferred with an inverted 10 ml glass pipette (Gibbs & Konwar, 1982) to Eppendorf tubes, where staining was performed.

Staining procedure

To label matrix material of the aggregates, lectins were employed to stain the lectin-specific EPS (Neu, 2000; Neu, *et al.*, 2001; Staudt, *et al.*, 2003). For the screening, different lectins (62 and 74 different lectins were tested in fall and in summer, respectively) were purchased from four suppliers (EY Laboratories, San Mateo, California, USA; Invitrogen, Eugene, Oregon, USA; Sigma, St. Louis, Missouri, USA; Vector Laboratories, Burlingame, California, USA). All lectins were either custom labeled with FITC or self-labeled with the fluorochrome Alexa Fluor 488 according to the data sheet of the supplier (kit from Molecular Probes, Eugene, Oregon, USA). To test the effect of season and the type of lectin on the glycoconjugate volume of the aggregates from the Danube, the lectins from *Aleuria aurantia* (AAL, Vector Laboratories, Burlingame, California, USA) or from *Phaseolus vulgaris* (PHA-E, Sigma Aldrich, St. Louis, Missouri, USA) were employed in parallel to stain the majority of lectin-specific glycoconjugates of the EPS (Neu, 2000; Neu, *et al.*, 2001; Staudt, *et al.*, 2003). The lectin from AAL was self-labeled with the fluorochrome Cy5 (Amersham, Buckinghamshire, UK) and PHA-E with Alexa Fluor 633 nm (Invitrogen) according to the data sheet of the supplier. The glycoconjugates of EPS were stained with different lectins as described previously (Neu, 2000). Briefly, for lectin staining, the lectins were diluted with deionized water to a final concentration of 0.1 g mL⁻¹ protein. 100 µl of this solution were added to each sample and incubated for 20 min in the dark. The aggregates were then carefully washed 3 times with tap water to remove unbound lectins and were never allowed to dry in the air. The stained samples were carefully transferred into cover well imaging chambers with gaskets (one chamber, 20 mm diameter, 0.5 mm deep, Invitrogen) or a Lab-Tek chambered coverglass system (8 chambers; Nalge Nunc International Corp., Naperville, Illinois), covered with tap water and immediately examined by Laser Scanning Microscopy (CLSM).

Lectin specificity test

Controls for lectin inhibition (Neu, 2000) were performed using different lectins (Table 1). The lectins were used at the same concentration as for staining (0.1 g mL^{-1} protein). A stock solution of each specific carbohydrate (0.1 g mL^{-1}) was prepared. This concentration as well as a dilution series (1:2, 1:4, 1:40, 1:400, 1:4000) was used for the inhibition experiment. For references, one sample was incubated solely with the specific carbohydrate stock solution and another one with the pure lectin. The procedure employed for this inhibition experiment was identical to the lectin staining (see above). $100 \mu\text{l}$ lectin solution and $100 \mu\text{l}$ specific carbohydrate solution were incubated for 20 min in the dark. Thereafter, the lectin-carbohydrate-solution and the aggregates were incubated for 20 min, washed three times with tap water, transferred into chambers and examined by CLSM. Inhibition of lectin binding to the EPS matrix in the presence of the specific monosaccharide was estimated by visual comparison and CLSM photomultiplier intensity of the fluorescence signal binding pattern of samples with and without added sugar. Furthermore, a ratio of the lectin signals to the reflection signals was calculated (see below).

Laser Scanning Microscopy

Aggregate structure was analyzed by CLSM using visible lasers for excitation and multi-channel recording. The 488 nm line was used for reflection signals of mineral compounds and cellular reflection (480 - 495 nm). FITC- and Alexa Fluor 488-labeled lectins were used for staining glycoconjugates (500 - 550 nm). The 633 nm line was employed for chlorophyll-*a* autofluorescence (650 - 800 nm) (Neu, 2000; Neu, *et al.*, 2004). To test the effect of season and type of lectin on glycoconjugate volume, the laser line 633 nm was used to detect lectin signals (650-750 nm; fluorochrome Cy5 / Alexa Fluor 633).

Aggregates from the Elbe River were analyzed by CLSM using a Leica TCS SP1, controlled by the LCS Version 2.61 Build 1537 174192 (Leica, Heidelberg, Germany), equipped with an upright microscope. For lectin screening, images were collected with a 40x 0.8 NA water lens. Aggregates from the River Danube were examined by CLSM using a TCS SP2 controlled by the LCS Version 2.5 Build 1227 192162 (Leica). Images were collected using an inverted DM IRB microscope and a HCXPL APO 40x 1.25 NA oil lens.

To test the effect of season and type of lectin on glycoconjugate volume, images were collected with a 63x 0.9 NA water lens.

Optical sections of aggregates up to a diameter of $100 \mu\text{m}$ were taken every $1 \mu\text{m}$. For aggregates larger than $100 \mu\text{m}$, a step size of $2 \mu\text{m}$ was used.

Quantification, calculation and statistical analysis

To quantify lectin and reflection signals, the freely available software Image J (<http://rsb.info.nih.gov/ij/>), developed in Java, was used (Staudt, *et al.*, 2004). Due to the very heterogeneous composition of the aggregates, automatic batch processing could not be used. Hence, for each aggregate, thresholds were set and analyzed for the reflection and lectin signals separately.

CLSM images were not further processed and no digital image filters were used. Adobe Photoshop CS2 was used to insert calibration bars into the images.

Actual aggregate volumes can not be determined by analyzing specific glycoconjugates, chlorophyll-*a* and inorganic, mineral components alone. The rest of the aggregates, such as nucleic acids, proteins, humic substances, lipids, other glycoconjugates etc., were not determined in this study. However, to gain information on the proportion of the specific glycoconjugates, the lectin to reflection ratio was introduced.

Reflection imaging can be performed with CLSM systems in the confocal mode. Note, however, that the reflection mode detects only the surface of the inorganic material and not the volume. This calls for cautious interpretation of the spatial information from the reflection mode. In our case, we did not use the calculated lectin to reflection ratio in a strict mathematical sense. Although the reflection signal provides information based only on an area, the lectin to reflection ratio can harbor ecological information. This ratio allows quantifying the proportion of specific glycoconjugates within an inorganic-organic moiety of aggregates. Moreover, changes in the EPS composition of the aggregates over time or at different locations could be detected. The higher the ratio, the more specific EPS glycoconjugate was present.

For statistical analysis, the software program SPSS 12.0 for Windows (SPSS, Chicago, Illinois, USA) was used. A Kolmogoroff-Smirnov test (K-S-test) was performed to determine whether the data exhibited normal distributions. Because the data exhibited no normal distributions, a non-parametric test (Mann-Whitney U-Test) was performed to test between aggregate qualities of the two rivers. To analyze differences in aggregate composition at different seasons within a river, a parametric test (Wilcoxon Test) was used.

Seasonal differences in the specific glycoconjugate volume data of the River Danube were tested for normal distribution (K-S-test) and homogeneity of variances (Levene-test). If the data fulfilled the criteria of normal distribution and homogeneity of variances, an ANOVA with seasons as grouping variable was carried out. The Tukey post-hoc test was applied to

determine, which differences were significant. If the data fulfilled the K-S-test but not the Levene-test, a parametric test (t-test, for dependent samples) was used.

Results

In a first step, unstained aggregates were observed. Images were scanned both in reflection and fluorescent modes. The reflection images were used to distinguish between organic and inorganic compounds. Chlorophyll-*a* signals of autotrophs were recorded in the far red channel (Fig. 1). Recording signals in the reflection mode demonstrated on one hand the variable mineral content of lotic aggregates and on the other hand differences in the structure and size of the aggregates when comparing both rivers. In the Danube, a flood event during summer sampling influenced aggregate size and quality.

Inhibition test

Some of the lectins were tested for their specificity (Tab. 1). Firstly, Danube and Elbe aggregates stained with an Alexa Fluor 488-labeled lectin *Aleuria aurantia* (AAL) were analyzed. Keeping the same settings at the CLSM, samples that were inhibited with different concentrations of L-Fucose were then analyzed. The CLSM data revealed a clear inhibition of the binding of AAL (Fig. 2). Microscope examination, however, still showed clear fluorescent signals even at the highest L-Fucose concentration. Therefore, further lectins were tested for their specificity (Tab. 1). All these lectins, inhibited with their specific sugars, also bound non-specifically to the EPS matrix.

The lectin from *Ulex europaeus* (UEA-I) labeled with the fluorochrome FITC was purchased from different companies such as EY Laboratories, Vector Laboratories and Sigma. UEA-I from Sigma was also self-labeled with Alexa Fluor 488. The results demonstrated that 1) the same lectin with the same fluorochrome from different companies showed different binding patterns to the EPS matrix (Fig. 3) and 2) all four lectins were only partially inhibited by L-Fucose.

Lectin screening and aggregate composition

Aggregates from the Danube and Elbe were analyzed by employing different carbohydrate-specific probes, to find the most suitable ones, in combination with CLSM. Visual comparison of the lectins tested on riverine aggregates showed that almost all had some binding pattern to the polymeric matrix. However, only a few lectins exhibited strong and clear binding to the EPS glycoconjugates of the aggregates. Images of selected lectins are presented in Figure 4;

they indicate the binding of lectins with the lectin-specific glycoconjugates of the riverine aggregates. The lectins stained major parts of the aggregates from both rivers during both sampling times. Furthermore, Danube and Elbe aggregates stained with the lectin from AAL showed that this lectin preferentially bound to the EPS matrix in summer, whereas in fall the lectin had a higher affinity to the aggregates' cell surface glycoconjugates (Fig. 4).

Some lectins differed strongly in their binding to glycoconjugates in the two rivers at the same season (Fig. 5). For example, large parts of the aggregates from the Elbe were stained with the lectin from *Canavalia ensiformis* (ConA), whereas ConA stained only minor parts of the Danube aggregates.

The lectin-glycoconjugate binding patterns of the riverine aggregates also changed over time (Fig. 6). In the Danube, lectins from *Dolichos biflorus* (DBA), *Narcissus pseudonarcissus* (NPA) and UEA-I stained major parts of the aggregates in fall, but gave weak signals in summer. In the Elbe, the lectin from *Tetragonolobus purpurea* stained the EPS matrix of the aggregates in fall. In that river, *Vigna radiata* (VRA) stained parts of the glycoconjugates in summer. In fall, VRA stained the EPS matrix of the aggregates very weakly.

In the Danube, the lectin to reflection ratio (i.e. the proportion of the specific glycoconjugate to the inorganic, mineral components) ranged from 0.01 to 7.36 (average 1.34) in fall and from 0.0 to 3.38 (average 0.32) in summer. In the Elbe, the lectin to reflection ratio ranged from 0.02 to 8.10 (average 1.95) in fall and from 0.0 to 5.07 (average 0.84) in summer. Regarding this ratio of all analyzed lectins, the two rivers differed significantly both in fall ($p < 0.01$, $n = 120$) and summer ($p < 0.01$, $n = 148$). In both rivers – Danube ($p = 0.03$, $n = 62$) and Elbe ($p < 0.01$, $n = 61$) – the glycoconjugates also varied significantly between seasons.

In order to determine which carbohydrates were dominant in the EPS of the aggregates, lectins were pooled based on their sugar specificity (Tab. 2). When pooled, the glycoconjugate composition of the aggregates did not differ significantly between both rivers in fall (Fig. 7a). In summer, however, the Elbe aggregates harbored significantly higher concentrations of specific carbohydrates (Fig. 7b). In both rivers, aggregate quality differed significantly when comparing both seasons (Fig. 7c and 7d): Higher concentrations of specific carbohydrates were present in fall in both rivers.

Effect of season and type of lectin on glycoconjugate volume

In general, the lectin from AAL stained a greater proportion of specific glycoconjugates of aggregates in the Danube River than the lectin from PHA-E during the four seasons (Fig. 8). Comparing the specific glycoconjugate volumes, stained with the two lectins AAL and PHA-

E, significant differences occurred in spring (t-test, $p < 0.001$, $n = 20$), summer (t-test, $p < 0.001$, $n = 30$) and fall (t-test, $p < 0.001$, $n = 20$), but no significant differences were found in winter (t-test, $p = 0.101$, $n = 23$).

Comparing the aggregates during the four seasons labeled with the lectin from PHA-E, no differences of the specific glycoconjugate volumes were found (Anova, $df_1 = 3$, $df_2 = 89$, $p = 0.738$). In contrast, the specific glycoconjugates determined by the lectin from AAL changed significantly during the seasons (Anova, $df_1 = 3$, $df_2 = 92$, $p = 0.001$): during winter the specific glycoconjugate volumes, labeled with AAL, showed significant differences compared to spring (Tukey, $p = 0.001$) and summer (Tukey, $p = 0.030$).

Discussion

Extracellular polysaccharides are the fundamental structural elements of the EPS matrix determining the mechanical stability of biofilms (Flemming & Wingender, 2003). Lectins are a useful probe to examine the 3-dimensional distribution of these glycoconjugates in fully hydrated biofilms (Neu & Lawrence, 1999). Aggregates are generally regarded as mobile biofilms and, therefore, results and assumptions of investigated biofilms are often automatically projected to aggregates. However, aggregates, especially river snow, are less well studied and may differ substantially from typical biofilm structures. To characterize the EPS of a system, a panel of lectins has to be selected and tested. Our study strongly supports the necessity of lectin screening to find the most suitable lectin or panel of lectins that will stain a major fraction of the EPS glycoconjugates, as reported also for microbial biofilms (Neu, *et al.*, 2001; Staudt, *et al.*, 2004).

Lectin specificity

The nominal specificity of a lectin is usually expressed in terms of the simple monosaccharide that best inhibits its effect. Hence, we investigated the monosaccharide specificity of the lectin AAL by adding different concentrations of the target monosaccharide L-Fucose to the lectin solutions before the staining procedure (Fig. 2). We were able to show that the lectin apparently bound to a specific target monosaccharide in the EPS matrix of the aggregates. But the lectin from AAL also bound non-specifically to the EPS matrix. The lectin from AAL, that we used was self-labeled with the fluorochrome Alexa Fluor 488 according to the supplier's data sheet. As no clear inhibition occurred, the question arose whether the lectin was over-labeled. This effect can occur when the incubation time of the protein and the fluorochrome is too long or the amount of protein is too small during the labeling process (see

supplier's data sheet). Therefore, the incubation time of the fluorochrome and the lectin from AAL was reduced from 60 to 15 minutes. Performing an inhibition test with this lectin, AAL still bound non-specifically. Johnsen *et al.* (2000) also found some lectin non-specifically bound to *Sphingomonas* biofilms after inhibition. Their interpretation was that some of the bound lectin, namely the part that does not bind in the presence of target sugars, is bound to specific sugar residues in the biofilm. The part that binds in the presence of target sugars is bound non-specifically to the biofilm.

So far, the known sugar specificity of lectins is restricted to the common carbohydrates listed in the suppliers' data sheet and is based on the influence of lectins on blood cell agglutination. Additionally, some lectins have an affinity not only for one specific monosaccharide, but also for di-, tri- and even oligosaccharides (Sharon & Lis, 2003). Natural samples no doubt contain unknown glycoconjugates or carbohydrate combinations; they may also bind to the applied lectins. Furthermore, binding may originate not only from the known sugars but also by other unknown lectin-protein interactions. Importantly, the assumed specificity of a lectin for a particular monosaccharide actually is an over-simplification (Brooks, *et al.*, 1997). Lectins will combine with monosaccharide moieties, and monosaccharides will inhibit lectin-induced agglutination. However, the combining site of the lectin is usually far more complex than this simple inhibition test would suggest. The actual structure recognized by a lectin's binding site when it combines with its natural ligand is generally larger and more complex than a single monosaccharide. Three monosaccharides, terminal and sub-terminal in the oligosaccharide chain, in a particular spatial arrangement, are thought to be involved. As a consequence, adding a simple monosaccharide to a lectin may yield a new and completely different binding pattern. Sometimes even part of the protein or lipid to which the oligosaccharides are attached is relevant (Brooks, *et al.*, 1997). Moreover, hydrophobic and electrostatic interactions not located at the sugar binding site may also play a role in lectin binding to tissue structures. Two lectins with identical monosaccharide specificities may actually recognize very different sugar structures and give surprisingly different results. Finally, note that beyond having carbohydrate-binding sites, lectins may contain one or more sites that interact with non-carbohydrate ligands (Barondes, 1988).

Fluorochrome labeling may also change lectin specificity. Neu *et al.* (2001) noted the influence of fluorine labeling on the glycoconjugate-lectin interaction. So far, tests indicated that FITC-labeled lectins had more specific binding patterns than TRITC-labeled ones (Neu, *et al.*, 2001). In the present study as well, lectin specificity was influenced by the fluorochrome, and different lectins reacted differently to different fluorine-labels (data not

shown). Moreover, the same lectin purchased from different companies bound differently to the glycoconjugates (Fig. 3). There is no clear explanation for this result. This calls for correctly providing the company name, product number etc., especially in ecological applications.

The tested lectins were isolated from plants, animals, fungi, lower plants and bacteria (Sharon & Lis, 2003). Very little is known regarding their natural binding sites. The structures that lectins recognize on cells and tissues are heterogeneous and largely uncharacterized. So far, the known sugar specificity of lectins is restricted to common carbohydrates as given by suppliers' data sheets. Nevertheless, these lectins can be usefully applied to different environmental samples to characterize the EPS (e.g. Decho & Kawaguchi, 1999; Holloway & Cowen, 1997; Neu, 2000; Staudt, *et al.*, 2003).

Structure and ecology of floating aggregates

Our lectin binding analysis shows that the Danube and Elbe Rivers apparently harbor different particle qualities (Fig. 5). The aggregates of different origin varied in their composition. Physical weathering of upland soils and rocks, riparian vegetation, biofilms, fecal pellets, autochthonous algae and macrophytes can influence the composition of inorganic and organic materials in riverine ecosystems (see review of Simon, *et al.*, 2002).

Moreover, we observed distinct glycoconjugate distributions in both rivers (Fig. 4, 7a and 7b) and also changes over time (Fig. 6, 7c and 7d). Changes in the glycoconjugates may be associated with changes in the community structure of microorganisms and/or in available nutrients. The ability to produce EPS is widespread among bacteria and archaea, but also occurs in eukaryotic microorganisms including microalgae such as diatoms, and fungi such as yeasts and molds (e.g. Flemming & Wingender, 2003; Hoagland, *et al.*, 1993).

A potential effect of the nutrient regime on the cellular composition and glycoconjugate chemistry was also proposed for lotic biofilms by Neu *et al.* (2005). Their results suggested that the relationship between bacteria and algae, as influenced by nutrients, plays an important role in determining the glycoconjugate structure. For the Danube, Besemer *et al.* (2005) showed that the compositional dynamics of the particle-associated bacterial communities were related to changes in the algal biomass and in concentrations of organic and inorganic nutrients. For the Elbe, seasonal dynamics in the structure and composition of the microbial river snow community have been shown by Böckelmann *et al.* (2000). The river snow community was characterized by a great bacterial diversity in spring. In summer the typical

features of the river snow aggregates were large amounts of green algae, diatoms and cyanobacteria. In autumn and winter, algae were absent and bacterial abundance increased. Moreover, viruses may also help explain a shift in the glycoconjugate composition. On the one hand, EPS may be produced during viral lysis (Peduzzi & Weinbauer, 1993); on the other hand, viral activity can influence the community composition of their hosts (Bouvier & del Giorgio, 2007; Weinbauer & Rassoulzadegan, 2003) and therefore probably also the EPS composition. Accordingly, differences in the microbial consortia may alter the EPS composition.

Based on the lectin screening and the lectin to reflection ratios in our study, the Danube and Elbe differed in their EPS composition. This serves as an example for the variability in the composition of floating aggregates, which has ecological implications. In riverine systems, for example, hydrology and different water age (in side arms or floodplain pools) apparently influence particle quality (Luef, *et al.*, 2007; Peduzzi & Luef, 2008). This also affects the abundance and activity of the associated microorganisms (bacteria, viruses), and the strongly colonized aggregates were mostly flocculent with a predominant organic matrix. In rivers, particulate organic matter is an important energy source for the heterotrophic biota. The bioavailability of particulate organic matter, however, strongly depends on its biochemical composition, diagenetic state (freshly produced vs. aged) and origin (allochthonous, autochthonous). Microorganisms typically better utilize younger and autochthonously produced material, whereas terrestrially derived material that enters running water is already largely degraded. Microbially produced EPS can be a highly labile food source (Decho & Lopez, 1993). Microbial exopolymers range from easily digestible carbon sources to relatively refractory ones, depending on their composition. Capsule EPS is significantly less digestible to consumers than slime EPS and has a high protein content; the loose slime EPS, in contrast, is largely composed of polysaccharides. Microbial cells are typically unable to utilize EPS that they have synthesized. However, heterologous species within the matrix can degrade and utilize the EPS, thereby also altering biofilm composition and structure (Sutherland, 2001). Furthermore, exopolymer microenvironments may also make recently adsorbed dissolved organic matter highly accessible to particle-ingesting animals. Dissolved organic matter readily associates with particulate EPS either through binding or colloidal trapping (Decho & Lopez, 1993). Hence, differences in the EPS composition may affect the digestibility to microorganisms or to protozoa/animals that ingest the microbial flora associated with floating aggregates or sediments. Variability in suspended matter quality

among various riverine environments at different seasons is therefore probably highly relevant for the respective food web.

Lectins are a remarkable, huge and amazingly diverse group of naturally occurring, specific, sugar-binding molecules. Our results clearly show that binding of lectins to river snow proves the presence of specific target monosaccharides in the EPS matrix of the aggregates. Lectins might also bind to non-EPS targets or bind non-specifically to the EPS matrix. Nonetheless, they are a valuable tool for assessing the glycoconjugate composition in riverine aggregates. Lectin binding analysis is useful to follow the production of lectin-specific glycoconjugates over time, and thus helps assess aggregation composition during high and low water conditions, during algal blooms or during different seasons (Fig. 8). However, the choice of the proper lectin is essential. Therefore, lectin screening is necessary to find the most suitable lectin or panel of lectins for aggregate analyses. Fluorescence lectin-binding analysis, in combination with CLSM, has a significant potential for studies on particle-related aspects relevant for biogeochemical cycling and the ecology of freshwater systems.

Acknowledgements

We thank the Austrian Science Foundation FWF (grant number P14721 to P.P.) and the European Commission (Marie-Curie-Training-Sites, grant number HPMT-CT-2001-00426) for financial support. We are grateful for technical help by U. Kuhlicke.

References

- Barondes SH (1988) Bifunctional properties of lectins: lectins redefined. *TBS* **13**: 480-482.
- Battin TJ, Kaplan LA, Newbold JD, Cheng X & Hansen C (2003) Effects of current velocity on the nascent architecture of stream microbial biofilms. *Appl Environ Microbiol* **69**: 5443-5452.
- Besemer K, Moeseneder MM, Arrieta JM, Herndl GJ & Peduzzi P (2005) Complexity of bacterial communities in a river-floodplain system (Danube, Austria). *Appl Environ Microbiol* **71**: 609-620.
- Böckelmann U, Manz W, Neu TR & Szewzyk U (2000) Characterization of the microbial community of lotic organic aggregates ("river snow") in the Elbe River of Germany by cultivation and molecular methods. *FEMS Microb Ecol* **33**: 157-170.
- Böckelmann U, Manz W, Neu TR & Szewzyk U (2002) Investigation of lotic microbial aggregates by a combined technique of fluorescent in situ hybridization and lectin-binding-analysis. *J Microbiol Methods* **49**: 75-87.
- Bouvier T & del Giorgio PA (2007) Key role of selective viral-induced mortality in determining marine bacterial community composition. *Environ Microbiol* **9**: 287-297.
- Brooks SA, Leathem AJC & Schumacher U (1997) *Lectin Histochemistry a concise practical handbook*. Bios Scientific Publishers, Oxford.
- Bura R, Cheung M, Liao B, *et al.* (1998) Composition of extracellular polymeric substances in the activated sludge floc matrix. *Water Sci & Technol* **37**: 325-333.
- Decho AW & Lopez GR (1993) Exopolymer microenvironments of microbial flora: multiple and interactive effects on trophic relationships. *Limnol Oceanogr* **38**: 1633-1645.
- Decho AW & Kawaguchi T (1999) Confocal Imaging of *in situ* natural microbial communities and their extracellular polymeric secretions (EPS) using Nanoplast resin. *BioTechniques* **27**: 1246-1252.
- Flemming H-C & Wingender J (2003) The crucial role of extracellular polymeric substances in biofilms. *Biofilms in wastewater treatment*, (Wuertz S, Bishop PL & Wilderer PA, eds.), p. 178-210. IWA Publishing.
- Gibbs RJ & Konwar LN (1982) Effect of pipetting on mineral flocs. *Environ Sci & Technol* **16**: 119-121.
- Hoagland KD, Rosowski JR, Gretz MR & Roemer SC (1993) Diatom extracellular polymeric substances: function, fine structure, chemistry, and physiology. *J Phycol* **29**: 537-566.

- Holloway CF & Cowen JP (1997) Development of a scanning confocal laser microscopic technique to examine the structure and composition of marine snow. *Limnol Oceanogr* **42**: 1340-1352.
- John A & Nielsen PH (1995) Extraction of extracellular polymeric substances (EPS) from biofilms using a cation exchange resin. *Water Sci & Technol* **32**: 157-164.
- Johnsen AR, Hausner M, Schnell A & Wuertz S (2000) Evaluation of fluorescently labeled lectins for noninvasive localization of extracellular polymeric substances in *Sphingomonas* biofilms. *Appl Environ Microbiol* **66**: 3487-3491.
- Luef B, Aspetsberger F, T. Hein, Huber F & Peduzzi P (2007) Impact of hydrology on free-living and particle-associated microorganisms in a river floodplain system (Danube, Austria). *Freshwater Biol* **52**: 1043 - 1057.
- McSwain BS, Irvine RL, Hausner M & Wilderer PA (2005) Composition and distribution of extracellular flocs and granular sludge. *Appl Environ Microbiol* **71**: 1051-1057.
- Neu TR (2000) *In situ* cell and glycoconjugate distribution in river snow studied by confocal laser scanning microscopy. *Aquat Microb Ecol* **21**: 85-95.
- Neu TR & Lawrence JR (1999) Lectin-binding analysis in biofilm systems. *Methods Enzymol* **310**: 145-152.
- Neu TR, Swerhone GDW & Lawrence JR (2001) Assessment of lectin-binding analysis for *in situ* detection of glycoconjugates in biofilm systems. *Microbiology* **147**: 299-313.
- Neu TR, Woelfl S & Lawrence JR (2004) Three-dimensional differentiation of photo-autotrophic biofilm constituents by multi-channel laser scanning microscopy (single-photon and two-photon excitation). *J Microbiol Methods* **56**: 161-172.
- Neu TR, Swerhone GDW, Böckelmann U & Lawrence JR (2005) Effect of CNP on composition and structure of lotic biofilms as detected with lectin-specific glycoconjugates. *Aquat Microb Ecol* **38**: 283-294.
- Peduzzi P & Weinbauer MG (1993) Effect of concentrating the virus-rich 2-200 nm size fraction of seawater on the formation of algal flocs (marine snow). *Limnol Oceanogr* **38**: 1562-1565.
- Peduzzi P & Luef B (2008) Viruses, bacteria and suspended particles in a backwater and main channel site of the Danube (Austria). *Aquat Sci* **70**: 186-194.
- Sharon N & Lis H (2003) *Lectins Second Edition*. Kluwer Academic Publishers, Dordrecht.
- Simon M, Grossart H-P, Schweitzer B & Ploug H (2002) Microbial ecology of organic aggregates in aquatic ecosystems. *Aquat Microb Ecol* **28**: 175-211.

Staudt C, Horn H, Hempel DC & Neu TR (2003) Screening of lectins for staining lectin-specific glycoconjugates in the EPS of biofilms. *Biofilms in medicine, industry and environmental technology*, (Lens P, Moran AP, Mahony T, Stoodley P & O'Flaherty V, eds.), p. 308-327. IWA Publishing, UK.

Staudt C, Horn H, Hempel DC & Neu TR (2004) Volumetric measurement of bacterial cells and extracellular polymeric substance glycoconjugates in biofilms. *Biotechnol Bioeng* **88**: 585-592.

Sutherland IW (2001) The biofilm matrix - an immobilized but dynamic microbial environment. *TIM* **9**: 222-227.

Weinbauer MG & Rassoulzadegan F (2003) Are viruses driving microbial diversification and diversity? *Environ Microbiol* **6**: 1-11.

Table 1: *Lectin inhibition test.* Lectin specificity as listed by the manufacturer. The specific sugars were used at a concentration of 0.1 g mL^{-1} . Lectin abbreviation in parentheses. Alexa Fluor 488 = A-488.

lectin from	label	carbohydrate-binding specificity
<i>Aleuria aurantia</i> (AAL)	FITC	Fucose
<i>Canavalia ensiformis</i> (ConA)	FITC	Glucose, Mannose
<i>Erythrina cristagalli</i> (ECA)	FITC	Galactose, Lactose
<i>Glycine max</i> (SBA)	FITC	Galactose, N-acetyl-D-galactosamine
<i>Homarus americanus</i> (HMA)	A-488	N-acetylneuraminic acid, N-acetyl-D-galactosamine
<i>Lens culinaris</i> (LcH)	FITC	Glucose, Mannose
<i>Ulex europaeus</i> (UEA-I)	FITC	Fucose

Table 2: Specificity of all tested lectins. Lectin specificity as listed by the manufacturer. Lectins were pooled together according to their sugar specificity. Lectin abbreviation in parentheses.

Carbohydrate-binding specificity	lectin from
Fucose	<i>Aleuria aurantia</i> (AAL), <i>Anguilla anguilla</i> (AAA), <i>Tetragonolobus purpurea</i> (Lotus), <i>Ulex europaeus</i> (UEA-I)
Galactose	<i>Aegopodium podagraria</i> (APP), <i>Agaricus bisporus</i> (ABA), <i>Allomyrina dochotoma</i> (Allo A), <i>Arachis hypogaea</i> (PNA), <i>Artocarpus integrifolia</i> (Jacalin), <i>Colchicum autumnale</i> (Ca), <i>Cytisus scoparius</i> (CSA), <i>Erythrina cristagalli</i> (ECA), <i>Glechoma hederacea</i> (GHA), <i>Glycine max</i> (SBA), <i>Griffonia (Bandeiraea) simplicifolia</i> (GS-I, BS-I), <i>Maclura pomifera</i> (MPA), <i>Marasmius oreades agglutinin</i> (MOA), <i>Momordica charantia</i> (MCA), <i>Morniga G</i> (MNA-G), <i>Pseudomonas aeruginosa</i> (PA-I), <i>Psophocarpus tetragonolobus</i> (PTA), <i>Pilota piumosa</i> (PPA), <i>Sambucus nigra</i> (SNA), <i>Sophora japonica</i> (SJA), <i>Trichosanthes kirilowii</i> (TKA), <i>Tulipa sp.</i> (TL), <i>Vigna radiata</i> (VRA), <i>Viscum album</i> (VAA), <i>Wisteria floribunda</i> (WFA)
Glucose	<i>Canavalia ensiformis</i> (ConA), <i>Dioclea grandiflora</i> (DGL), <i>Lens culinaris</i> (LcH), <i>Vicia faba</i> (VFA)
Lactose	<i>Aegopodium podagraria</i> (APP), <i>Arachis hypogaea</i> (PNA), <i>Bryonia dioica</i> (BDA), <i>Colchicum autumnale</i> (Ca), <i>Cytisus scoparius</i> (CSA), <i>Erythrina cristagalli</i> (ECA), <i>Maackia amurensis</i> (MAA), <i>Psophocarpus tetragonolobus</i> (PTA), <i>Sambucus nigra</i> (SNA), <i>Trichosanthes kirilowii</i> (TKA), <i>Tulipa sp.</i> (TL), <i>Wisteria floribunda</i> (WFA)
Mannose	<i>Canavalia ensiformis</i> (ConA), <i>Dioclea grandiflora</i> (DGL), <i>Galanthus nivalis</i> (GNA), <i>Hippeastrum hybrid</i> (HHA, HHL), <i>Lathyrus odoratus</i> (LDA), <i>Lens culinaris</i> (LcH), <i>Narcissus pseudonarcissus</i> (NPA), <i>Pisum sativum</i> (PSA), <i>Vicia faba</i> (VFA)
Melibiose	<i>Bryonia dioica</i> (BDA), <i>Cytisus scoparius</i> (CSA), <i>Maclura pomifera</i> (MPA)
N-acetyl-D-galactosamine	<i>Aegopodium podagraria</i> (APP), <i>Amaranthus caudatus</i> (ACA), <i>Bauhinia purpurea</i> (BPA), <i>Bryonia dioica</i> (BDA), <i>Caragana arborescens</i> (CAA), <i>Codium fragile</i> (Cod), <i>Colchicum autumnale</i> (Ca), <i>Cytisus scoparius</i>

	(CSA), <i>Dolichos biflorus</i> (DBA), <i>Griffonia (Bandeiraea) simplicifolia</i> (GS-I, BS-I), <i>Erythrina cristagalli</i> (ECA), <i>Glechoma hederacea</i> (GHA), <i>Glycine max</i> (SBA), <i>Helix aspersa</i> (HAA), <i>Helix pomatia</i> (HPA), <i>Homarus americanus</i> (HMA), <i>Iberis amara</i> (IAA), <i>Momordica charantia</i> (MCA), <i>Phaseolus lunatus</i> (LBA), <i>Salvia sclarea</i> (SSA), <i>Sambucus nigra</i> (SNA), <i>Sophora japonica</i> (SJA), <i>Triticum vulgare</i> (WGA), <i>Tulipa sp.</i> (TL), <i>Vicia villosa</i> (VVA), <i>Wisteria floribunda</i> (WFA)
N-acetyl-D-glucosamine	<i>Canavalia ensiformis</i> (ConA), <i>Datura stramonium</i> (DSA), <i>Erythrina corallodendron</i> (Ecora), <i>Helix aspersa</i> (HAA), <i>Laburnum alpinum</i> (LAA I), <i>Lycopersicon esculentum</i> (LEA), <i>Marasmius oreades agglutinin</i> (MOA), <i>Phytolacca americana</i> (PWA), <i>Polyporus squamosus</i> (PSL), <i>Solanum tuberosum</i> (STA), <i>Triticum vulgare</i> (WGA), <i>Urtica dioica</i> (UDA), <i>Vicia faba</i> (VFA)
N-acetylneuraminic acid	<i>Homarus americanus</i> (HMA), <i>Limax flavus</i> (LFA), <i>Limulus polyphemus</i> (LPA)
Sialic acid	<i>Cancer antennarius</i> (CCA), <i>Maackia amurensis</i> (MAA), <i>Triticum vulgare</i> (WGA)
not inhibited by simple sugars	<i>Cicer arietinum</i> (CPA), <i>Euonymus europaeus</i> (EEA), <i>Iberis amara</i> (IAA), <i>Phaseolus vulgaris</i> (PHA-L), <i>Robinia pseudoacacia</i> (RPA), <i>Vicia graminea</i> (VGA)
specificity not determined	<i>Mangifera indica</i> (MIA), <i>Naja naja mosambica</i> (Naja), <i>Persea americana</i> (PAA), <i>Tritrichomonas mobilensis</i> (TML)

Figure legends

Figure 1: Confocal laser scanning micrographs of aquatic aggregates. Reflection imaging (mineral compounds, inorganic matrix, cellular reflection) as well as autofluorescence of phototrophic organisms (algae) from the Danube River and the Elbe River sampled in summer. The images are presented as maximum intensity projections. Color allocation: reflection signal = white, autofluorescence of algae = blue.

Figure 2: Lectin inhibition test. Control experiment with the lectin from *Aleuria aurantia* (AAL) labeled with the fluorochrome Alexa Fluor 488 (conc. 0.1 g mL^{-1}) and its target carbohydrate L-Fucose (conc. 0.1 g mL^{-1}). Lectin inhibition starting at a high carbohydrate concentration to a dilution of 1:40,000. Aggregates from the Elbe River were analyzed.

Figure 3: Example of lectin-binding analysis with *Ulex europaeus* (UEA-I) purchased from different companies. Color allocation: reflection signal = white, autofluorescence of algae = blue, lectin = green. Alexa fluor 488 = A-488. Length of calibration bar is $20 \text{ }\mu\text{m}$.

Figure 4: Examples of lectin-binding analyses demonstrating similar binding patterns to aggregates from the Danube and Elbe Rivers. Images are presented as maximum intensity projections. Numbers indicate the ratio lectin signals to reflection signals. Lectin abbreviation in parentheses. Color allocation: reflection signal = white, autofluorescence of algae = blue, lectin = green. Alexa fluor 488 = A-488. Length of calibration bar is $20 \text{ }\mu\text{m}$.

Figure 5: Examples of lectin-binding analyses demonstrating the different binding patterns to aggregates from the Danube and Elbe Rivers at the same season. Images are presented as maximum intensity projections. Numbers indicate the ratio lectin signals to reflection signals. Lectin abbreviation in parentheses. Color allocation: reflection signal = white, autofluorescence of algae = blue, lectin = green. Alexa fluor 488 = A-488. Length of calibration bar is $20 \text{ }\mu\text{m}$.

Figure 6: Examples of lectin-binding analyses demonstrating the different binding patterns to aggregates from the Danube and Elbe Rivers at different seasons. Images are presented as maximum intensity projections. Numbers indicate the ratio lectin signals to reflection signals. Lectin abbreviation in parentheses. Color allocation: reflection signal = white, autofluorescence of algae = blue, lectin = green. Length of calibration bar is $20 \text{ }\mu\text{m}$.

Figure 7: Comparison of the lectin to reflection ratio of the Danube and Elbe Rivers in fall (a) and summer (b). Variations of the specific glycoconjugates were compared in the Danube (c) and Elbe (d) between seasons. Lectins were pooled according to their sugar specificity. Data are presented as box plots. The boundary of the box closest to zero indicates the 25th percentile, a line within the box marks the median, and the boundary of the box farthest from zero indicates the 75th percentile. Error bars above and below the box indicate the 90th and 10th percentiles. A minimum number of data points are needed to compute each set of percentiles. At least three points are required to compute the 25th and 75th percentiles, and at least nine points are required for the 10th and 90th percentiles. Therefore, specific sugars with less than three data points are not included.

NeuraminicNAc = N-acetylneuraminic acid, GalNAc = N-acetylgalactosamine, GlcNAc = N-acetylglucosamine; for significant differences, two asterisks indicate** = $p < 0.01$, one asterisk indicates* = $0.05 < p \leq 0.01$.

Figure 8: Average volumes of the specific glycoconjugate of aggregates from the Danube River stained with the lectin from *Aleuria aurantia* (AAL) and the lectin from *Phaseolus vulgaris* (PHA-E) during the four seasons. Samples were taken in spring (05/03/2005), summer (07/20/2005), fall (10/13/2005) and winter (01/08/2006). In spring 20, summer 30, fall 20 and winter 23 aggregates were stained with each lectin and analyzed at each sampling day. Error bars indicate the standard error.

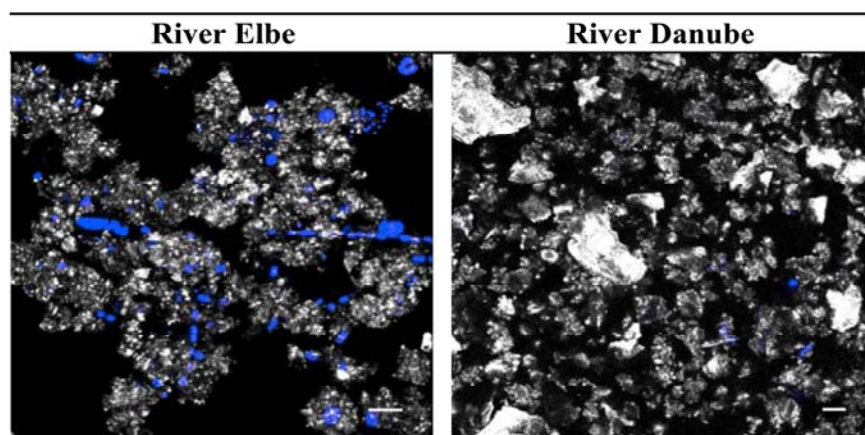


Figure 1

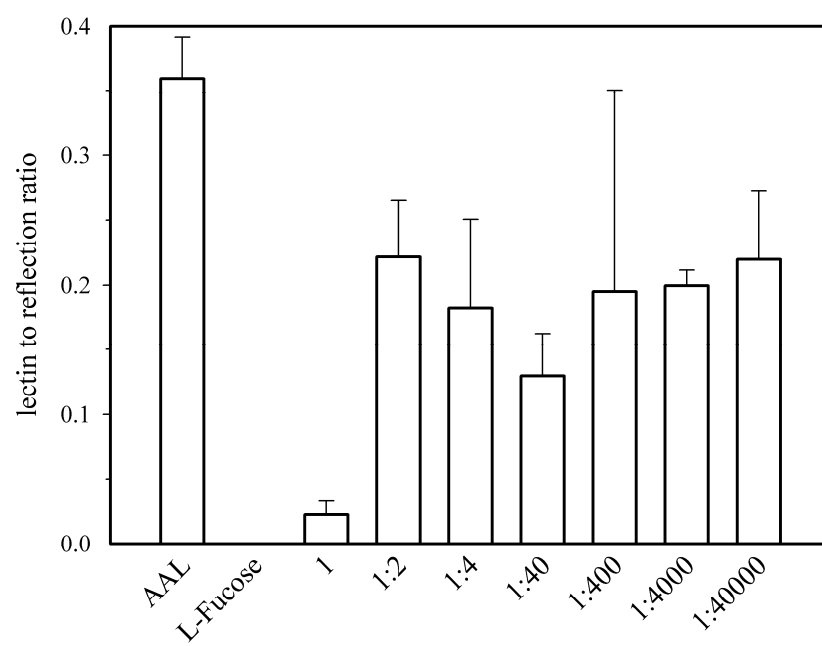


Figure 2

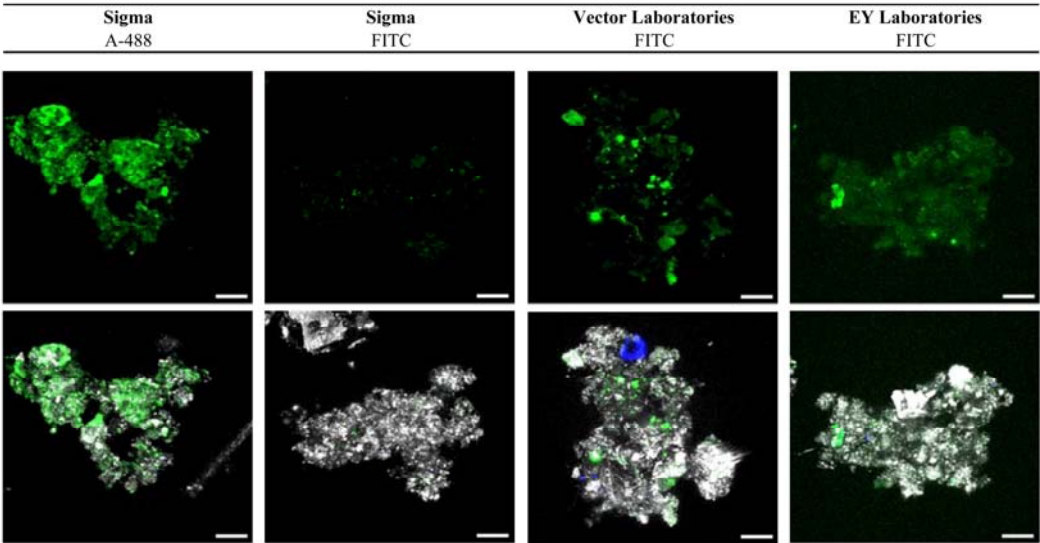


Figure 3

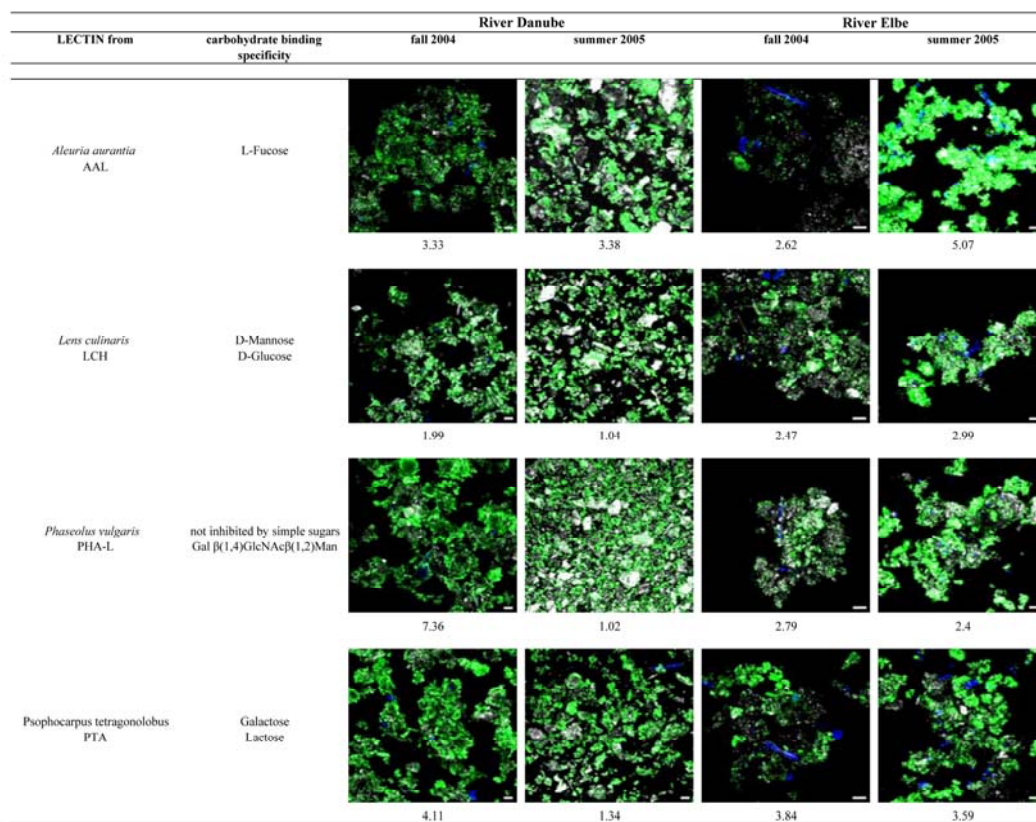


Figure 4

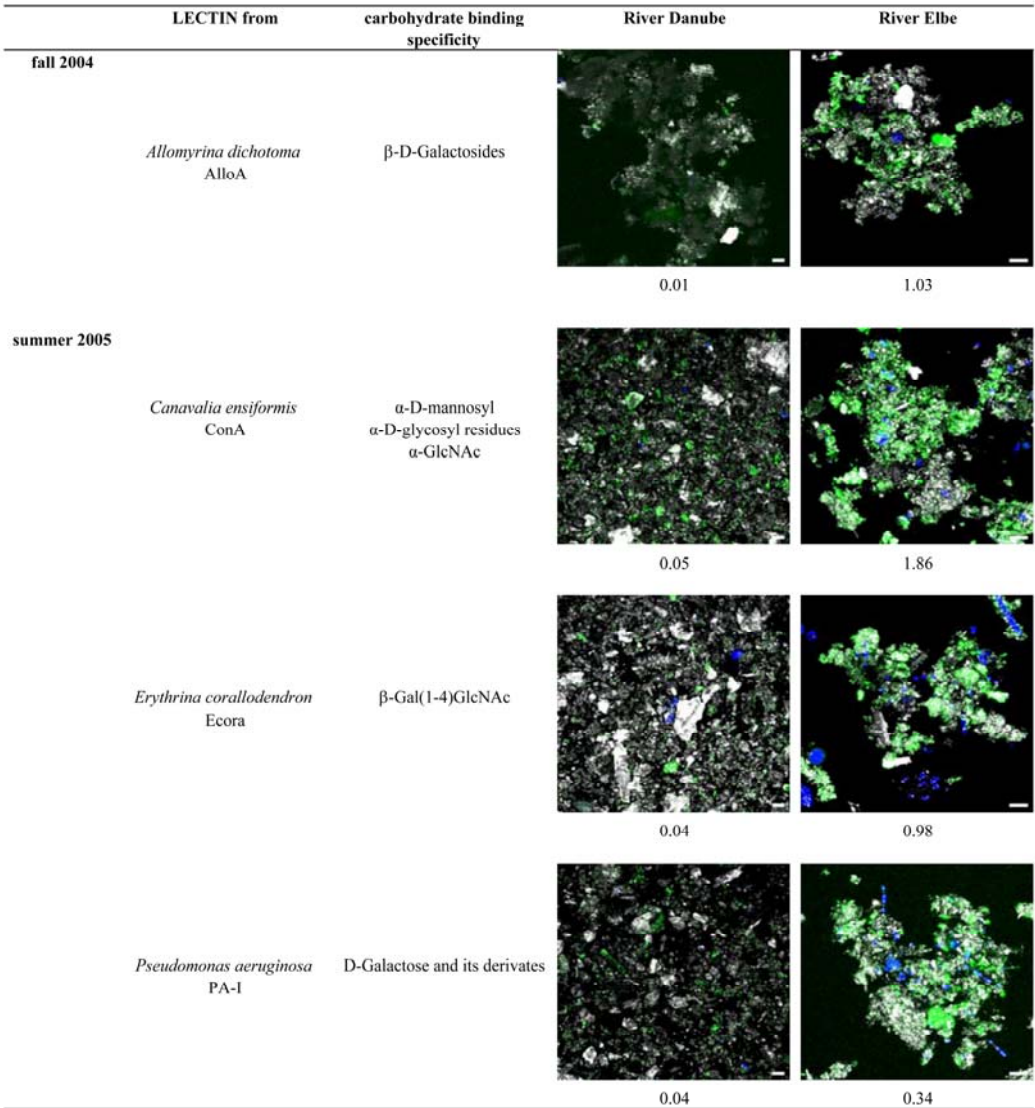


Figure 5

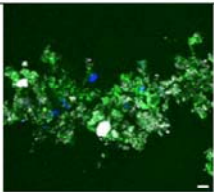
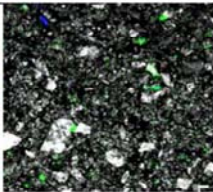
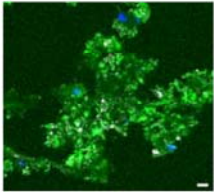
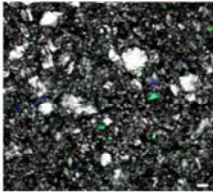
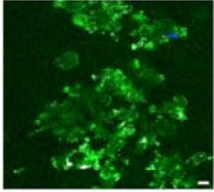
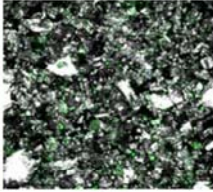
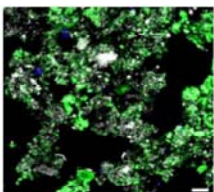
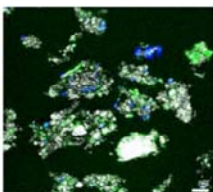
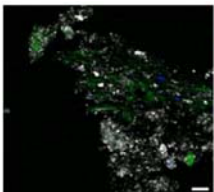
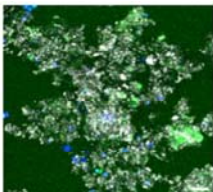
	LECTIN from	carbohydrate binding specificity	fall 2004	summer 2005
River Danube	<i>Dolichos biflorus</i> DBA	terminal non-reducing α -N-acetyl-D-galactosamine	 0.22	 0.01
	<i>Narcissus pseudonarcissus</i> NPA	Mannose	 0.33	 0.00
	<i>Ulex europaeus</i> UEA-I	α -L-Fucose	 0.44	 0.01
River Elbe	<i>Tetragonolobus purpurea</i> Lotus	α -L-Fucose	 2.03	 0.15
	<i>Vigna radiata</i> VRA	α -D-Galactose	 0.03	 0.06

Figure 6

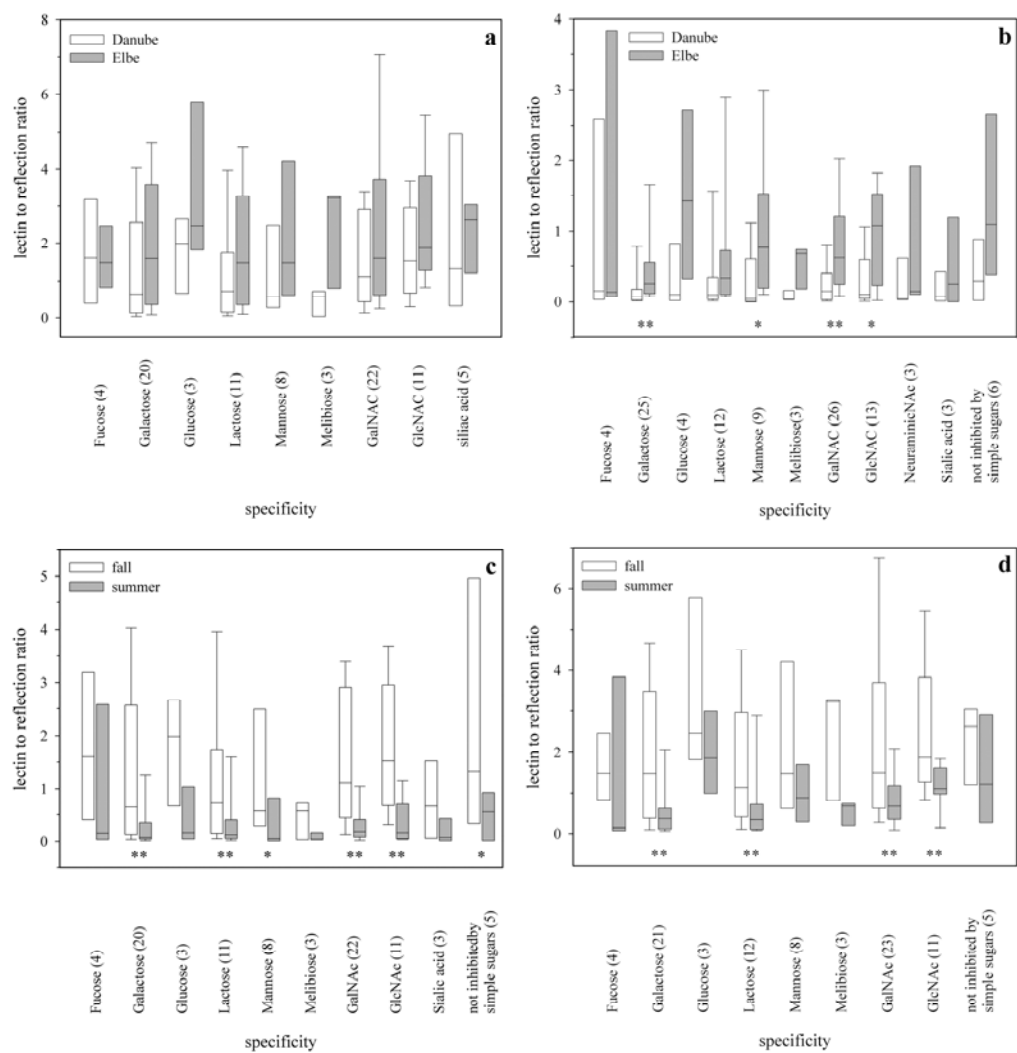


Figure 7

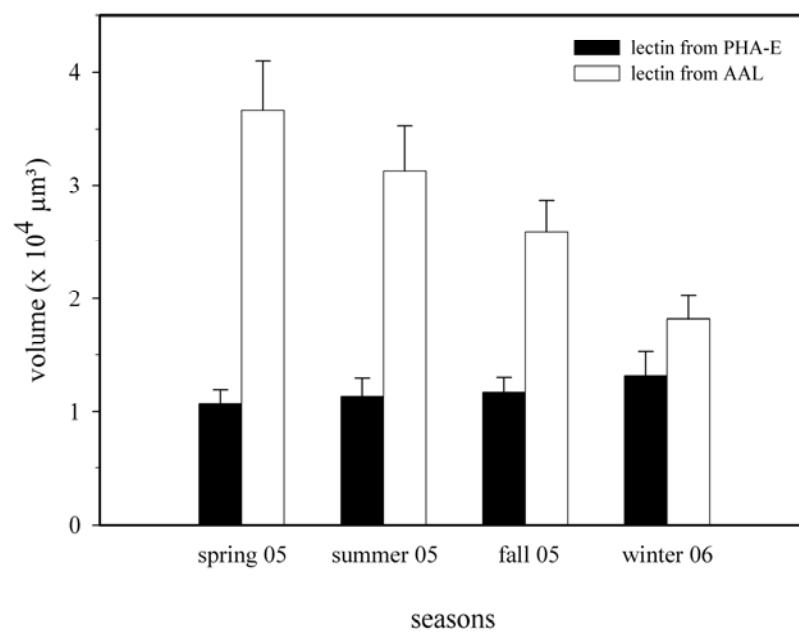


Figure 8

Chapter 2

The Potential of Confocal Laser Scanning Microscopy in Combination with Statistical and Image Analysis to Investigate Volume, Structure and Composition of Riverine Aggregates

Birgit Luef, Thomas R. Neu, Irene Zweimüller, Peter Peduzzi
(submitted to Limnology and Oceanography)

Abstract

Floating riverine aggregates are composed of a complex mixture of inorganic and organic components from the respective aquatic habitat. Their architecture and integrity is supplemented by the presence of extracellular polymeric substances (EPS) of microbial origin. They are also a habitat for virus-like particles, bacteria, fungi, algae and protozoa.

In this study we present different confocal laser scanning microscopy strategies to examine aggregates collected from the Danube and Elbe Rivers. In order to collect multiple information, various approaches were necessary. Small aggregates were examined directly. When analyzing large and dense aggregates, limitations of the technique were overcome by cryo-sectioning and post-staining of the samples. The staining procedure included positive staining (specific glycoconjugates, cellular nucleic acid signals) as well as negative staining (aggregate volume) and multi-channel recording. Data sets of cellular nucleic acid signals (CNAS) and the structure of aggregates were visualized and quantified using digital image analysis. The Danube and Elbe Rivers differed in their aggregate composition and in the relative contribution of EPS and CNAS volume to the aggregate volume; these contributions also changed over time. We report different spatial patterns of CNAS inside riverine aggregates, depending on aggregate size and season. The spatial structure of CNAS inside riverine aggregates was more complex in the Elbe than in the Danube. Based on our samples, we discuss the strengths and challenges involved when scanning and quantifying riverine aggregates.

Introduction

In rivers, primary particles are frequently and perhaps characteristically transported as larger flocculated aggregates. They are structurally very stable because they are exposed to a constant shear force resulting in relatively small aggregates compared to aggregates in lakes and marine systems (Simon et al., 2002; Zimmermann-Timm, 2002). Abiotic mechanisms such as physical coagulation, collision frequency and stickiness are involved in particle aggregation (Droppo et al., 2005). These aggregates, which are generally regarded as mobile biofilms, can be very heterogeneous in their composition. Up to 97% of the biofilm matrix is actually water (Sutherland, 2001). Apart from water, biofilms may consist of dissolved, colloidal and particulate materials of varying size and composition (Droppo et al., 2005). They are composed of a complex mixture of components including inorganic (minerals), living organic (bacteria, fungi, algae, protozoa and viruses) and non-living organic (extracellular polymeric substances (EPS), allochthonous and autochthonous detritus, lignins,

tannins, etc.) material from the respective aquatic habitat and its terrestrial environment (e.g. Simon et al., 2002). Cellular material within a biofilm can vary greatly. Measurements of organic carbon contents suggest that cellular material represents 2-15 % of the biofilm (Sutherland, 2001). Up to 95 % of the biofilm is composed of EPS (Lawrence et al., 1991; Skillman et al., 1999; Flemming and Wingender, 2003). The actual structure of the biofilm matrix varies greatly depending on the microbial cells present, their physiological status, the nutrients available and the prevailing physical conditions (Sutherland, 2001).

Knowledge about the structure and the function of aggregates, both in environmental and engineered systems, is very important (Droppo et al., 2005). In engineered systems such as wastewater treatment plants, understanding flocculation can help to manage that process. In environmental systems, such structure-function relationships can provide information for modelling ecological processes. Numerous methods are available to help characterize aggregate properties. Microscopic as well as photographic techniques have been used to analyze aggregate structure. In recent years, confocal laser scanning microscopy (CLSM) data sets allow the visualization and quantification of three-dimensional (3-D) structures (Holloway and Cowen, 1997; Neu and Lawrence, 1999; Staudt et al., 2004; Zippel and Neu, 2005; Luef et al., submitted-a; Luef et al., submitted-b).

In this study, we analyzed aggregates from the Danube and Elbe Rivers by collecting reflection, nucleic acid, glycoconjugate and negative stain signals using CLSM. Although most of the detected nucleic acid signals derive from bacteria, we refer to them as cellular nucleic acid signals including potential virus signals (CNAS; Luef et al., submitted-a). Nucleic acid signals can potentially also be obtained from fungi, algae and protozoa, but the detection of extracellular DNA can be excluded due to its type of appearance (Böckelmann et al., 2006). Data sets of EPS, CNAS and aggregate structure were visualized and quantified by using digital image analysis. Based on our samples, we discuss the strengths and challenges in scanning and quantifying riverine aggregates using CLSM.

Material and Methods

Study sites and sampling

The Danube River was sampled at Wildungsmauer (Austria), river kilometer 1894, located in the National Park area on the southern bank of the river. Samples of the Elbe River were collected on the left downstream bank at river kilometer 318, near Magdeburg (Germany). Water samples from the Danube River were taken in spring (05/03/2005), summer (07/20/2005), fall (10/13/2005) and winter (01/08/2006). From the Elbe River, water samples

were taken in spring (03/21/2005), summer (08/08/2005), fall (11/03/2005) and winter (01/23/2006). Sampling depth was approximately 30 cm.

Riverine aggregates were sampled in 1L plexiglass bottles. The samples were always kept at +4 °C until analysis, which was completed within 24 h (Bura et al., 1998). With an inverted 10 ml glass pipette (Gibbs and Konwar, 1982), the aggregates were carefully transferred to Eppendorf tubes, where staining was performed.

Staining procedure

To stain the major parts of the matrix material of the aggregates, lectins from *Aleuria aurantia* (AAL; Vector Laboratories, Burlingame, California, USA) labeled with the fluorochrome Cy5 (Amersham, Buckinghamshire, UK) or *Phaseolus vulgaris* (PHA-E; Sigma Aldrich, St. Louis, Missouri, USA), labeled with fluorochrome Alexa Fluor 633 (A-633; Invitrogen, Eugene, Oregon, USA), were employed in parallel to stain the lectin-specific EPS (Neu, 2000; Neu et al., 2001; Staudt et al., 2003). The lectins were self-labeled according to the data sheet of the supplier.

The glycoconjugates of EPS were stained with one of the lectins as described previously (Neu, 2000). Briefly, for lectin staining, the lectins were diluted with deionized water to a final concentration of 0.1 g mL⁻¹ protein. 100 µl of this solution were added to each sample and incubated for 20 min in the dark. The aggregates were then carefully washed 3 times with tap water to remove unbound lectins and were never allowed to dry in the air.

After staining the lectin-specific EPS compounds, SYBR Green I (concentration of 1 µl mL⁻¹ deionized water; Invitrogen) was directly applied to the aggregates and incubated for 5 min to detect aggregate-associated CNAS on/in the fully hydrated aggregates. SYBR Green I is a nucleic-acid-specific stain widely used to detect prokaryotes and virus particles in aquatic environments (Noble and Fuhrman, 1998).

The dimensions and volumes of the aggregates were determined by a negative staining procedure. Lawrence et al. (1994) demonstrated the use of fluorescein and size-fractionated fluor-conjugated dextrans in conjunction with scanning confocal laser microscopy to directly monitor and determine diffusion coefficients within biofilms. We took advantage of this method to determine aggregate volumes. Different probes and fluorochrome-staining-solutions such as dextrans (Invitrogen), rhodamines (Invitrogen), fluorescein (Sigma Aldrich, St. Louis, Missouri, USA), Cy5 (Amersham) and Alexa Fluor 568 (A-568, Invitrogen) were tested. These stains and probes are characterized by their chemical properties and molecular weights and were used at different concentrations. Probes and fluorochrome-staining-

solutions such as dextrans, rhodamines, fluorescein and Cy5 were not appropriate for this analysis, probably due to their molecular weight or their binding properties (data not shown). Negative staining with A-568 allowed calculating the aggregate volumes. Hence, to analyze our samples, we stained the water phase – the volume of the scanned box which was not occupied by the aggregate – with the fluorochrome A-568 ($C_{37}H_{33}N_3O_{13}S_2$, MW = 791.80). The positive stained samples were carefully transferred into cover well imaging chambers (0.5 mm, Invitrogen), covered with 150 μ l Alexa Fluor 568 and immediately examined by CLSM.

Confocal Laser Scanning Microscopy

Aggregates were analyzed by CLSM using a Leica TCS SP1, controlled by the LCS Version 2.61 Build 1537 174192 (Leica, Heidelberg, Germany), equipped with an upright microscope. Images were collected with a 63x 0.9 NA water lens.

The aggregate structure was analyzed by CLSM using visible lasers (488 nm, 568 nm and 633 nm). Emission signals were detected from 480-500 nm (inorganic, mineral compounds; reflection signals), 500-550 nm (DNA signals, SYBR Green I), 570-625 nm (negative stain signals, A-568) and from 650-750 nm (lectin signals, fluorochrome Cy5 or A-633).

Optical sections of aggregates were taken every 1 μ m.

Cryo-sections

Conventional analyses of larger riverine aggregates (traditional staining procedure and scanning with a view from the top) were limited by laser penetration and diffusion of staining solutions. To obtain information on the distribution of lectin-specific glycoconjugates and CNAS inside riverine aggregates, cryo-sections were performed (Huang et al., 1996; Zippel and Neu, 2005). Aggregates from the Danube and Elbe were embedded in liquid cryostat medium (Neg-50 by Richard-Allan Scientific), frozen at -26 °C and physically sectioned (50 μ m) with a cryo-microtome (Leica CM3050S). Thereafter, sections were stained with lectins and SYBR Green I (see above), embedded in water, and covered with a coverslip before analysis by CLSM (see above).

Quantification & visualization

Quantification of LSM data sets of the whole aggregate (optically sectioned material) and cryo-sections was done with the freely available software Image J (<http://rsb.info.nih.gov/ij/>), developed in Java (Staudt et al., 2004). To analyze cryo-sections with the software Image J, special plug-ins were developed. After setting thresholds to avoid counting background

pixels, each cryo-section was divided into three sectors. Within each sector, one subsample extending across the whole dimension of the aggregate's cryo-section was chosen. The dimension of the aggregate was given by the lectin-specific glycoconjugate. The software cropped each subsample, rotated it backwards (turned around the x-axis), divided each into 1 μm slices, and counted the pixels of the CNAS.

The IDL-based program Confocal Analysis (ConAn) version 1.31 was also applied. The software ConAn was developed by BioCom for the Helmholtz Centre for Environmental Research – UFZ in Magdeburg. This software analyzes complex 3-D data sets, including visualization, quantification and calculation of structural parameters. This program can handle multi-channel data and co-localization of data; different structural parameters can be calculated.

For each channel and data set, the threshold was set manually. Due to the very heterogeneous composition of the aggregates, automatic batch processing could not be applied.

To visualize 3-D data sets, Imaris 4.2 (Bitplane AG, Zurich, Switzerland) and Amira 3.0 (TGS, San Diego, California) were used. For each channel and image, thresholds were set manually. Adobe Photoshop CS2 was used to insert calibration bars into the images.

Calculations and statistics

For statistical analysis, the software program SPSS 12.0 for Windows (SPSS, Chicago, Illinois, USA) was used. The criteria of normal distribution (K-S-test) and homogeneity of variances (Levene-test) were not met, so seasonal differences in the data were determined with a non-parametric test (Friedman test). The Tamhane post-hoc test (which does not require homogeneity of variances in the data) was used to determine significant differences between seasons. Differences between the two rivers were tested using the Mann-Whitney-U-test.

To determine the distribution of CNAS within riverine aggregates, cryo-sections were analyzed. Only those subsamples that included a minimum of 10 slices containing CNAS were included in the analysis; this is because fluorescence signals of the same bacterium were found in up to 10 slices. Two approaches were used: the first to detect abundance differences between the subsamples of the three sectors, the second to characterize the internal structure of the cryo-sections using a finer spatial resolution.

1) The mean abundances of CNAS within each subsample were calculated. Then, differences between the two outer subsamples to the middle subsample were computed to detect potential spatial accumulation of cells. The averages of these two differences were tested against zero

using a Wilcoxon test. Mean differences between abundances will only be significantly different from zero if CNAS are more abundant either on the two outer subsamples or in the middle subsample of the cryo-section.

2) To test whether CNAS occurred in accumulations anywhere within the cryo-sections of the aggregates and to test for regularity in distributions of CNAS within the cryo-sections, we calculated the spatial autocorrelation (Legendre and Legendre, 1998), which is a mathematical tool for finding repeating patterns in samples taken in regular spatial intervals. Autocorrelations are the correlations between values of the same sample series separated by so-called lags. The lag numbers indicate the distance between the consecutive values used to calculate the autocorrelation, e.g. autocorrelation with lag 1 is the correlation coefficient between the 1st and the 2nd, the 2nd and the 3rd up to the $n^{\text{th}}-1$ and the n^{th} value. Consequently, autocorrelations with low lag numbers describe the similarities between neighboring values, whereas high autocorrelation for higher lag numbers indicate a spatial regularity on a larger distance scale. Since the total number of slices per subsample was variable, autocorrelations for lags 1 to one fourth of the total number of slices were calculated. If the autocorrelation values were higher than twice the standard error for positive autocorrelations, they were considered significant. The highest autocorrelations always occurred at lag 1 and then typically decreased monotonously. The first local maximum was defined as the number of lags with significant positive autocorrelations, starting from lag 1 until the significance level was reached or the autocorrelations started to increase again. This first maximum provides information on the width of the CNAS layers. The width of the layers in μm can be calculated from the number of lags of the first local maximum + 1. Local secondary maxima were only counted if 1) positive autocorrelations were higher than twice the standard error and 2) the difference between local maximum and presiding minimum was higher than 0.05 autocorrelation. These secondary maxima indicate a regular spatial distribution of CNAS within the cryo-section, pointing to the repeating occurrence of CNAS-layers (whose width can be estimated from the first maximum). For example, if a secondary maximum occurs at lag 20, most CNAS-layers will be placed approx. 20 μm apart. To characterize the position of secondary maxima, we used the lag numbers at which the respective secondary maxima occurred. For further calculations, we defined the the following variables: layer width (calculated from the first local maximum as described above), spatial structure (the number of secondary local maxima), diameter of cryo-section (the total number of slices of each subsample), and percentage of CNAS (the percentage of slices that harbored CNAS within each subsample).

The structural parameters derived from the autocorrelation analysis (layer width and spatial structure) may not be independent from aggregate size and the overall occurrence of CNAS within it. Hence, two linear regressions were carried out to define this relationship, with the diameter of cryo-section and percentage of CNAS as independent variables and layer width and spatial structure as dependent variables. The residuals from these two regressions gave estimates for layer width and spatial structure without the effect of aggregate size and percentage of CNAS. As mentioned before, each cryo-section was divided into three sectors and, within each sector, one random subsample was chosen. For these 3 groups of subsamples the regressions described above were calculated separately to 1) determine whether the position within the aggregate had a strong effect on the regressions and 2) to avoid having strongly dependent samples within one regression analysis. The residuals of these regressions were used as dependent variables in a second set of regressions, where season and river (dummy-coded) were defined as the independent variables. The objective was to determine whether seasonal or between-river differences in the spatial structure could be detected when the effect of aggregate size and percentage of CNAS was factored out.

Results

Abiotic and biotic parameters characterizing the two rivers Danube and Elbe

The Danube River and Elbe River were characterized by an annual mean discharge of 1818 m³s⁻¹ and 469 m³s⁻¹, respectively, during the sampling period. In the Elbe, a flood occurred in late March/early April. In the Danube, summer sampling occurred during a flood event. The measured chemical characteristics, particle abundance, seston parameters and chlorophyll-*a* values for both rivers during the four seasons are summarized in Table 1. On average, nutrients, seston parameters, particle abundance and chlorophyll-*a* values were higher in the Elbe than in the Danube.

Scanning aggregates under in situ conditions

Aggregates were examined after a conventional staining procedure and scanned by simple view from the top. The aggregates incorporated a high amount of non-cellular matter such as sand, clay and detritus. This limited diffusion of the staining solution, laser penetration and detection of emission signals in our samples. This approach enabled us to properly investigate only the outer 20 µm of the aggregates (Fig. 1).

Distribution of aggregates' components based on the outer 20 μm *1) Specific glycoconjugate composition of aggregates*

Firstly, the aggregate volume was calculated by subtracting the negative stain volume from the scanned box volume. In some cases the fluorochrome A-568 penetrated into the aggregate matrix and revealed the existence of channels and pores within aggregates. Therefore, colocalization of the specific glycoconjugate and the negative stain was used to calculate the aggregate volume. Colocalization is a tool for quantifying the degree of association or co-distribution of labeled structures between any two channels in an image (Pawley, 2006). In the first step of the calculation we subtracted the volume of colocalized EPS and negative stain from the negative stain; in the second step we subtracted this term from the scanned box volume. During the four seasons in the Elbe River, on average 59.95 % (S.E. 1.68 %) and 36.49 % (S.E. 2.69) in the Danube River of the aggregate volume were labeled with lectins (Fig. 2a). When comparing the relative contribution of the EPS volume to the aggregate volume from both rivers during the four seasons, significant differences occurred in spring, summer and fall (Mann-Whitney-U-test, $p < 0.001$, 0.034, < 0.001 , $n = 53$, 49 and 57 for spring, summer and fall, respectively). No significant differences were found in winter (Mann-Whitney-U-test, $p = 0.318$, $n = 51$).

Comparing the relative contribution of EPS volume to aggregate volume of the Danube (Friedman test, $n = 14$, $p < 0.001$) and the Elbe (Friedman test, $n = 14$, $p = 0.003$) on a seasonal basis, significant differences occurred in both rivers. In the Danube, spring values were significantly lower than in summer (Tamhane, $p < 0.001$), fall (Tamhane, $p < 0.001$) and winter (Tamhane, $p < 0.001$). Furthermore, the relative contribution of the EPS volume in summer was also significantly higher than in fall (Tamhane, $p < 0.001$). During fall in the Elbe, this relative contribution was significantly higher compared to spring (Tamhane, $p = 0.008$), summer (Tamhane, $p < 0.001$) and winter (Tamhane, $p < 0.001$).

2) CNAS associated with aggregates

On average, the relative contribution of CNAS volume to aggregate volume was higher in the Elbe (mean 1.53 %, S.E. 0.23) versus the Danube (mean 1.00 %, S.E. 0.30) during the four seasons. When comparing these values from both rivers during the four seasons, significant differences occurred in spring, fall and winter (Mann-Whitney-U-test, $p < 0.001$, 0.007, 0.006, $n = 52$, 57 and 51 for spring, fall and winter, respectively), but no significant differences occurred in summer (Mann-Whitney-U-test, $p = 0.20$, $n = 49$) (Fig. 2b).

When testing for seasonality in this relative contribution within the rivers, both the Danube (Friedman test, $n = 13$, $p < 0.001$) and the Elbe (Friedman test, $n = 26$, $p < 0.001$) exhibited significant differences. During spring in the Danube, the relative contribution of the CNAS volume was significantly than in fall (Tamhane, $p < 0.001$). In the Elbe, values were significantly lower in spring versus summer (Tamhane, $p = 0.02$), fall (Tamhane, $p = 0.02$) and winter (Tamhane, $p < 0.001$). Furthermore, the relative contribution was also significantly lower in summer than in winter (Tamhane, $p = 0.001$).

Cryo-sections

Cryo-sections in combination with post-staining provide information on the presence and distribution of CNAS and glycoconjugates inside the aggregates (Fig. 3).

Forty-six cryo-sections were analyzed to obtain quantitative information on the CNAS distribution within riverine aggregates. Firstly, we tested whether the subsamples (see methods) differed in their CNAS distribution. No differences were found either in the Danube (Wilcoxon test, $n = 66$, $p = 0.529$) or in the Elbe (Wilcoxon test, $n = 56$, $p = 0.429$) using data from all seasons.

Secondly, we tested whether CNAS exhibited a homogeneous distribution or whether they occur in accumulations within the aggregates. Autocorrelations describe the spatial distribution of CNAS within riverine aggregates. Two examples are given in Figure 4. Figure 4a-c depicts a thick layer width of CNAS (45 μm) and no further significant spatial structure. In comparison, Figure 4d-f depicts a relatively thin layer width (12 μm) and a clear spatial structure. In the Danube, this width averaged 10.38 μm , in the Elbe 9.95 μm (Fig. 5a). On average, the spatial distribution of CNAS was more complex in the Elbe River (Fig. 5b). In the Danube, 42% of the examined subsamples contained at least one secondary maximum; the respective value for the Elbe was 52%. For the Elbe the secondary maxima were positioned over a wider range of lags (highest values: 87 compared to 75 for the Danube), with most values occurring either between 10 and 15 lags or 20 and 25 lags. In the Danube most values occurred either between 10 and 15 lags or 25 and 30 lags.

Furthermore, two sets of linear regressions were carried out with cryo-section diameter and percentage of CNAS as independent variables and layer width and spatial structure as dependent variables (Tab. 2). The three separate regressions for the subsamples gave similar, but not identical results: slopes for each parameter had the same direction and were within the same order of magnitude within one set of regressions. Ten out of the 12 slope values showed

a p-value of < 0.05 . Generally, layer width as well as spatial structure could be significantly predicted by the cryo-section diameter and the CNAS percentage: Increasing diameters of the cryo-sections led to thicker CNAS layers and more spatial structure. Layer width also increased with increasing CNAS percentage, but spatial structure was reduced as this percentage increased. Thus, differences in layer width and spatial structure also reflect differences in aggregate size and colonization.

To make these parameters comparable between aggregates of different diameters, the residuals of these regressions were used for further analysis, specifically as dependent variables in a second set of regressions in which season and river were defined as the independent variables (for details see Tab. 3). In summer the layer widths of CNAS were significantly thinner than predicted by diameter and percentage of CNAS. This effect did not depend on the river, as the identity of the river was not selected as an independent variable. When the differences in aggregate size were factored out, the spatial structure was more complex in the Elbe than in the Danube River, and spatial complexity was also higher in summer and spring compared to the other seasons, as indicated by the slopes of the regressions.

Discussion

We used visible laser light of various wavelengths in combination with fluorescently labeled probes to describe EPS and CNAS abundance and the structure of floating riverine aggregates by CLSM. Due to their size and fragility, aggregates were quite difficult to examine under *in situ* conditions. Nevertheless, CLSM allows analyzing properties of fully hydrated aggregates without fixation and dehydration.

Handling, staining and analyzing aggregates

Within 30 minutes after sampling, aggregates settle in the sampling bottles and co-aggregation of smaller aggregates into larger and loosely associated aggregates may occur (Droppo et al., 2005). Droppo et al. (1996) developed a nondestructive technique to stabilize aggregates in low-melting agarose. However, lectin-binding-analyses after aggregate stabilization in agarose did not work due to interference of the lectin with the agarose (B.L., personal observation).

Bura et al. (1998) demonstrated that the loss of EPS constituents in activated sludge flocs occurred after 24 h at 4 °C. DNA and acidic polysaccharides were the most labile

components. The analysis of the EPS composition therefore requires fresh samples. All of our samples were analyzed within 24 h.

Although aggregates are exposed to variable physical stress in their natural environments, care must be taken to maintain the structural integrity of riverine aggregates. While mounting and staining probably do not alter aggregates significantly, fixation, freezing and dehydration may damage their native structure (Droppo et al., 2005). So far, transmission electron microscopy was the method of choice to investigate the microstructures of aquatic aggregates (e.g. Leppard et al., 1996). This approach offers high resolution but usually requires fixation and/or dehydration in order to examine the 3-D structure. Recently, CLSM has become a key instrument for investigating fully hydrated biofilms and aquatic aggregates (e.g. Lawrence et al., 1991; Neu, 2000; Battin et al., 2003; Luef et al., submitted-a; Luef et al., submitted-b). For *in situ* analysis of hydrated aggregates, a range of fluorescence stains – specific for polysaccharides, nucleic acids, proteins and lipids – are available. Lectins are a useful probe to examine the 3-D distribution of glycoconjugates in fully hydrated biofilms (Neu and Lawrence, 1999). Luef et al. (submitted-b) showed that binding of lectins to river snow proves the presence of specific target monosaccharides in the aggregates' EPS matrix. Accordingly, lectin binding analysis may be useful to follow the production of lectin-specific glycoconjugates over time. Knowledge about the internal distribution of polymeric substances (Fig. 2a) and CNAS (Fig. 2b) will clearly help understand the relationship of structure, function and spatial dynamics in aquatic aggregates.

Quantification of CLSM data sets

After applying CLSM, the data can be visualized and quantified. Such quantification, however, remains difficult because the composition of environmental samples may be highly complex. Ample software is available for quantifying CLSM data sets (Heydorn et al., 2000; Yang et al., 2000; Daims et al., 2006), although such complex images remain difficult to interpret and their meaning is often inconclusive (Beyenal et al., 2004). The capabilities of such software have two aspects: on the one hand, image quality can be improved dramatically. On the other hand, they can also generate artifacts. Image quality is critical and depends on the quality of the input data.

In this study we applied the algorithm colocalization, which is a very powerful tool for determining the degree of associated labeled structures. Obtaining reliable data requires considering that: 1) the signal intensity between the two channels has to be relatively balanced, 2) the used fluorochromes should have a wide separation between their emission

spectra, 3) background noise, blur, autofluorescence, non-specific labeling, reflections and bleed-through have a major impact on colocalization quantification, 4) setting thresholds to eliminate noise and background in the two channels is a critical step and 5) optical misalignment of the instrument also impacts the result (Pawley, 2006).

Often a deconvolution algorithm is applied to 3-D sets. It eliminates blur and noise and increases contrast and axial resolution to restore image clarity (Pawley, 2006). We did not apply deconvolution to our 3-D data sets, although small objects such as bacteria become more distorted than bigger objects. Deconvolution is a mathematical transformation. It can encompass many different methods such as blind deconvolution, nearest neighbor, maximum likelihood or Wiener filtering. Note, however, that such procedures are critically dependent on the assumptions of linearity and shift invariance. In many biological specimens, for example, fluorescence light is not linear due to strong absorption effects. Furthermore, the point spread function often changes with depth within a biological sample. Deconvolution can be easily applied to perfect shapes such as spheres, but the shapes of e.g. bacteria are not known. Reasonable and reliable solutions using deconvolution require non-linear methods, which are more complex, time consuming to compute and usually require multiple computation rounds, whereby uncertainties remain.

Visualization, calculation and quantification

Aggregate size is a widely used parameter for characterizing aggregates. Generally, their sizes are observed in 2 dimensions and there is no simple way to estimate exact size and shape. In the literature the equivalent spherical diameter (ESD) is often used to estimate aggregate size (Peduzzi and Weinbauer, 1993; Berger et al., 1996; Long and Azam, 1996; Luef et al., 2007). However, aggregates are 3-D, irregularly shaped and have pores (Droppo et al., 2005). Many methods such as coulter counter, photographic techniques or laser-based sizing instruments have been developed for size measurements (e.g. (Kranck and Milligan, 1980; Hofmann, 2004). Staudt et al. (2004) showed that digital image analysis of confocal stacks allows the spatial and temporal binding of different lectins to be quantitatively evaluated.

Our volume determinations may have limitations due to CLSM drawbacks such as scattering properties of aggregates, depth of laser penetration and diffusion properties of staining solutions (Fig. 1 and 3a). Using only one lectin to label the specific glycoconjugate of the aggregate matrix may underestimate actual volume. Lectins might also bind to non-EPS targets or bind non-specifically to the EPS matrix (Luef et al., submitted-b). Nevertheless, the

use of CLSM data sets (including cryo-sectioning and the mathematical model of colocalization) yields superior estimates of aggregate volumes.

Relationship between CNAS and EPS within aggregates

Flemming and Wingender's (2003) review demonstrated that the EPS matrix enables microorganisms to live continuously at high cell densities, to form stable mixed populations, leading to synergistic microconsortia. The EPS matrix constitutes a medium for communication processes between cells because it holds the bacteria close to each other. Such close contact of aggregated cells and the accumulation of DNA in the EPS matrix may facilitate horizontal gene transfer. Furthermore, rapid adaptation of bacteria to changing environmental conditions might not be necessary in a biofilm matrix, which provides a buffer against changing organic nutrients (Sutherland, 2001). Although microbial cells are generally unable to utilize EPS that they have synthesized, heterologous species within the matrix can degrade and utilize them, thus also altering biofilm composition and structure in a dynamic way (Sutherland, 2001). A function frequently attributed to EPS is their general protective effect on biofilm organisms against adverse abiotic and biotic influences such as biocides, including disinfectants and antibiotics from the environment.

Ecological aspects of riverine aggregates

Microbial aggregates in marine systems (Alldredge and Silver, 1988), in freshwater lakes (Grossart and Simon, 1993), and lotic habitats (Böckelmann et al., 2000; Böckelmann et al., 2002; Neu, 2000) represent hot spots of high nutrient concentrations and microbial activity.

In rivers, particulate organic matter is an important energy source for heterotrophic biota. The composition of aggregates varies depending on their origin (soil, rock, riparian vegetation, biofilms, macrophytes, autochthonous algae, etc.) and therefore influences the associated microorganisms (see reviews of Simon et al., 2002 and Zimmermann-Timm, 2002). For example, hydrology apparently influences particle quality, which in turn also affects the abundance and activity of the associated bacteria and viruses (Aspetsberger et al., 2002; Luef et al., 2007; Peduzzi and Luef, 2008). Those aggregates dominated by mineral particles are less densely colonized by bacteria than aggregates consisting of mostly organic compounds (Berger et al., 1996; Zimmermann, 1997; Luef et al., 2007). The Danube and Elbe Rivers appear to harbor different particle qualities (Luef et al., submitted-b). The respective aggregates differ in their glycoconjugate composition, which also changes over time. In our

study, over the annual cycle, the relative contribution of the specific glycoconjugates and associated CNAS to the aggregate volume was on average higher in the Elbe (Fig. 2a and 2b). Moreover, when averaging the four seasons, more chlorophyll-*a*, a higher proportion of particulate organic matter and more ambient nutrients were found in the Elbe than in the Danube (Tab. 1). This supports the observed differences in aggregate composition and structure. Besemer et al. (2005) showed for the Danube that the compositional dynamics of the particle-associated bacterial communities were related to changes in the algal biomass and in concentrations of organic and inorganic nutrients. In the Elbe, the structure and composition of the microbial river snow community showed seasonal dynamics (Böckelmann et al., 2000). The river snow community was characterized by a great bacterial diversity in spring. In summer the typical aggregate features were large amounts of green algae, diatoms and cyanobacteria. In autumn and winter, algae were absent and bacterial abundance increased.

We found different spatial patterns and amounts of CNAS inside riverine aggregates, depending on aggregate size and season (Fig. 4 and 5; Tab. 2 and 3). Aggregation of small particles to large aggregates may benefit microorganisms. Changes in water column conditions may affect microorganisms associated with aggregates less than their free-living counterparts because the former maintain their own microenvironments. Moreover, the aggregate matrix may protect the bacteria from protozoa predation pressure. Concentration gradients of gases (Ploug and Passow, 2007), nutrients (Alldredge, 2000) and microbial activity (Ploug and Grossart, 1999) exist in aggregates. Some studies have focused on anoxic micro-niches inside marine snow aggregates. Reducing micro-zones with sulfide production were found immediately adjacent to oxic zones (Shanks and Reeder, 1993). Experimental results, however, have shown that aggregates are seldom anoxic unless they occur in oxygen minimum zones (Ploug et al., 1997). The oxygen microenvironment of aggregates decreased dramatically when they were sitting on a solid surface compared with when they were sinking (Ploug and Jorgensen, 1999). Thus, the composition and structure of aggregates, chemical gradients and the assemblage of microorganisms create microhabitats inside aggregates.

Summary

The Danube and Elbe Rivers differed in their aggregate composition. Over the annual cycle, the relative contribution of the specific glycoconjugates and associated CNAS to the aggregate volume changed over time. Different spatial patterns of CNAS inside riverine aggregates, depending on aggregate size and season, were found. The spatial structure of

CNAS inside riverine aggregates was more complex in the Elbe than in the Danube. This information underlines the substantial value of visualizing and quantifying CNAS and glycoconjugate distribution in aggregates for understanding the ecology of floating aquatic aggregates. Although analyzing riverine aggregates by CLSM poses a broad range of challenges, these techniques and applications yield a better insight into the relationship of the EPS matrix and microbial organisms in riverine aggregates.

Acknowledgements

We thank the University of Vienna (research fellowship, grant number: F055-B) and the Austrian Science Foundation FWF (grant number P17798 to P.P.) for financial support.

We are grateful for technical help by U. Kuhlicke and for K. Garny's expertise on the computer software for visualization. Thanks are due to M. Baborowski and C. Fesl for measuring particle abundances.

References

- Allredge, A. (2000) Interstitial dissolved organic carbon (DOC) concentrations within sinking marine aggregates and their potential contribution to carbon flux. *Limnol Oceanogr* **45**: 1245-1253.
- Allredge, A.L., and Silver, M.W. (1988) Characteristics, dynamics and significance of marine snow. *Prog Oceanogr* **20**: 41-82.
- Aspetsberger, F., Huber, F., Kargl, S., Scharinger, B., Peduzzi, P., and Hein, T. (2002) Particulate organic matter dynamics in a river floodplain system: impact of hydrological connectivity. *Arch Hydrobiol* **156**: 23-42.
- Battin, T.J., Kaplan, L.A., Newbold, J.D., and Hansen, C.M.E. (2003) Contribution of microbial biofilms to ecosystem processes in stream mesocosms. *Nature* **426**.
- Berger, B., Hoch, B., Kavka, G., and Herndl, G.J. (1996) Bacterial colonization of suspended solids in the River Danube. *Aquat Microb Ecol* **10**: 37-44.
- Besemer, K., Moeseneder, M.M., Arrieta, J.M., Herndl, G.J., and Peduzzi, P. (2005) Complexity of bacterial communities in a river-floodplain system (Danube, Austria). *Appl Environ Microbiol* **71**: 609-620.
- Beyenal, H., Lewandowski, Z., and Harkin, G. (2004) Quantifying biofilm structure: facts and fiction. *Biofouling* **20**: 1-23.
- Böckelmann, U., Manz, W., Neu, T.R., and Szewzyk, U. (2000) Characterization of the microbial community of lotic organic aggregates ("river snow") in the Elbe River of Germany by cultivation and molecular methods. *FEMS Microb Ecol* **33**: 157-170.
- Böckelmann, U., Manz, W., Neu, T.R., and Szewzyk, U. (2002) Investigation of lotic microbial aggregates by a combined technique of fluorescent *in situ* hybridization and lectin-binding-analysis. *J Microbiol Methods* **49**: 75-87.
- Böckelmann, U., Janke, A., Kuhn, R., Neu, T., Wecke, J., Lawrence, J., and Szewzyk, U. (2006) Bacterial extracellular DNA forming a defined network-like structure. *FEMS Microbiol Lett* **262**: 31-38.
- Bura, R., Cheung, M., Liao, B., Finlayson, J., Lee, B.C., Droppo, I.G. et al. (1998) Composition of extracellular polymeric substances in the activated sludge floc matrix. *Water Sci & Technol* **37**: 325-333.
- Daims, H., Lückner, S., and Wagner, M. (2006) *daime*, a novel image analysis program for microbial ecology and biofilm research. *Environ Microbiol* **8**: 200-213.
- Droppo, I., Flannigan, D., Leppard, G., Jascot, C., and Liss, S. (1996) Floc stabilization for multiple microscopic techniques. *Appl Environ Microbiol* **62**: 3508-3515.

- Droppo, I.G., Leppard, G.G., Liss, S.N., and Milligan, T.G. (2005) *Flocculation in natural and engineered environmental systems*. Boca Raton, Florida: CRC Press.
- Flemming, H.-C., and Wingender, J. (2003) The crucial role of extracellular polymeric substances in biofilms. In *Biofilms in wastewater treatment*. Wuertz, S., Bishop, P.L., and Wilderer, P.A. (eds): IWA Publishing, pp. 178-210.
- Gibbs, R.J., and Konwar, L.N. (1982) Effect of pipetting on mineral flocs. *Environ Sci & Technol* **16**: 119-121.
- Grossart, H.-P., and Simon, M. (1993) Limnetic macroscopic organic aggregates (lake snow): Occurrence, characteristics, and microbial dynamics in Lake Constance. *Limnol Oceanogr* **38**: 532-546.
- Heydorn, A., Nielsen, A.T., Hentzer, M., Sternberg, C., Givskov, M., Ersboll, B.K., and Molin, S. (2000) Quantification of biofilm structures by the novel computer program COMSTAT. *Microbiology* **146**: 2395-2407.
- Hofmann, T. (2004) Die Welt der vernachlässigten Dimensionen Kolloide. *Chem. Unserer Zeit* **38**: 24-35.
- Holloway, C.F., and Cowen, J.P. (1997) Development of a scanning confocal laser microscopic technique to examine the structure and composition of marine snow. *Limnol Oceanogr* **42**: 1340-1352.
- Huang, C.-T., McFeters, G.A., and Stewart, P. (1996) Evaluation of physiological staining, cryoembedding and autofluorescence quenching techniques on fouling biofilms. *Biofouling* **9**: 269-277.
- Kranck, K., and Milligan, T. (1980) Macroflocs: production of marine snow in the laboratory. *Mar Ecol Prog Ser* **3**: 19-24.
- Lawrence, J.R., Wolfaardt, G.M., and Korber, D.R. (1994) Determination of diffusion coefficients in biofilms by confocal laser microscopy. *Appl Environ Microbiol* **60**: 1166-1173.
- Lawrence, J.R., Korber, D.R., Hoyle, B.D., Costerton, J.W., and Caldwell, D.E. (1991) Optical sectioning of microbial biofilms. *J Bacteriol* **173**: 6558-6567.
- Legendre, P., and Legendre, L. (1998) *Numerical ecology*. Amsterdam, The Netherlands: Elsevier.
- Leppard, G.G., Heissenberger, A., and Herndl, G.J. (1996) Ultrastructure of marine snow. I. Transmission electron microscopy methodology. *Mar Ecol Prog Ser* **135**: 289-298.
- Long, R.A., and Azam, F. (1996) Abundant protein-containing particles in the sea. *Aquat Microb Ecol* **10**: 213-221.

- Luef, B., Neu, T.R., and Peduzzi, P. (submitted-a) Imaging and quantifying virus fluorescence signals on aquatic aggregates: an unresolved problem? *FEMS Microbiol Ecol*.
- Luef, B., Peduzzi, P., and Neu, T.R. (submitted-b) Fluorescence lectin-binding analysis in riverine aggregates (river snow): a critical examination. *FEMS Microbiol Ecol*.
- Luef, B., Aspetsberger, F., T. Hein, Huber, F., and Peduzzi, P. (2007) Impact of hydrology on free-living and particle-associated microorganisms in a river floodplain system (Danube, Austria). *Freshwater Biol* **52**: 1043 - 1057.
- Neu, T.R. (2000) *In situ* cell and glycoconjugate distribution in river snow studied by confocal laser scanning microscopy. *Aquat Microb Ecol* **21**: 85-95.
- Neu, T.R., and Lawrence, J.R. (1999) Lectin-binding analysis in biofilm systems. *Methods Enzymol* **310**: 145-152.
- Neu, T.R., Swerhone, G.D.W., and Lawrence, J.R. (2001) Assessment of lectin-binding analysis for *in situ* detection of glycoconjugates in biofilm systems. *Microbiology* **147**: 299-313.
- Noble, R.T., and Fuhrman, J.A. (1998) Use of SYBR Green I for rapid epifluorescence counts of marine viruses and bacteria. *Aquat Microb Ecol* **14**: 113-118.
- Pawley, J.B.e. (2006) *Handbook of biological confocal microscopy, third edition*. New York, USA: Springer Science+Business Media, LLC.
- Peduzzi, P., and Weinbauer, M.G. (1993) Effect of concentrating the virus-rich 2-200 nm size fraction of seawater on the formation of algal flocs (marine snow). *Limnol Oceanogr* **38**: 1562-1565.
- Peduzzi, P., and Luef, B. (2008) Viruses, bacteria and suspended particles in a backwater and main channel site of the Danube (Austria). *Aquat Sci* **70**: 186-194.
- Ploug, H., and Grossart, H.-P. (1999) Bacterial production and respiration in suspended aggregates - a matter of the incubation method. *Aquat Microb Ecol* **20**: 21-29.
- Ploug, H., and Jorgensen, B. (1999) A net-jet flow system for mass transfer and microsensor studies of sinking aggregates. *Mar Ecol Prog Ser* **176**: 279-290.
- Ploug, H., and Passow, U. (2007) Direct measurement of diffusivity within diatom aggregates containing transparent exopolymer particles. *Limnol Oceanogr* **52**: 1-6.
- Ploug, H., K hl, M., Buchholz-Cleven, B., and Jorgensen, B. (1997) Anoxic aggregates - an ephemeral phenomenon in the pelagic environment? *Aquat Microb Ecol* **13**: 285-294.
- Shanks, A., and Reeder, M. (1993) Reducing microzones and sulfide production in marine snow. *Mar Ecol Prog Ser* **96**: 43-47.

- Simon, M., Grossart, H.-P., Schweitzer, B., and Ploug, H. (2002) Microbial ecology of organic aggregates in aquatic ecosystems. *Aquat Microb Ecol* **28**: 175-211.
- Skillman, L.C., Sutherland, I.W., and Jones, M.V. (1999) The role of exopolysaccharides in dual species biofilm development. *J Appl Microbiol Symp Suppl* **85**: 13S-18S.
- Staudt, C., Horn, H., Hempel, D.C., and Neu, T.R. (2003) Screening of lectins for staining lectin-specific glycoconjugates in the EPS of biofilms. In *Biofilms in medicine, industry and environmental technology*. Lens, P., Moran, A.P., Mahony, T., Stoodley, P., and O'Flaherty, V. (eds). UK: IWA Publishing, pp. 308-327.
- Staudt, C., Horn, H., Hempel, D.C., and Neu, T.R. (2004) Volumetric measurement of bacterial cells and extracellular polymeric substance glycoconjugates in biofilms. *Biotechnol Bioeng* **88**: 585-592.
- Sutherland, I.W. (2001) The biofilm matrix - an immobilized but dynamic microbial environment. *TIM* **9**: 222-227.
- Yang, X., Beyenal, H., Harkin, G., and Lewandowski, Z. (2000) Quantifying biofilm structure using image analysis. *J Microbiol Methods* **39**: 109-119.
- Zimmermann-Timm, H. (2002) Characteristics, dynamics and importance of aggregates in rivers - an invited review. *Internat Rev Hydrobiol* **87**: 197-240.
- Zimmermann, H. (1997) The microbial community on aggregates in the Elbe estuary, Germany. *Aquat Microb Ecol* **13**: 37-46.
- Zippel, B., and Neu, T.R. (2005) Growth and structure of phototrophic biofilms under controlled light conditions. *Water Sci & Technol* **52**: 203-209.

Table 1: Selection of abiotic and biotic parameters characterizing the Danube and Elbe Rivers during the four seasons of the sampling period.

Chemical analyses of nitrogen (N-NO_3 = nitrate, N-NO_2 = nitrite, N-NH_4 = ammonium) and phosphorus (P-PO_4 = orthophosphate, $\text{P}_{\text{soluble}}$ = total soluble reactive phosphorus, P_{total} = total phosphorus) were performed based on German Standard Methods for the Examination of Water, Wastewater and Sludge. Determination of total suspended solids (TSS), particulate organic matter (POM) and chlorophyll-*a* concentrations are published elsewhere (Luef et al., 2007). In the Danube River, particle abundance was measured with a Galai CIS100L Laser Analyzer (Ankersmid Ltd., Yokneam, Israel) and in the Elbe River with the optical measuring instrument PartmasterL (AUCOTEAM GmbH Berlin, Berlin, Germany). The measuring range for particle abundance was from 2 to 200 μm .

	Danube River				Elbe River			
	spring	summer	fall	winter	spring	summer	fall	winter
discharge (m ³ s ⁻¹)	2809	2656	1236	935	1459	330	260	379
conductivity (μS cm ⁻¹)	415	367	408	552	1262	1106	1523	1380
P-PO ₄ (μg L ⁻¹)	31	30	34	48	53	78	61	81
P-P _{soluble} (μg L ⁻¹)	36	35	35	49	61	83	70	88
P _{total} (μg L ⁻¹)	74	87	56	63	202	129	352	145
N-NO ₃ (μg L ⁻¹)	2487	1497	1829	3048	2526	3478	5627	5802
N-NO ₂ (μg L ⁻¹)	49.1	14.9	6.5	13.3	9.7	0.6	20.1	45.1
N-NH ₄ (μg L ⁻¹)	3	44	35	9	25	13	164	90
particles (x 10 ⁷ L ⁻¹)	1.07	2.61	0.36	0.05	25.21	11.38	4.18	3.83
relative contribution of POM to TSS (%)	11.02	6.98	16.24	30.41	16.15	36.01	16.35	40.36
chlorophyll- <i>a</i> (μg L ⁻¹)	0.97	0.56	0.75	0.37	0.87	10.37	1.03	0.43

Table 2: *Effect of aggregate size and colonization on layer width of CNAS (cellular nucleic acid signals including potential virus signals) and spatial structure within the three subsamples.* Multiple linear regression analysis (method: include), independent variables: aggregate diameter (= total number of slices in the respective subsample) and % CNAS (% of slices in the subsample containing CNAS), dependent variable a) layer width and b) spatial structure (= number of secondary maxima found in the respective subsample; see text). 1st, 2nd & 3rd sector refers to the position of the subsample within the cyrosection. Reg. coef. = regression coefficient.

a) layer width of CNAS

	1 st sector		2 nd sector		3 rd sector	
r ²	0.268		0.174		0.245	
p-value	0.001		0.010		0.002	
	reg. coef.	p-value	reg. coef.	p-value	reg. coef.	p-value
intercept	-4.229	0.244	-2.942	0.547	0.096	0.971
slope of diameter	0.033	0.010	0.043	0.004	0.025	0.006
slope of % CNAS	0.160	0.000	0.083	0.131	0.098	0.006

b) spatial structure

	1 st sector		2 nd sector		3 rd sector	
r ²	0.155		0.321		0.402	
p-value	0.035		0.000		0.000	
	reg. coef.	p-value	reg. coef.	p-value	reg. coef.	p-value
intercept	1.575	0.016	0.768	0.128	0.053	0.900
slope of diameter	0.001	0.790	0.004	0.004	0.006	0.000
slope of % CNAS	-0.017	0.023	-0.016	0.007	-0.012	0.036

Table 3: *Differences in layer width of CNAS (cellular nucleic acid signals including potential virus signals) and spatial structure (corrected for aggregate size) between seasons and the two rivers.* Multiple linear regression analysis (method: backward selection), independent variables: river (sample from 1 = Elbe, 0 = Danube), spring (sample from spring = 1, other seasons = 0), summer, fall, winter: analogously to spring; dependent variable residual layer width (= residuals from regressions given in Tab. 1a) and residual spatial structure (= residuals from regressions given in Tab. 1b). Reg. coef. = regression coefficient.

	residual layer width		residual spatial structure	
r^2	0.040		0.053	
p-value	0.015		0.023	
	reg. coef.	p-value	reg. coef.	p-value
intercept	0.778	0.203	-0.306	0.015
slope of river			0.299	0.047
slope of spring			0.458	0.052
slope of summer	-2.877	0.015	0.399	0.017
slope of fall				
slope of winter				

Figure legends

Figure 1: 3-D reconstruction of a riverine aggregate. Four-channel presentation of mineral compounds, glycoconjugates, CNAS (cellular nucleic acid signals including potential virus signals) and as well as negative stain. Area with polygons indicate the aggregate volume without specific glycoconjugates and CNAS, detected after negative staining. Color allocation: reflection mode = white, nucleic acid = green, glycoconjugates = red.

Figure 2: Average relative contribution of the specific glycoconjugate volume to the aggregate volume (a) and the average relative contribution of the CNAS (cellular nucleic acid signals including potential virus signals) volume to the aggregate volume (b) from the Danube and Elbe River during the four seasons. Error bars indicate standard error of all inspected aggregates.

Figure 3: Single scan of an unsectioned aggregate. CNAS (cellular nucleic acid signals including potential virus signals) and glycoconjugates deeper inside cannot be investigated due to scattering properties (black) of the aggregates themselves and the limited depth of laser penetration (a). Single scan of a cryo-section showing distribution of CNAS and glycoconjugates inside an aggregate (b). Color allocation: nucleic acid = green, glycoconjugates = red, yellow = CNAS in or in contact with lectin-specific extracellular polymeric substances, negative stain (Alexa Fluor 568) = blue. Length of calibration bar 10 μm .

Figure 4: Single scans of different cryo-sections showing distribution of CNAS (cellular nucleic acid signals including potential virus signals) and glycoconjugates inside an aggregate (a, d). Insert of (d) shows CNAS in detail. White rectangle indicates subsample for CNAS volume calculation. The distribution of the calculated CNAS volumes within the subsamples of the cryo-sections is presented (b, e). Spatial autocorrelation presents the distribution and accumulations of CNAS within the cryo-sections of the aggregates (c, f). Autocorrelations for lags 1 to one fourth of the total number of slices were calculated. The first local maximum provides information on CNAS layer width. Secondary maxima indicate a regular spatial distribution of CNAS within the cryo-section, pointing to the repeating occurrence of CNAS-layers (whose width can be estimated from the first maximum). Black lines indicate the level of significance (twice the standard error). Color allocation: nucleic acid = green,

glycoconjugates = red, yellow = CNAS in or in contact with lectin-specific extracellular polymeric substances. Length of calibration bar 15 μm .

Figure 5: Comparison of the Danube and Elbe Rivers based on (a) the layer width which harbors CNAS (cellular nucleic acid signals including potential virus signals) and (b) the occurrence of secondary maxima. Cryo-sections of all four seasons are considered.

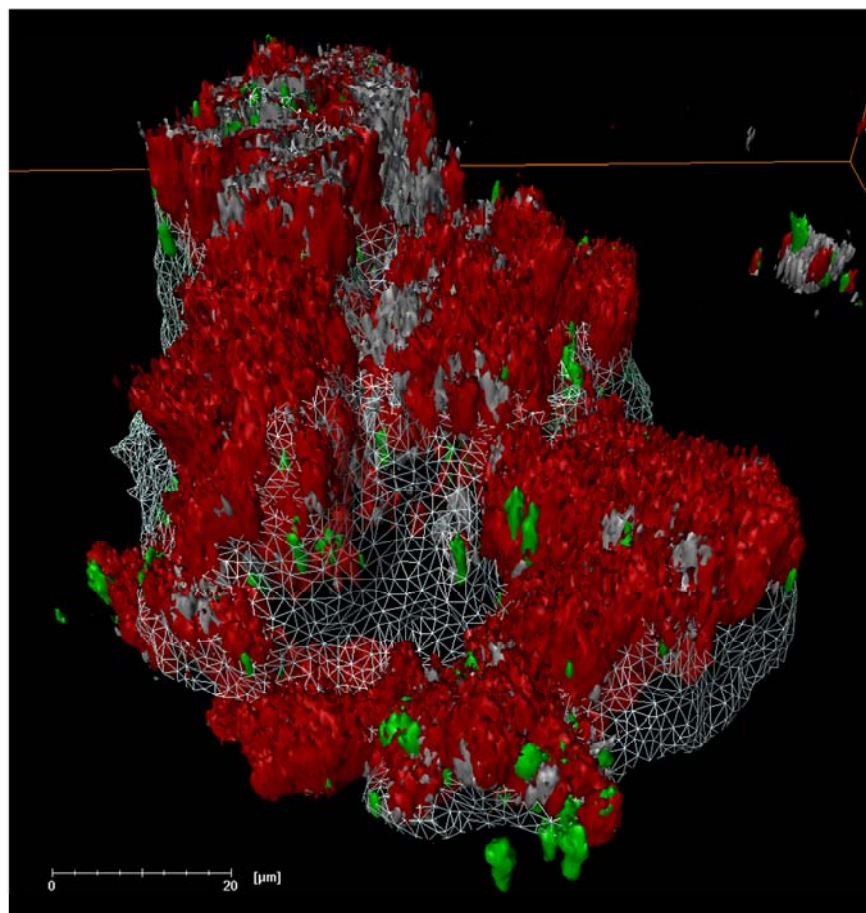


Figure 1

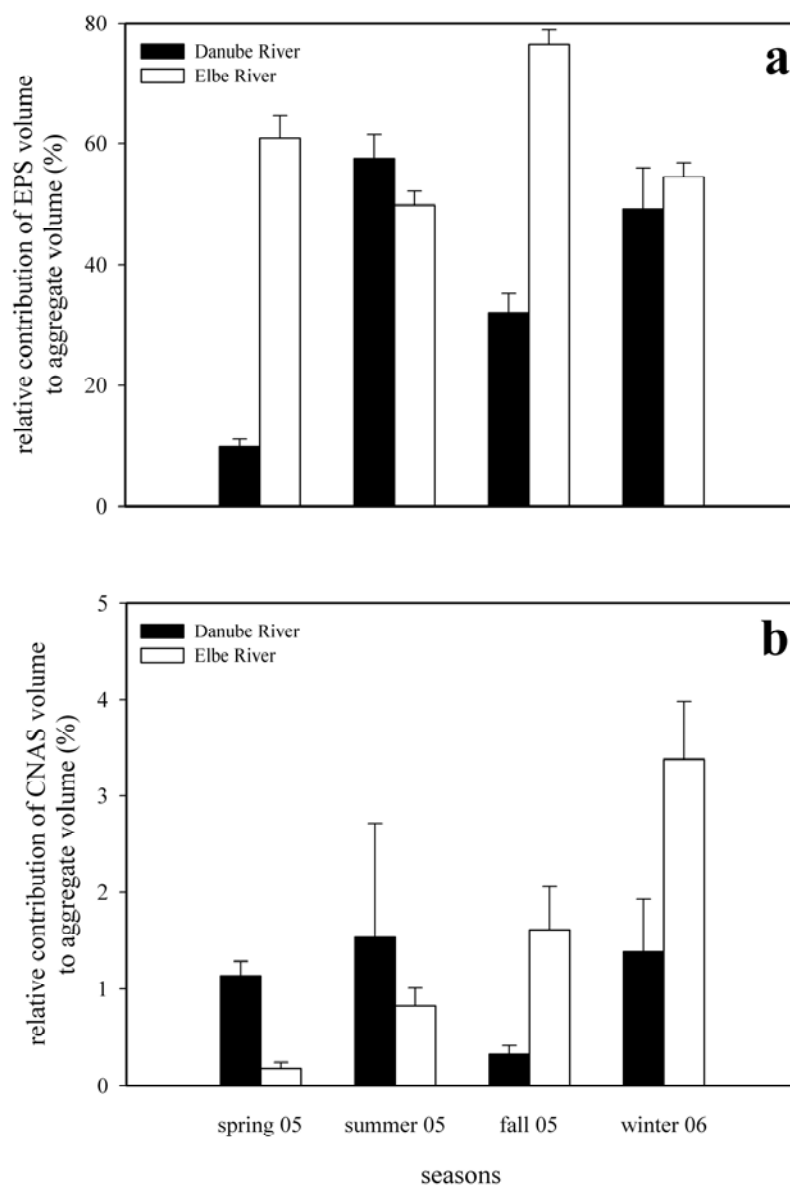


Figure 2

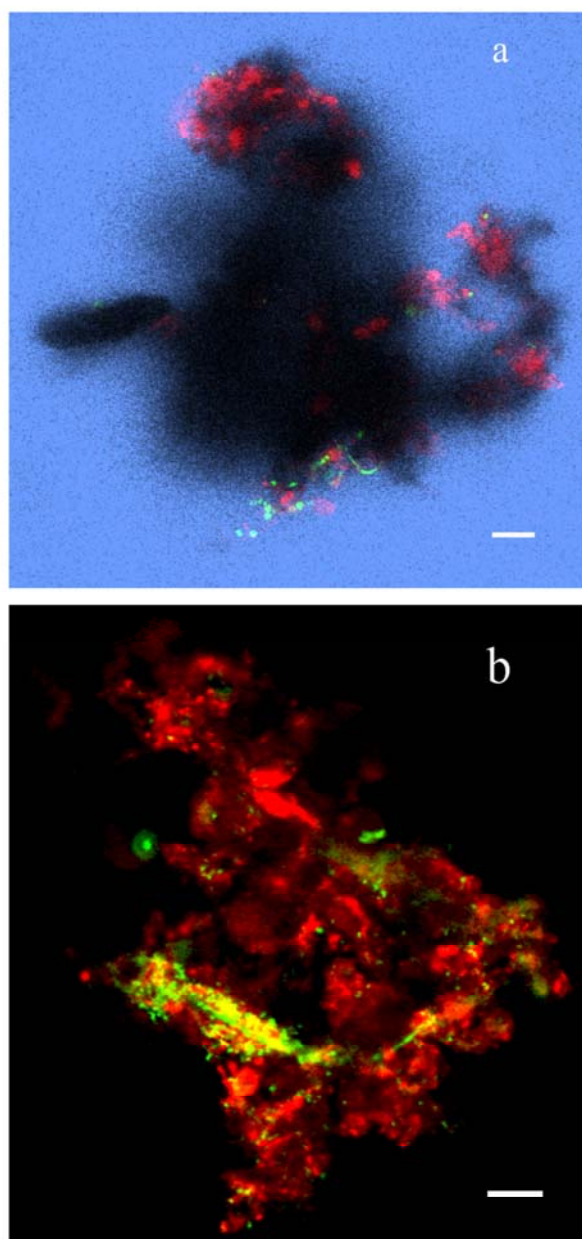


Figure 3

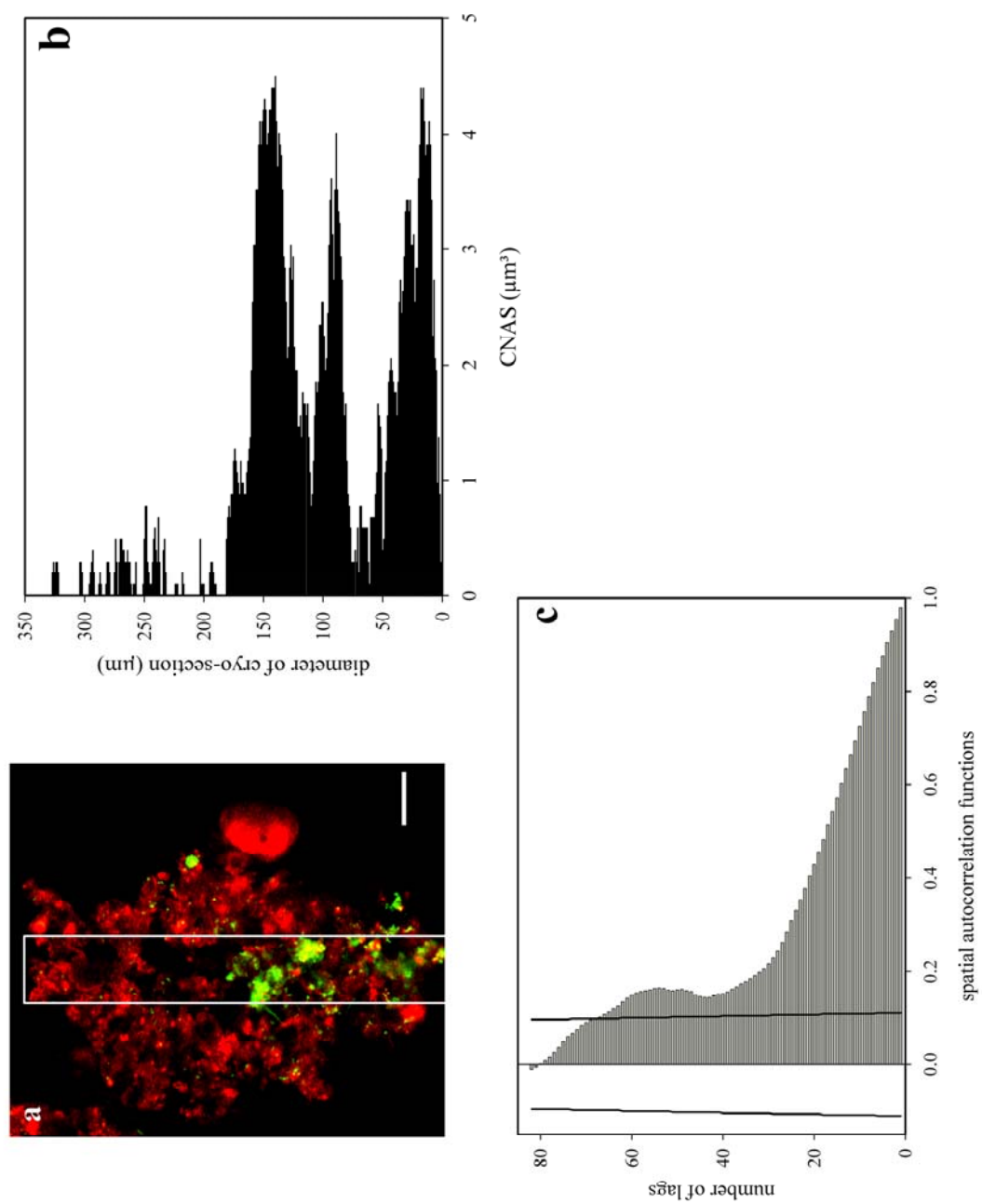


Figure 4a-c

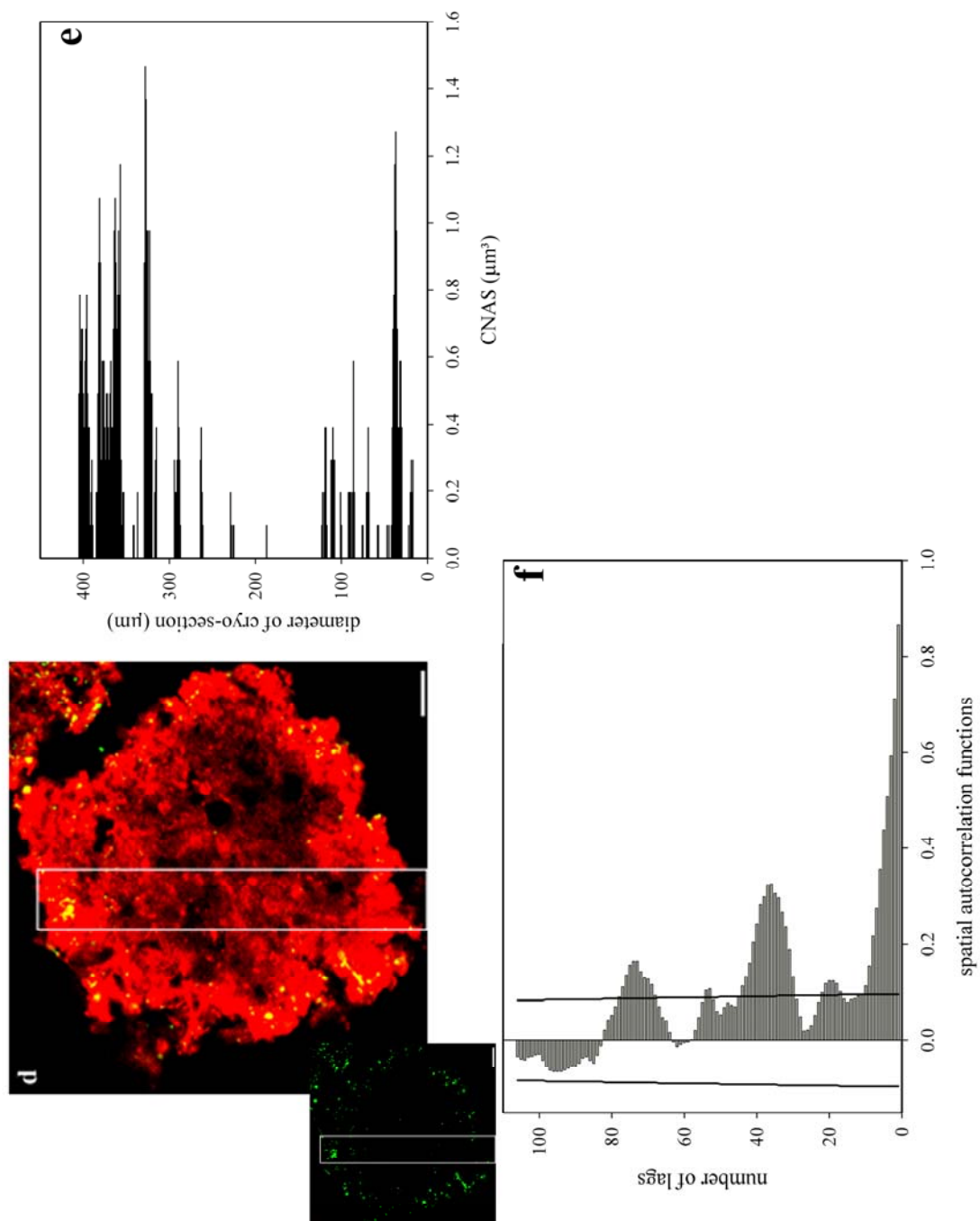


Figure 4d-f

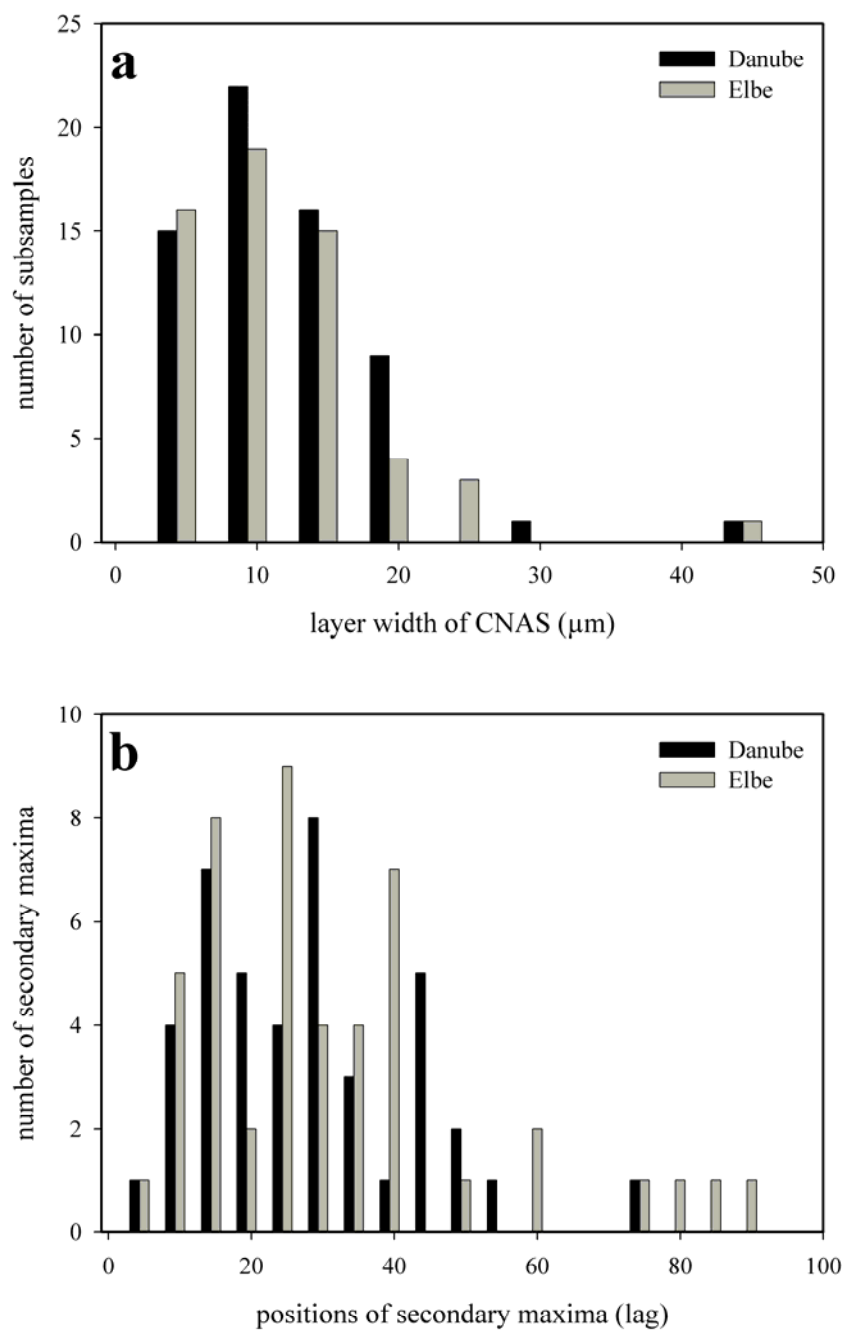


Figure 5

Chapter 3

Imaging and Quantifying Virus Fluorescence Signals on Aquatic Aggregates: an Unresolved Problem?

Birgit Luef, Thomas R. Neu and Peter Peduzzi
(submitted to FEMS Microbiology Ecology)

Abstract

The development of accurate methods to detect and enumerate viruses is an important issue in aquatic microbial ecology. In particular, viruses attached to floating aggregates is a largely ignored field both in marine and inland water ecology. Data on total abundance and the colonization of aggregates by viruses are rare, mainly due to methodological difficulties. In the present study we used confocal laser scanning microscopy (CLSM) to resolve fluorescence signals of single viruses and bacterial cells in a complex three-dimensional matrix of riverine aggregates. CLSM in combination with different fluorochromes is a very promising approach for obtaining information both on aggregate architecture and on the spatial distribution of viruses attached to fully hydrated aggregates. Aggregates from the Danube River harbored up to 5.39×10^9 viruses cm^3 . We discuss the problems associated with different methods such as sonication or directly counting viruses on aggregates, both combined with epifluorescence microscopy and CLSM, to quantify viruses on suspended particles.

Introduction

Viruses are highly abundant in aquatic systems, affect phyto- and bacterioplankton growth, may regulate the genetic diversity of their hosts, and potentially influence the cycling of organic carbon and nutrients (see reviews of Wommack & Colwell, 2000; Weinbauer, 2004). In order to understand the potential impact of viruses on microorganisms, it is important to detect and enumerate the viruses. Typically, viral abundance in aquatic systems ranges between $< 10^4$ and $> 10^8$ mL^{-1} . Compared to free-living forms, viruses associated with aggregates have received little attention, perhaps largely due to methodological difficulties. Nevertheless, the occurrence and importance of viruses in sediments (see review of Danovaro, *et al.*, 2008; Danovaro, *et al.*, 2008) and on floating aggregates (Peduzzi & Weinbauer, 1993; Simon, *et al.*, 2002; Luef, *et al.*, 2007; Mari, *et al.*, 2007; Peduzzi & Luef, 2008) is documented. So far, viruses associated with aggregates were analyzed using different techniques such as sonication (Danovaro, *et al.*, 2001) or direct observation (Luef, *et al.*, 2007), both combined with conventional epifluorescence microscopy (EFM) and transmission electron microscopy (TEM; Peduzzi & Weinbauer, 1993). Recently, Mari *et al.* (2007) described an indirect approach to enumerate viruses inside transparent exopolymeric particles using magnetic isolation and flow cytometry.

In recent years, confocal laser scanning microscopy (CLSM) has been introduced into the field of microbial ecology to investigate three-dimensional (3-D) objects such as fully

hydrated biofilms and aggregates in both freshwater and marine environments (e.g. Holloway & Cowen, 1997; Neu & Lawrence, 1999; Neu, 2000; Neu, *et al.*, 2001). No attempt has yet been made to detect particle-associated viruses via CLSM. Viruses are typically below the detection limit of light microscopy. Therefore, visualizing viruses requires a fluorescence staining procedure such as with SYBR stains (Noble & Fuhrman, 1998; Chen, *et al.*, 2001; Wen, *et al.*, 2004). Significant advantages of CLSM include the elimination of out-of-focus information and the possibility for horizontal and vertical optical thin sectioning of thick, hydrated biological samples. Hence, our investigation applies CLSM in combination with SYBR staining to visualize the 3-D distribution of viruses. In addition, we quantify the CLSM data sets of virus signals in fully hydrated riverine aggregates. We then discuss different methods for quantifying viruses associated with aquatic aggregates in combination with advanced imaging techniques.

Material and Methods

Sampling of aggregates

Water samples from the Danube River (Wildungsmauer, Austria, stream kilometer 1894) were taken in early May and late July 2005 at a sampling depth of approximately 30 cm. In July, samples were taken after a flood event. Lotic aggregates were sampled in 1L plexiglass bottles. The samples were always kept at +4 °C until analysis, which was completed within 24 h (Bura, *et al.*, 1998).

Extraction of viruses by sonication

To confirm that viruses can be properly detected also by CLSM, we dislodged viruses from aggregates by sonication. Therefore, we adopted the method, used for sediments by Weinbauer *et al.* (1998) and Danovaro *et al.* (2001), to enumerate viruses on floating aggregates. Water samples were filtered onto 3µm Isopore Membrane filters (TSTP, 25 mm diameter, Millipore) to obtain the particle – associated microbial fraction. Filters were stored in 4.5ml 0.02µm - filtered water and fixed with formaldehyde (2 % final concentration). Tetra sodium pyrophosphate (final conc. 5 mMolar) was added to the samples, which were incubated for one hour on a shaker. The samples were sonicated three times for one minute on ice, pulsing at 40 Watt using a B. Braun Diessel Biotech Sonifier (4 mm needle diameter; Labsonic U, Melsungen, Germany). The sonication was interrupted for 30 s every minute. Afterwards samples were filtered onto Whatman Anodisc filters (pore size 0.02µm, 25 mm diameter, Whatman, Maidstone, England) and stained with SYBR Green I (Invitrogen,

Eugene, Oregon, USA) according to Noble & Fuhrman (1998). Filters were mounted on glass slides with an antifade mounting solution (Citifluor AF1, Citifluor, London, UK). Viruses were detected under the CLSM (see below).

Staining & CLSM

To label matrix material of the riverine aggregates, the lectin from *Aleuria aurantia* (AAL, Vector Laboratories, Burlingame, California, USA) was employed to stain the lectin-specific glycoconjugates of the extracellular polymeric substances (EPS) (Neu, 2000; Neu, *et al.*, 2001; Staudt, *et al.*, 2003). The lectins were self-labeled with the fluorochrome Cy5 according to the data sheet of the supplier (Amersham, Buckinghamshire, UK). Lectin staining of the glycoconjugates of EPS (100 $\mu\text{g mL}^{-1}$) was done as described previously (Neu, 2000). For staining, the lectin was diluted with deionized water to a final concentration of 0.1 mg mL^{-1} protein. 100 μl of this solution were added to each sample and were incubated for 20 min in the dark. The aggregates were then carefully washed 3 times with tap water to remove unbound lectins. The aggregates were never allowed to dry in the air. To detect aggregate-associated bacteria and viruses on the fully hydrated aggregates, the samples were stained with the nucleic-acid-specific-stain SYBR Green I (Noble & Fuhrman, 1998). After staining the lectin-specific EPS compounds, SYBR Green I (1 $\mu\text{l mL}^{-1}$ deionised water) was directly applied to the aggregates and incubated for 5 min. The stained samples were carefully transferred into cover well imaging chambers (0.5 mm, Invitrogen), covered with tap water and immediately examined by CLSM.

CLSM was performed using a Leica TCS SP1, controlled by the LCS Version 2.61 Build 1537 174192 (Leica, Heidelberg, Germany), equipped with an upright microscope. For detecting viruses, images were taken with a 100x 1.4 NA oil lens. Aggregate structure was analysed by CLSM using visible lasers (488 nm and 633 nm). Emission signals were detected from 500-550 nm and from 650-750 nm. Optical sections of aggregates were taken every 0.2 μm .

Cryo-embedding, Cryo-sections & CLSM

To quantify viruses and bacteria on riverine aggregates, also cryo-sections were performed. Aggregates from the Danube were embedded in liquid cryostat medium (Neg-50 by Richard-Allan Scientific), frozen at $-26\text{ }^{\circ}\text{C}$ and physically sectioned (10 μm) with a cryomicrotome (Leica CM3050S) (Huang, *et al.*, 1996). Thereafter, sections were stained with lectins and a nucleic acid stain (see above), were embedded in water, and covered with a coverslip before

analysis. The sections of the aggregates were examined by CLSM using a TCS SP2 controlled by the LCS Version 2.5 Build 1227 192162 (Leica). Images were collected using an inverted DM IRB microscope and a 100x 1.4 NA oil lens. Aggregate structure was analysed by CLSM using visible lasers (488 nm and 633 nm). Emission signals were detected from 480-500 nm and from 650-750 nm.

Quantification & Visualization

To quantify virus signals, the freely available software Image J (<http://rsb.info.nih.gov/ij/>), developed in Java (Staudt, *et al.*, 2004) or, alternatively, the IDL based program Confocal Analysis (ConAn) version 1.31, was applied. The software ConAn was developed by BioCom for the Helmholtz Centre for Environmental Research – UFZ in Magdeburg.

To quantify lectin signals, the software Image J was used. For each aggregate, the threshold was set manually. Due to the very heterogeneous composition of the aggregates, automatic batch processing could not be applied.

To visualize 3-D data sets, Imaris 4.2 (Bitplane AG, Zurich, Switzerland) was used. Thresholds were set manually. Adobe Photoshop CS2 was used to insert calibration bars into the images.

Results

Confocal laser scanning microscopy (CLSM) & visualization

In a first step, we had to confirm that virus signals can be also detected properly by CLSM. Therefore, samples were sonicated, filtered, stained and analyzed by CLSM (Fig. 1). Viruses and bacteria appeared brightly and could be easily distinguished based on size and light intensity. Other than in conventional EFM, almost no disturbing background fluorescence was present when using CLSM. To obtain information about the spatial distribution of viruses attached to aggregates, the fully hydrated aggregates were analyzed directly by CLSM after staining. This is the first time that viral, bacterial and glycoconjugate distribution has been visualized together by means of CLSM in fully hydrated aggregates. The serial optical sections, as shown in Figure 2, provide insight into the arrangement of viruses, bacteria and the matrix of heterogeneous aggregates. In addition, Figure 3 shows the presence of viruses and lectin-specific glycoconjugates, their location and also their co-localization in a 3-D reconstruction.

CLSM & quantification

The software Image J and ConAn enabled quantification of the lectin-specific glycoconjugates and of the bacteria, but not of the viruses. Although the diverse programs could not identify virus signals correctly, the human eye could easily distinguish between a virus and an occasional background pixel. Nonetheless, counting viruses manually in untreated aggregates was not manageable. The main obstacle was to identify whether the DNA signals were viruses or sections of bacteria: therefore, each section of an image stack had to be compared to determine whether the fluorescence signals were virus-derived or merely a section of a bacterium. Performing this comparison for each fluorescence signal is too laborious, especially for heavily colonized aggregates.

Cryo-sections, however, allowed detecting the distribution of viruses, bacteria and polymeric constituents inside the aggregate with more accurate resolution in a reasonable time (Fig.4). Potential limitations of the CLSM technique due to scattering, laser penetration and diffusion of staining solutions can be overcome by analysis of cryo-sectioned post-stained samples. Abundance data were therefore gained from cryo-sections of aggregates which were counted manually. Abundances of bacteria and viruses associated with Danube aggregates are summarized in Table 1. In spring, for example, aggregates harbored on average of 17.27×10^8 bacteria and 18.77×10^8 viruses cm^{-3} lectin-specific glycoconjugate. In summer, after a flood event, the corresponding average values were 1.55×10^8 bacteria and 2.48×10^8 viruses cm^{-3} lectin-specific glycoconjugate.

Discussion*CLSM, visualization & quantification*

In recent years, CLSM has become an indispensable tool for studying 3-D biofilm and aggregate architectures, their chemical compositions and associated microbial communities (e.g. Böckelmann, *et al.*, 2002; Staudt, *et al.*, 2003; Neu, *et al.*, 2004). To our knowledge no one has yet attempted to detect viruses attached to aquatic aggregates by CLSM. Generally, interactions between natural virus assemblages and suspended particulate matter are poorly documented. Particularly in riverine systems, where suspended matter is an important factor, very little information is available on the interaction of viruses with aggregates. We therefore used CLSM to resolve single virus signals and bacteria in a complex 3-D matrix of riverine aggregates (Fig. 2 and 3). In combination with different fluorochromes, this allowed us to obtain information on both aggregate architecture and the spatial distribution of viruses in fully hydrated aggregates.

Since viruses attached to riverine aggregates were detectable, we attempted to quantify the virus signals. Ample software is available for quantifying CLSM data. This includes freely available as well as commercial software. None of the programs, however, is suitable for multi-purpose applications.

One crucial step in digital image analysis is setting thresholds (Xavier, *et al.*, 2001; Beyenal, *et al.*, 2004). Thresholding is a segmentation method that essentially reduces 256 gray scale levels images to binary images in order to separate the image into biomass and interstitial space. To extract statistically meaningful parameters from image series, the thresholding has to be reproducible. There are no general rules for setting thresholds. The operator uses his or her best judgment, setting the gray-scale level such that the binary image appears to capture the essence of the EPS structure, viral and bacterial signals. Setting the thresholds manually is quite time consuming, and variability between operators in choosing the threshold adversely affects the measurements obtained from the binary image. Most computer programs are equipped with automatic image thresholding procedures. Such procedures must be tested carefully prior to use. Changes in thresholding can alter the numerical values of diverse parameters (Beyenal, *et al.*, 2004). We tried different automated methods of thresholding. As the aggregate structures were so heterogeneous, the computer programs did not have a sufficiently precise automatic procedure to yield reproducible results compared to the human operator.

Setting the thresholds manually, the computer program ConAn and J-Image allowed us to estimate bacterial and EPS volumes, but it was not possible to accurately quantify viruses. Two important points have to be considered for digital image analysis and especially for virus quantification: firstly, virus signal intensity versus background signal, and secondly virus signal size versus pixel size. The above computer programs failed to distinguish between virus and background pixels, probably because the algorithms were insufficiently sensitive. Viruses and bacteria attached to aggregates were therefore counted manually. Nevertheless, CLSM is recommended as the method of choice to resolve single viruses in a complex 3-D matrix of fully hydrated riverine aggregates. Although more sensitive and precise algorithms for thresholding may become available, thresholding remains difficult because riverine aggregates have a very complex composition.

Comparison of different methods to quantify viruses and bacteria attached to riverine aggregates

Direct counts provide a wealth of basic information on viruses in aquatic ecosystems. This calls for accurate methods to detect and enumerate viruses on particles as well. Generally, two major approaches have been used for such enumerations: one is based on TEM, the other on DNA/RNA staining techniques using EFM.

Using TEM for example, riverine aggregates can be embedded in Nanoplast in combination with uranylacetate counter-staining (Leppard, *et al.*, 1996). TEM offers high resolution and therefore clearly identifies accumulations of viruses. But TEM requires fixation and/or dehydration in order to examine the 3-D aggregate structure. Both processes can produce severe artefacts, especially in highly hydrated samples. Moreover, TEM is very time consuming and expensive.

Sonication is widely used to dislodge viruses from sediments, aggregates, etc., combined with EFM (see review of Danovaro, *et al.*, 2008). Using CLSM we also accurately detected dislodged viruses (Fig. 1). However, sonication appears to be a useful method for reasonably quantifying viruses on floating aggregates, but does not supply any information on the spatial distribution of viruses on the aggregates.

Luef, *et al.* (2007) directly observed particle-attached viruses and bacteria in combination with conventional EFM. This technique had limitations in distinguishing between stained viruses and background fluorescence from deeper layers of the aggregate. Occasional high densities of attached bacteria also hampered the precise detection of single virus signals. Examining a sample by EFM required frequently adjusting the plane of focus. Furthermore, bacteria and viruses underneath the aggregates or deeper inside were undetectable.

The major disadvantage of fluorescence microscope techniques is image degradation by out-of-focus information originating from focal planes located above or below the objects of interest. CLSM systems provide the opportunity to extend light microscopy studies beyond the limitations of traditional EFM (Lawrence, *et al.*, 2002).

For CLSM-based quantification, not the entire aggregates were analyzed. Riverine aggregates incorporate a high amount of non-cellular matter such as sand, clay and detritus which limit diffusion of the staining solution, laser penetration and detection of emission signals in thick samples (Luef, *et al.*, submitted). Thus, large aggregates had to be embedded and physically sectioned into slices using cryo-sectioning. Cryo-sections allow much better detection of the distribution of viruses, bacteria and polymeric constituents inside the aggregates. From each

slice, bacterial and viral abundances were counted manually due to the above mentioned difficulties when using digital image analysis.

CLSM allowed clear recognition of virus accumulations (Fig. 5), although sometimes the quantification of single virus signals and clear identification within such accumulations was still hampered. It was also occasionally difficult to distinguish single virus-particles in aggregates containing high densities of stained cells and/or a matrix that was also stainable with nucleic acid dyes. Nevertheless, CLSM is a very promising approach for obtaining abundances of viruses attached to or within aggregates.

The resolution of any linear imaging system is given by its point spread function, which quantifies the blur of an object point in the image. The sharper the point spread function, the better the resolution. In 1873, Ernst Abbe discovered that lens-based optical microscopes cannot resolve objects that are closer together than half of the wavelength of light. Recently, however, Schmidt *et al.* (2008) introduced a fluorescence microscope that creates nearly spherical focal spots of 40 to 45 nm ($\lambda/16$) in diameter. Combinations of stimulated emission depletion microscopy with 4Pi will probably push the z resolution to < 10 nm (Hell, 2007). Perhaps methods such as stimulated emission depletion, which sharpen the point spread function, will yield even better resolution/images of viruses attached to aggregates.

Interactions of viruses and particulate material

The literature on the interaction between suspended matter and the natural assemblage of viruses infecting microplankton organisms, such as bacteria and phytoplankton, is surprisingly scarce. Particularly in freshwater systems, where suspended matter is often a prominent factor, very little information is available on the interaction of viruses with aggregate-associated host bacteria. But even for marine systems, we know little about virus – particle interactions.

Few studies on the abundance of viruses attached to or within organic aggregates are available (Peduzzi & Weinbauer, 1993; Simon, *et al.*, 2002; Luef, *et al.*, 2007; Peduzzi & Luef, 2008). Marine snow particles from the Northern Adriatic Sea harbored 5.6×10^{10} viral particles cm^{-3} aggregate based on ultrathin-sections and subsequent TEM investigations (Peduzzi & Weinbauer, 1993). In the present study, up to 5.39×10^9 viruses cm^{-3} lectin-specific glycoconjugate were found in the Danube when analyzed by CLSM (Tab. 1). A comprehensive overview of studies on viruses attached to different substrata in inland waters is given by Peduzzi & Luef (in press). For example, Luef *et al.* (2007) and Peduzzi & Luef

(2008) showed that $0.01 - 0.89 \times 10^7$ viruses mL^{-1} water were attached to particles in the Danube and its floodplain system. In the Talladega Wetland, Alabama, viruses attached to surfaces ranged from 1.3×10^6 virus particles cm^{-2} on macrophytes to 1.1×10^7 virus particles cm^{-2} on wood (Farnell-Jackson & Ward, 2003). In the Mahoning River, Ohio, viral abundances ranged from 1.65 to 6.68×10^8 g ash-free dry mass (Lemke, *et al.*, 1997), leaves harbored $4.81 - 21.8 \times 10^8$ viruses g^{-1} and sediment samples $4.71 - 8.91 \times 10^6$ viruses g^{-1} (Baker & Leff, 2004). At Lake Hallwil, Switzerland, $0.2 - 0.9 \times 10^8$ viruses cm^{-2} biofilm, $3.5 - 10.6 \times 10^7$ viruses mg^{-1} C_{org} plant litter and $1.9 - 5.3 \times 10^9$ viruses cm^{-3} sediment were found (Filippini, *et al.*, 2006). Furthermore, quite recently Danovaro *et al.* (2008) gave a broad overview of viruses in both freshwater and marine sediments. In inland waters, viral abundances range from $>0.01 - 203.3 \times 10^8$ viruses g^{-1} dry sediment. A literature comparison of viral abundances associated with aggregates, biofilms, sediments etc. is very difficult due to the different methods used and the variable units presented. Nonetheless, such associated viruses apparently reveal some dependency on the type of the particulate matter, such as particle size and quality (Lemke, *et al.*, 1997; Farnell-Jackson & Ward, 2003; Luef, *et al.*, 2007).

Flood & Ashbolt (2000) observed that wetland biofilms could entrap viral-sized particles and concentrate them over 100-fold compared with abundances in the surrounding water column. In a study on viral decay in the Gulf of Mexico, free-living viruses may bind irreversibly to loosely associated aggregates, thereby losing their infectivity (Suttle & Chen, 1992). On the other hand, viral association with colloidal and particulate materials can prolong their survival (Kapuscinski & Michell, 1980), and phage production and transduction frequencies can increase in the presence of particulate matter (Kokjohn, *et al.*, 1991; Ripp & Miller, 1995).

Virus infection of bacteria and virus-induced bacterial mortality on aggregates are probably similar to that in free-living bacterial communities (Proctor & Fuhrman, 1991; Simon, *et al.*, 2002).

Viral infection of bacterial cells attached to aggregates may be impeded by various structures, including the bacterial extracellular polymer. Specific phages can degrade susceptible biofilms and continue to infect biofilm bacteria during the degradation of extracellular polymeric substances (Hughes, *et al.*, 1998). Many phages, but not all, may use polysaccharases or polysaccharide lyases (Hughes, *et al.*, 1998; Sutherland, *et al.*, 2004). Viruses can indirectly produce EPS by lysing bacteria and phytoplankton biomass and may play an important role in flocculation processes (Peduzzi & Weinbauer, 1993).

Based on the above outlined information it becomes evident that visualizing and quantifying virus distribution on particles is important in microbial ecology of floating aggregates in aquatic systems. This new technique should contribute among others to elucidate the significance of viruses on suspended matter.

Conclusions

CLSM in combination with different fluorochromes represents an *in situ* approach that yields information both on the architecture of aggregates and on the spatial distribution of bacteria, viruses and polymeric constituents. For the first time viral, bacterial and glycoconjugate distribution could be visualized by means of CLSM in fully hydrated aggregates. Although some difficulties occurred when quantifying viruses attached to aggregates, CLSM is proposed as the method of choice for investigating multiple constituents in fully hydrated suspended matter.

Acknowledgements

We thank the Austrian Science Foundation FWF (grant number P14721 and P17798 to P.P.) for financial support. We are grateful for technical expertise and help by U. Kuhlicke.

References

- Baker PW & Leff LG (2004) Seasonal patterns of abundance of viruses and bacteria in a Northeast Ohio (USA) stream. *Arch Hydrobiol* **161**: 225-233.
- Beyenal H, Lewandowski Z & Harkin G (2004) Quantifying biofilm structure: facts and fiction. *Biofouling* **20**: 1-23.
- Böckelmann U, Manz W, Neu TR & Szewzyk U (2002) Investigation of lotic microbial aggregates by a combined technique of fluorescent in situ hybridization and lectin-binding-analysis. *J Microbiol Methods* **49**: 75-87.
- Bura R, Cheung M, Liao B, *et al.* (1998) Composition of extracellular polymeric substances in the activated sludge floc matrix. *Water Sci & Technol* **37**: 325-333.
- Chen F, Lu J-R, Binder BJ, Liu Y-C & Hodson RE (2001) Application of digital image analysis and flow cytometry to enumerate marine viruses stained with SYBR Gold. *Appl Environ Microbiol* **67**: 539-545.
- Danovaro R, Dell'Anno A, Trucco A, Serresi M & Vanucci S (2001) Determination of virus abundance in marine sediments. *Appl Environ Microbiol* **67**: 1384-1387.
- Danovaro R, Dell'Anno A, Corinaldesi C, Magagnini M, Noble R, Tamburini C & Weinbauer M (2008) Major viral impact on the functioning of benthic deep-sea ecosystems. *Nature* **454**: 1084-1087.
- Danovaro R, Corinaldesi C, Filippini M, *et al.* (2008) Viriobenthos in freshwater and marine sediments: a review. *Freshwater Biol* **53**: 1186-1213.
- Farnell-Jackson EA & Ward AK (2003) Seasonal patterns of viruses, bacteria and dissolved organic carbon in a riverine wetland. *Freshwater Biol* **48**: 841-851.
- Filippini M, Buesing N, Bettarel Y, Sime-Ngando T & Gessner MO (2006) Infection paradox: high abundance but low impact of freshwater benthic viruses. *Appl Environ Microbiol* **72**: 4893-4898.
- Flood JA & Ashbolt NJ (2000) Virus-sized particles can be entrapped and concentrated one hundred fold within wetland biofilm. *Adv Environ Res* **3**: 403-411.
- Hell SW (2007) Far-field optical nanoscopy. *Science* **316**: 1153-1158.
- Holloway CF & Cowen JP (1997) Development of a scanning confocal laser microscopic technique to examine the structure and composition of marine snow. *Limnol Oceanogr* **42**: 1340-1352.
- Huang C-T, McFeters GA & Stewart P (1996) Evaluation of physiological staining, cryoembedding and autofluorescence quenching techniques on fouling biofilms. *Biofouling* **9**: 269-277.

- Hughes KA, Sutherland IW & Jones MV (1998) Biofilm susceptibility to bacteriophage attack: the role of phage-borne polysaccharide depolymerase. *Microbiology* **144**: 3039-3047.
- Hughes KA, Sutherland IW, Clark J & Jones MV (1998) Bacteriophages and associated polysaccharide depolymerases - novel tools for study of bacterial biofilms. *J Appl Microbiol* **85**: 583-590.
- Kapuscinski RB & Michell R (1980) Processes controlling virus inactivation in coastal waters. *Water Res* **14**: 363-371.
- Kokjohn TA, Sayler GS & Miller RV (1991) Attachment and replication of *Pseudomonas aeruginosa* bacteriophages under conditions simulating aquatic environments. *Gen Microbiol* **137**: 661-666.
- Lawrence JR, Korber DR, Wolfaardt GM, Caldwell DE & Neu TR (2002) Analytical imaging and microscopy techniques. *Manual of environmental microbiology, second edition*, (Hurst CJ, Crawford RL, Knudsen GR, McInerney MJ & Stetzenbach LD, eds.), p. 39-61. ASM, Whashington DC.
- Lemke M, Wickstrom C & Leff L (1997) A preliminary study on the distribution of viruses and bacteria in lotic environments. *Arch Hydrobiol* **141**: 67-74.
- Leppard GG, Heissenberger A & Herndl GJ (1996) Ultrastructure of marine snow. I. Transmission electron microscopy methodology. *Mar Ecol Prog Ser* **135**: 289-298.
- Luef B, Aspetsberger F, T. Hein, Huber F & Peduzzi P (2007) Impact of hydrology on free-living and particle-associated microorganisms in a river floodplain system (Danube, Austria). *Freshwater Biol* **52**: 1043 - 1057.
- Luef B, Neu TR, Zweimüller I & Peduzzi P (submitted) The potential of Confocal Laser Scanning Microscopy in combination with statistical and image analysis to investigate volume, structure and composition of riverine aggregates. *Limnol Oceanogr*.
- Mari X, Kerros M-E & Weinbauer MG (2007) Virus attachment to transparent exopolymeric particles along trophic gradients in the southwestern lagoon of New Caledonia. *Appl Environ Microbiol* **73**: 5345-5252.
- Neu TR (2000) *In situ* cell and glycoconjugate distribution in river snow studied by confocal laser scanning microscopy. *Aquat Microb Ecol* **21**: 85-95.
- Neu TR & Lawrence JR (1999) Lectin-binding analysis in biofilm systems. *Methods Enzymol* **310**: 145-152.
- Neu TR, Swerhone GDW & Lawrence JR (2001) Assessment of lectin-binding analysis for *in situ* detection of glycoconjugates in biofilm systems. *Microbiology* **147**: 299-313.

- Neu TR, Woelfl S & Lawrence JR (2004) Three-dimensional differentiation of photo-autotrophic biofilm constituents by multi-channel laser scanning microscopy (single-photon and two-photon excitation). *J Microbiol Methods* **56**: 161-172.
- Noble RT & Fuhrman JA (1998) Use of SYBR Green I for rapid epifluorescence counts of marine viruses and bacteria. *Aquat Microb Ecol* **14**: 113-118.
- Peduzzi P & Weinbauer MG (1993) Effect of concentrating the virus-rich 2-200 nm size fraction of seawater on the formation of algal flocs (marine snow). *Limnol Oceanogr* **38**: 1562-1565.
- Peduzzi P & Luef B (2008) Viruses, bacteria and suspended particles in a backwater and main channel site of the Danube (Austria). *Aquat Sci* **70**: 186-194.
- Peduzzi P & Luef B (in press) Viruses. *Encyclopedia of Inland Waters*, (Likens GE, ed.), Elsevier, Oxford.
- Proctor LM & Fuhrman JA (1991) Roles of viral infection in organic particle flux. *Mar Ecol Prog Ser* **69**: 133-142.
- Ripp S & Miller RV (1995) Effects of suspended particulates on the frequency of transduction among *Pseudomonas aeruginosa* in a freshwater environment. *Appl Environ Microbiol* **61**: 1214-1219.
- Schmidt R, Wurm CA, Jakob S, Engelhardt J, Egner A & Hell SW (2008) Spherical nanosized focal spot unravels the interior of cells. *Nat Methods* **5**: 539-544.
- Simon M, Grossart H-P, Schweitzer B & Ploug H (2002) Microbial ecology of organic aggregates in aquatic ecosystems. *Aquat Microb Ecol* **28**: 175-211.
- Staudt C, Horn H, Hempel DC & Neu TR (2003) Screening of lectins for staining lectin-specific glycoconjugates in the EPS of biofilms. *Biofilms in medicine, industry and environmental technology*, (Lens P, Moran AP, Mahony T, Stoodley P & O'Flaherty V, eds.) p. 308-327. IWA Publishing, UK.
- Staudt C, Horn H, Hempel DC & Neu TR (2004) Volumetric measurement of bacterial cells and extracellular polymeric substance glycoconjugates in biofilms. *Biotechnol Bioeng* **88**: 585-592.
- Sutherland IW, Hughes KA, Skillman LC & Tait K (2004) The interaction of phage and biofilms. *FEMS Microbiol Lett* **232**: 1-6.
- Suttle CA & Chen F (1992) Mechanisms and rates of decay of marine viruses in seawater. *Appl Environ Microbiol* **58**: 3721-3729.

Weinbauer MG, Beckmann C & Höfle MG (1998) Utility of green fluorescent nucleic acid dyes and aluminium oxide membrane filters for rapid epifluorescence enumeration of soil and sediment bacteria. *Appl Environ Microbiol* **64**: 5000-5003.

Weinbauer MG (2004) Ecology of prokaryotic viruses. *FEMS Microbiol Rev* **28**: 127-181.

Wen K, Ortmann AC & Suttle CA (2004) Accurate estimation of viral abundance by epifluorescence microscopy. *Appl Environ Microbiol* **70**: 3862-3867.

Wommack KE & Colwell RR (2000) Virioplankton: viruses in aquatic ecosystem. *Microbiol Mol Biol Rev* **64**: 69-114.

Xavier JB, Schnell A, Wuertz S, Palmer R, White DC & Almeida JS (2001) Objective threshold selection procedure (OTS) for segmentation of scanning laser confocal microscope images. *J Microbiol Methods* **47**: 169-180.

Table 1: Quantification of viruses and bacteria on riverine aggregates on cryo-sections. VBR: virus to bacterium ratio.
n: number of analyzed cryo-sections.

		n	minimum	maximum	mean	standard error
spring	bacteria ($\times 10^8 \text{ cm}^{-3}$ specific glycoconjugate)	34	0.35	96.02	17.27	3.39
	viruses ($\times 10^8 \text{ cm}^{-3}$ specific glycoconjugate)	34	1.75	53.86	18.77	2.42
	VBR	34	0.39	5.00	1.65	0.18
summer	bacteria ($\times 10^8 \text{ cm}^{-3}$ specific glycoconjugate)	33	0.20	7.45	1.55	0.25
	viruses ($\times 10^8 \text{ cm}^{-3}$ specific glycoconjugate)	33	0.31	11.47	2.48	0.40
	VBR	33	0.24	8.00	2.25	0.32

Figure legends

Figure 1: CLSM maximum intensity projection showing particle-derived viruses and bacteria on a filter after sonication. White arrows point to viruses, yellow ones to bacteria. Calibration bar: 5 μm .

Figure 2: CLSM image series of a riverine aggregate in axial direction. Dual channel presentation of specific glycoconjugates, bacteria and viruses. Images were collected at a step size of 0.2 μm . Arrow points to viruses. Color allocation: nucleic acid = green, glycoconjugates = red. Calibration bar: 30 μm .

Figure 3: 3-D volume reconstructions from a riverine aggregate. (a) and (b) represent different views of the aggregate. Arrows point to viruses. Color allocation: nucleic acid = green, glycoconjugates = red. Calibration grid: 5 μm .

Figure 4: Single scan of a cryo-section showing distribution of viruses, bacteria and glycoconjugates inside an aggregate (a). View of one channel to present bacteria and viruses (b). White arrows point to viruses. Color allocation: nucleic acid = green, glycoconjugates = red. Calibration bar: 10 μm .

Figure 5: 3-D volume reconstruction from a riverine aggregate. For deconvolution the method classic maximum likelihood estimation was applied. The program Huygens 3.0.0, SVI (Scientific Volume Imaging b.v., Netherland) was used. Arrows point to viruses. Color allocation: nucleic acid = green, glycoconjugates = red. Calibration grid: 5 μm .

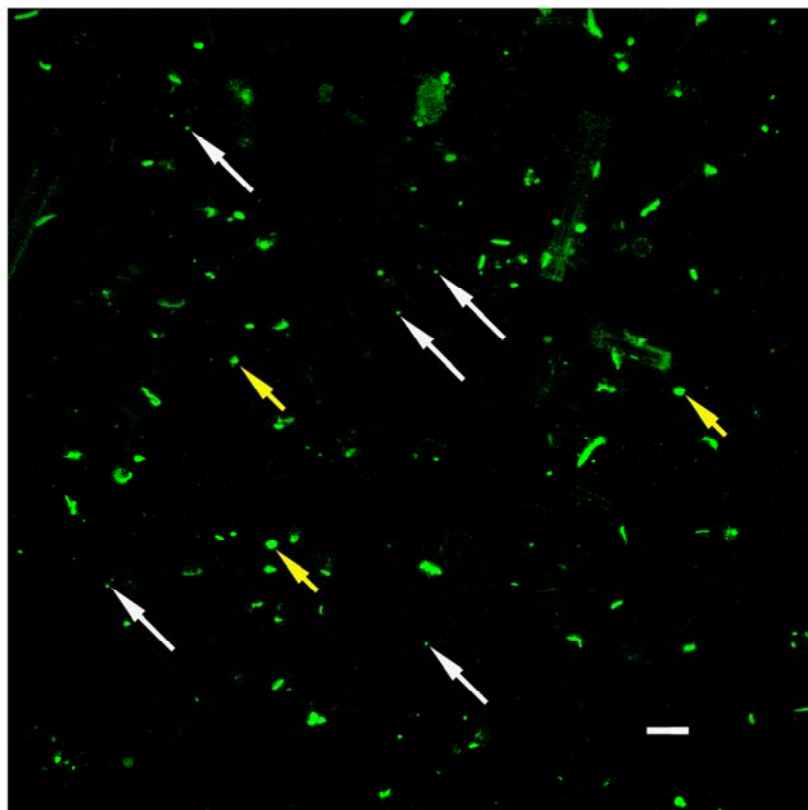


Figure 1

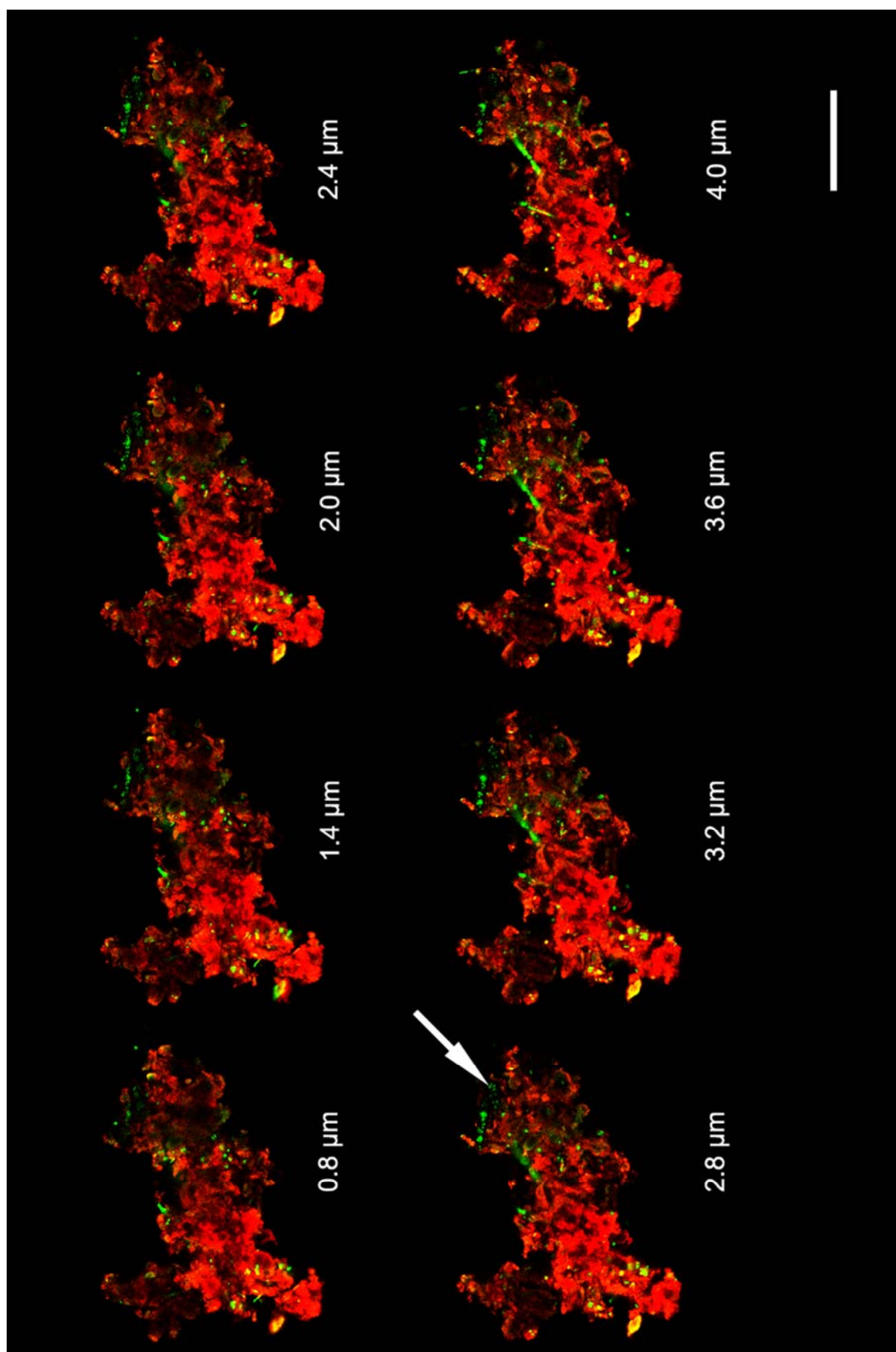


Figure 2

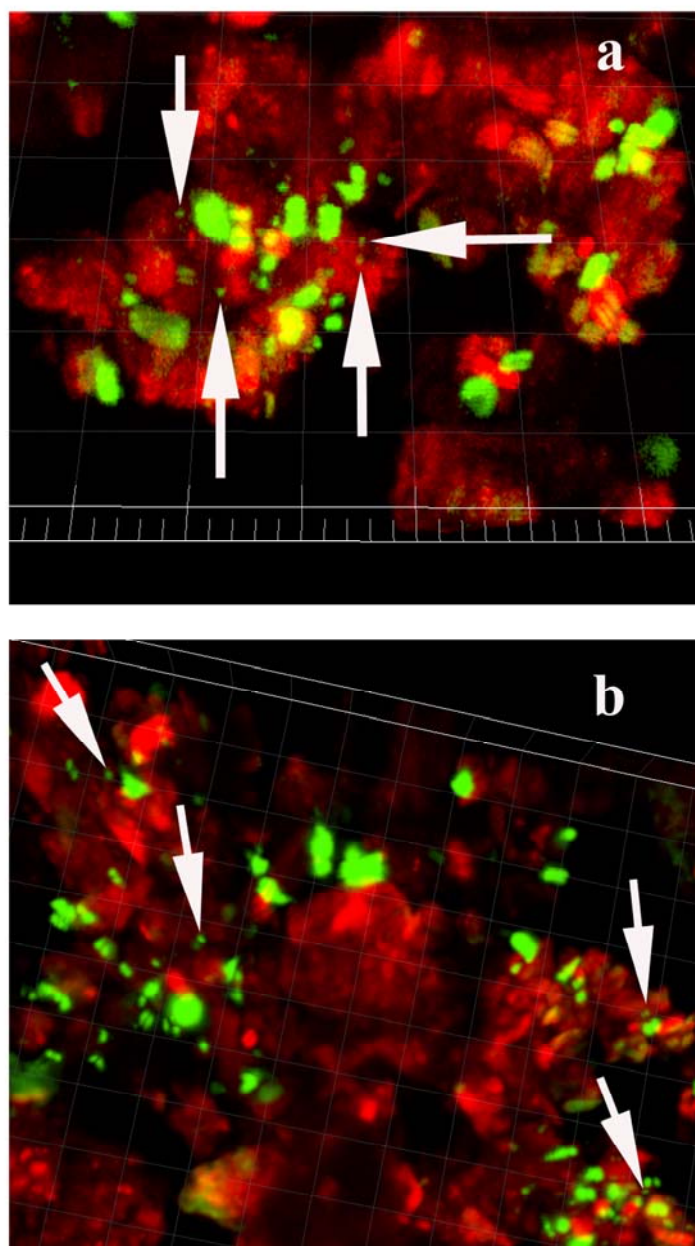


Figure 3

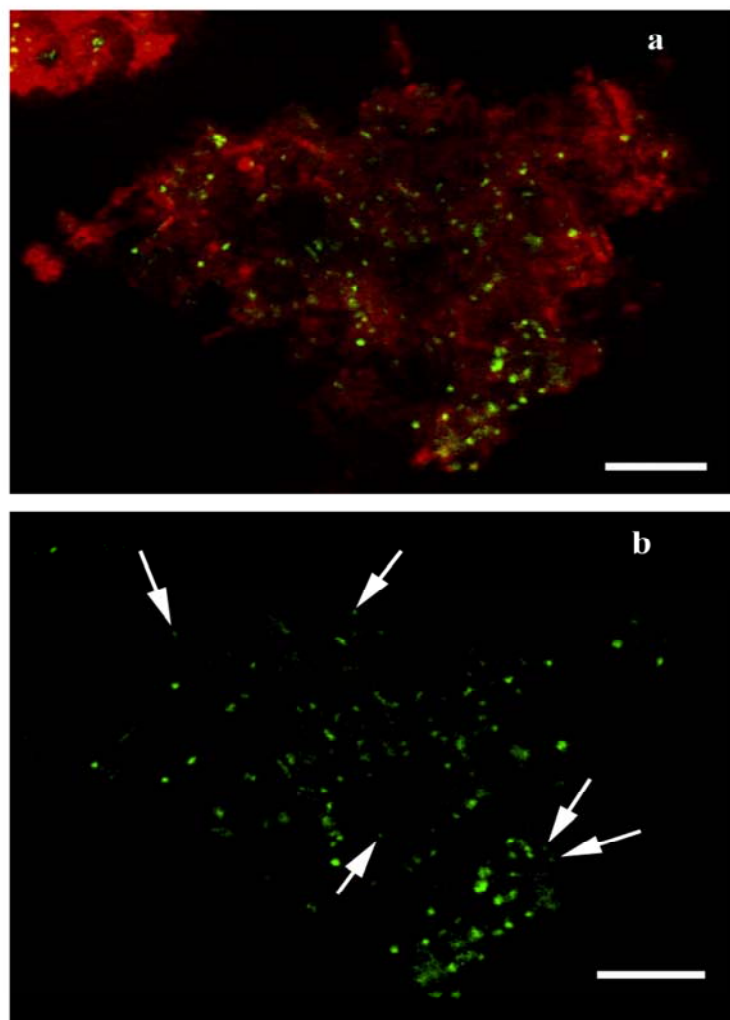


Figure 4

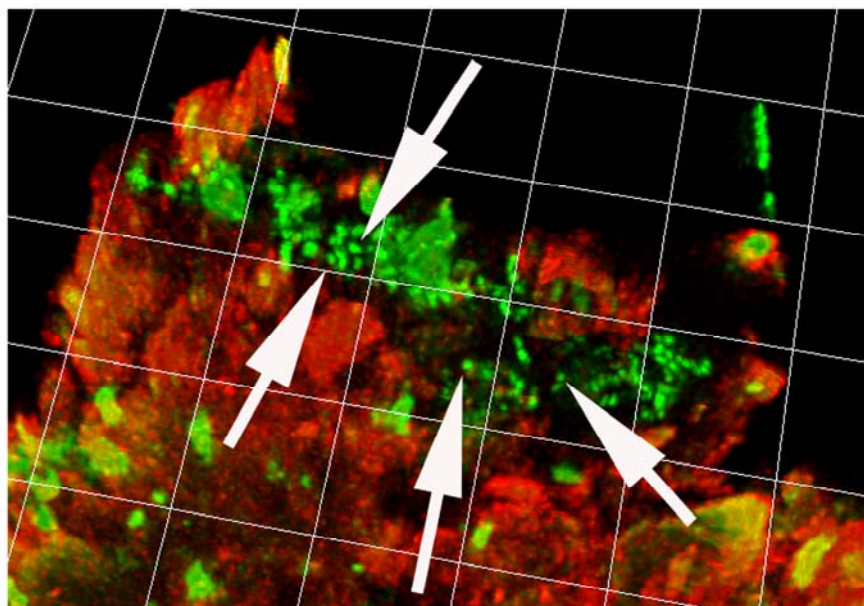


Figure 5

Chapter 4

Online Program “VIPCAL” for Calculating Lytic Viral Production and Lysogenic Cells Based on a Viral Reduction Approach

Birgit Luef, Franz Luef and Peter Peduzzi

(under revision at Environmental Microbiology)

Abstract

Assessing viral production (VP) requires robust methodological settings combined with precise mathematical calculations. This contribution improves and standardizes mathematical calculations of VP and the assessment of the proportion of lysogenic cells in a sample. We present an online tool “**Viral Production Calculator**” (VIPCAL, <http://www.univie.ac.at/nuhag-php/vipcal>) that calculates lytic production and the percentage of lysogenic cells based on data obtained from a viral reduction approach (VRA). The main advantage of our method lies in its universal applicability, even to different piecewise-linear curves. We demonstrate the application of our tool for calculating lytic VP and the proportion of lysogenic bacteria in an environmental sample. The program can also be used to calculate different parameters for estimating virus-induced mortality, including the percentage of lytically infected cells, lysis rate of bacteria, percentage of bacterial production lysed, proportion of bacterial loss per day, viral turnover time as well as dissolved organic carbon and nitrogen release. VIPCAL helps avoid differences in the calculation of VP and diverse viral parameters between studies and laboratories, which facilitates interpretation of results. This tool represents a methodological step forward that can help improve our understanding of the role of viral activity in aquatic systems.

Introduction

Aquatic viruses infect all members of the microbial food web and are significant biological agents in microbial processes (Fuhrman, 1999). Estimates of bacterial mortality due to phage production suggest that viruses can be responsible for up to 100 % of bacterial mortality (Proctor and Fuhrman, 1990; Proctor et al., 1993; Hennes and Simon, 1995; Noble and Fuhrman, 2000). Moreover, viruses may significantly impact natural bacterial abundance, productivity and community composition (Fuhrman and Schwalbach, 2003; Schwalbach et al., 2004; Weinbauer, 2004; Hewson and Fuhrman, 2006; Bouvier and del Giorgio, 2007). Therefore, information on viral survival mechanisms and viral life strategies is of considerable interest. Viruses display different types of life cycles, the most common being lytic and lysogenic infections. In most aquatic environments, the lytic cycle is the dominant method of viral replication and ultimately destroys the infected cells. In the lysogenic cycle, the phage infects a host cell and the phage’s genome typically remains in the host in a dormant stage known as a prophage. The prophage replicates along with the host until environmental stimuli such as UV radiation, temperature etc. cause proliferation of new phages via the lytic cycle (see review of Weinbauer, 2004). Lysogeny may be an important

survival mechanism for viruses where host densities or resources are low (Wilson and Mann, 1997) or when the destruction rate of free phages is too high to allow for lytic replication (Lenski, 1988). Temperate viruses may affect host assemblage composition, either by lysis or by other mechanisms, e.g., by resistance to lytic virus infection (Hewson and Fuhrman, 2007a). Lysogeny also occurs in natural populations of the Cyanobacteria such as *Synechococcus* spp. (Ortmann et al., 2002), and this interaction exhibits a seasonal pattern (McDaniel et al., 2002).

Estimating the significance of the lysogenic pathway in natural viral populations requires determining the percentage of cells that are lysogens. Different approaches have been used to assess the frequency of lysogenic cells: (Jiang and Paul, 1994) searched for lysogenic strains within cultures of marine bacteria using mitomycin C. Water samples were directly exposed to an inducing agent (sunlight, mitomycin C) to estimate the lysogenic frequency within bacteria (Jiang and Paul, 1996; Cochran and Paul, 1998; Williamson et al., 2002). In these studies, lysogenic induction from natural bacterioplankton was investigated based on significant changes in viral (increase) and bacterial (decreases) abundances.

A very comprehensive overview of assumptions, advantages and disadvantages of different viral production (VP) techniques is given in Winget et al. (2005). The viral reduction approach (VRA) provides rapid and reproducible estimates of VP, which can be measured directly (Weinbauer and Suttle, 1996; McDaniel et al., 2002; Weinbauer et al., 2002; Wilhelm et al., 2002; Hewson and Fuhrman, 2003; Mei and Danovaro, 2004; Winter et al., 2004; Helton et al., 2005; Winget et al., 2005; Hewson and Fuhrman, 2007b; Williamson et al., 2008). VRA allows direct observation of VP from natural microbial communities if certain assumptions are made (see Winget et al., 2005). In this approach, the viral abundance of a water sample is reduced with virus-free water in order to minimize or even to stop new infections. This technique allows monitoring even small changes in the lytically produced viral abundance based on changes in viral direct counts (VDC) over time. Additionally, when estimating the amount of lysogens within bacteria, water samples have to be treated with an inducing agent. To induce the lytic cycle in lysogenized bacteria, mitomycin C and UV C radiation are the most powerful agents (Jiang and Paul, 1994; Wilcox and Fuhrman, 1994; Jiang and Paul, 1996; Weinbauer and Suttle, 1996; Tapper and Hicks, 1998). If the inducing agent stimulates virus release, the abundance of viruses increases in the water samples.

In order to obtain a standardized, improved calculation, we programmed an online tool for estimating lytically and lysogenically produced viruses during a VRA. We demonstrate the application of our program for assessing lytic VP and the proportion of lysogenic cells in

environmental samples. Furthermore, other viral parameters can be calculated, including the percentage of lytically infected cells, lysis rate of bacteria, percentage of bacterial production lysed, proportion of bacterial loss per day, viral turnover time as well as dissolved organic carbon and nitrogen release.

Materials and Methods

Study site

The samples for the experiments were collected from the Danube River (Vienna, Austria) and an isolated subsystem called Lobau. The study site and the sampling stations are published elsewhere (Peduzzi and Luef, 2008).

Virus production (VP) – experimental design of the virus reduction approach (VRA)

To measure VP, a VRA was used and performed as follows: A prokaryotic concentrate was produced. Due to very high particle loads, sample water was pre-filtered through 3.0 µm pore size filters (SSWP, 47 mm diameter, Millipore). 200 mL of this filtered water was concentrated to approx. 1 mL using Vivaspins (20 mL concentrator, Membrane: 0.2 µm PES, VivaScience AG, Sartorius Group, Hannover, Germany) by repeated centrifugation for 1 min at 2900 rpm using a Beckmann table centrifuge. The filter was never allowed to fully dry. Then the concentrate was diluted with virus-free water (from the same water sample) up to 3 mL. To obtain virus-free water, 3.0 µm pre-filtered sample water was first filtered through 0.22 µm Sterivex (Sterivex GV 0.22 µm, Millipore). This filtrate was further passed through filter cartridges (Vivaflow 50, 30,000 Dalton cut off, Hannover, Germany) using a peristaltic pump. An aliquot of the prokaryotic concentrate was added to 50 mL virus-free ultrafiltrate. Two types of incubations, which were done in duplicates, were performed simultaneously per sample: To the first incubation, mitomycin C (Roth, Karlsruhe, Germany) was added at a final concentration of 1.0 µg mL⁻¹. The second one was incubated without the antibiotic. Subsamples were taken every 4 to 6 h for a total period of up to 24 h to enumerate viruses at regular intervals. At the start of the experiment, bacterial abundance was also determined. The experiments were performed at *in situ* temperature in the dark.

Abundance of viruses and bacteria

For assessing viral and bacterial abundances of the prefiltered samples, water samples were fixed with formaldehyde (2 % final concentration). Samples were filtered onto Anodisc filters (pore size 0.02 µm, 25 mm diameter, Whatman, Maidstone, England). The filters were stored

at -20 °C in a freezer until further processing. Viruses and bacteria were stained with SYBR Gold (Molecular Probes, Eugene, Oregon, USA). Slides were prepared by using a modified method of Noble and Fuhrman (1998). The original SYBR Gold stock solution (10,000x) was diluted to a working solution (3.3x) before use. The filters were stained sample side up for 20 min in a plastic petri dish in the dark. After staining, the filters were placed on a Kimwipe until they were dry. Each filter was then mounted on a glass slide with an antifade mounting solution (Citifluor AF1, Citifluor, London, UK) and was inspected immediately. Microorganisms were enumerated under an epifluorescence microscope (Nikon E 800, Nikon, Tokyo, Japan) at 1250-fold magnification. On each filter, twenty to thirty fields were counted to determine the total number of viruses and bacteria.

Bacterial secondary production (BSP)

BSP of the free-living fraction was determined by prefiltering samples through a 3.0 µm filter (Millipore TSTP, 47 mm diameter). BSP was assessed using the [³H]-thymidine incorporation technique (Fuhrman and Azam, 1982) and applying a conversion factor proposed by Bell (1993). Triplicate samples (5 mL) were incubated for 0.5 to 1 h at in situ temperature in the laboratory. Two sub-samples were treated with formalin and served as a blank.

Determination of the burst size

Aliquots of unfiltered water (10 mL) were fixed with glutaraldehyde (2% final concentration) and were immediately centrifuged onto Formvar-coated copper grids (400 mesh) in a swing-out rotor (SW41Ti, Beckman) at 6000 x g and 4 °C for 1 h. Grids were stained with 1% uranyl acetate for about 1 min and rinsed 3 times with deionized distilled water. Transmission electron microscopy (Zeiss EM 902), operated at 80 kV, was used to estimate the sample-specific burst size as the average number of viral particles in all visibly infected bacteria (Weinbauer et al., 1993). A bacterium was infected when phages inside the cells could be clearly recognized based on their shape and size.

Results and Discussion

Computations of VP

Lytic viral production estimated by the virus reduction approach was initially published by Wilhelm et al. (2002). Viral production rates were determined from first-order regressions of viral abundance vs. time, thus implying a continuous increase in viral abundance.

Weinbauer et al. (2002) published a model for estimating lytic and lysogenic VP as follows: Lytic VP is the difference between viral abundance in the stationary phase of the incubations without added mitomycin C and viral abundance at the start of the experiment. Lysogenic VP is the difference between viral abundance in the incubations with and without mitomycin C-treatment.

For lytic VP, Winter et al. (2004) developed the model further and discussed the potential occurrence of 2 peaks in viral abundance during the incubations. Lytic VP was calculated as the slope between the minimum (V_{\min}) and the maximum viral abundance (V_{\max}). For experiments in which 2 peaks of viral abundance occurred, VP was calculated according to the following formula:

$$VP = [(V_{\max 1} - V_{\min 1}) + (V_{\max 2} - V_{\min 2})] / (t_{\max 2} - t_{\min 1}),$$

where t = time (incubated hours). Lysogenic VP was not considered in this study.

Figure 1 displays different outcomes of VRAs throughout our experimental incubations. Comparing VDC (with and without mitomycin C) at the commencement of an experiment sometimes revealed a difference in these two treatments (Fig. 1b, c). Continuous growth in viral abundance, as observed by Wilhelm et al. (2002), was rarely found (Fig. 1a). In some of our incubations, viral abundance decreased or remained constant before it increased (Fig. 1b, c). Instead of a continuous increase, two or sometimes even three increases in viral abundance, followed by decreases, were observed (Fig. 1c). This was also reported by Winter et al. (2004) and Winget et al. (2005). Explanations for this viral response in experimental incubations include the release of viruses with different latent periods as well as new infection and cell death from viruses released in early lysis events.

Hence, our approach for the computation of the lytic VP rates in a VRA is as follows:

Let $VDC_{\min 1}, VDC_{\max 1}, \dots, VDC_{\min n}, VDC_{\max n}$ be the starting and end points and $t_{\min 1}, t_{\max 1}, \dots, t_{\min n}, t_{\max n}$ the time-intervals between min and max values. Then

$$VP = [(VDC_{\max 1} - VDC_{\min 1}) / (t_{\max 1} - t_{\min 1}) + \dots + (VDC_{\max n} - VDC_{\min n}) / (t_{\max n} - t_{\min n})] / n$$

is the mean lytic VP for the experiment.

Regarding the viral abundances without mitomycin C, lytic VP in the experiment is determined for each time period with a net increase. Calculating the arithmetic mean of these VP rates gives the mean lytic VP per hour.

Using the above-mentioned models by Weinbauer et al. (2002) and Winter et al. (2004), problems in the computation of lysogenic VP can arise due to (i) different viral abundances at the onset of the experiment, (ii) the occurrence of 2 or more peaks in viral abundance and (iii)

different slopes of the two curves (with and without mitomycin C), sometimes causing several points of intersection.

Therefore, in our study, the lysogenic VP is represented by a difference curve, which is developed by calculating

$$VDC_{\text{mitomycin C}} - VDC_{\text{without mitomycin C}}$$

for the whole experiment.

Hence, the lysogenic VP rate for each net increase is computed from the difference curve as follows:

Let $VDC_{\min 1}$, $VDC_{\max 1}$, ..., $VDC_{\min n}$, $VDC_{\max n}$ be the starting and end points and $t_{\min 1}$, $t_{\max 1}$, ..., $t_{\min n}$, $t_{\max n}$ the time-intervals between min and max values of the difference curve. Then

$$VP = [(VDC_{\max 1} - VDC_{\min 1}) / (t_{\max 1} - t_{\min 1}) + \dots + (VDC_{\max n} - VDC_{\min n}) / (t_{\max n} - t_{\min n})]$$

is the whole lysogenic VP within the experiment.

If the VDCs are higher in the treatment without mitomycin C than in the treatment with mitomycin C (which may occasionally occur), then the difference curve reaches values less than or equal to zero. In this case, the lysogenic VP of the experiment is usually simply computed from the time-periods in which the difference curve has values greater than or equal to zero (Fig. 2c). Combining the approaches of Weinbauer et al. (2002) and Winter et al. (2004) sometimes yields negative values because the differences in slopes are not taken into account. Therefore, the computation of a difference curve ensures consistent calculation of positive values of lysogenically produced viruses.

Finally, the lysogenic viral production is translated into the percentage of lysogenic cells. The slope of the difference curve is equal to the lysogenic production rate, if there is a continuous increase of the lysogenically produced viruses during an experiment. When 2 peaks in viral abundance occur during the incubations, we add up the lysogenic viral production in the time-periods with a net increase. This yields the following formula for the proportion of lysogenic cells:

$$\% \text{ of lysogenic cells} = 100 \times [(VP_{\text{lysogenic } 1}) / BS \times B_0] + \dots + 100 \times [(VP_{\text{lysogenic } n}) / BS \times B_0].$$

Demonstration of the program VIPCAL

We developed the program VIPCAL, which computes the lytic VP and the percentage of lysogenic cells based on data from a VRA. Parameters describing virus-induced mortality can also be calculated (Tab. 1).

The program, which is written in PHP-scripts, is an online tool available at <http://www.univie.ac.at/nuhag-php/vipcal>. The main advantage of our method lies in its universal applicability to all possible outcomes of a VRA-experiment.

Here, we demonstrate the application of the program for calculating lytic VP and the proportion of lysogenic cells in an environmental sample (Fig. 2). After starting the program, you can choose between two modes, a demo that introduces the program based on an example, and another for the input of new data. When choosing “new data”, the input field appears (Fig. 2a) and the sampling times have to be entered first. After entering each data point, press the enter button. Then enter the viral abundances – incubated with and without mitomycin C – for each sampling point of the experiment. Note, that for correct calculation using VIPCAL, the VDC values must be expressed in 10^6 mL^{-1} . Replicates of viral abundance determinations can be entered. Separate each value by a semicolon. For further calculations, the program uses the mean viral abundance of each sampling point. Entering only the VDC without mitomycin C yields only lytic VP. Enter the following parameters to compute the percentage of lytically infected cells, lysis rate of bacteria, percentage of bacterial production lysed (also often called virus-mediated mortality), proportion of bacterial loss per day, viral turnover time and dissolved organic carbon and nitrogen release: bacterial abundance at the beginning of the VRA (in 10^6 mL^{-1} ; replicates of bacterial abundance counts can be entered); viral and bacterial abundance (in 10^6 mL^{-1}), bacterial secondary production (in $10^6 \text{ cells mL}^{-1} \text{ h}^{-1}$), the burst size in the original sample, as well as the carbon and nitrogen contents of a bacterial cell (e.g. Lee and Fuhrman, 1987; Simon and Azam, 1989; Fukuda et al., 1998; Gundersen et al., 2002). You can enter a variety of burst sizes. Separate each burst size by a semicolon. After entering all the data, press the pushbutton “compute”, and VIPCAL calculates the lytic and lysogenic VP of the respective experiment. When the results appear on the applet window, the mean lytic VP is calculated (Fig. 2b). If you press the “plot-button”, a graphic representation of the two experimental curves (with and without mitomycin C) is provided, along with the computed difference curve, which corresponds to the lysogenically produced viral abundances (Fig. 2c). Based on the VRA the percentage of lysogenic cells is computed. Calculating the proportion of lysogenic cells provides information on whether the investigated environment favours the lysogenic life cycle or not. Note, however, that manipulations during the VRA may alter the proportions within the bacterial community. The calculation of the percentage of lysogenic cells is based on the assumption that the burst size is the same in lytically and lysogenically infected cells. Furthermore, not all lysogens can be induced with mitomycin C; therefore, this method most likely estimates the minimum percentage of bacteria in a community that are lysogens (Ortmann et al., 2002).

The necessary manipulation steps in a VRA often reduce the initial bacterial abundance in the incubation. Therefore, VP estimates for the original environment should be corrected for the

loss of bacteria between the original water and the incubation (Wilhelm et al., 2002; Winget et al., 2005). In VIPCAL, lytic VP rates can be corrected by the loss-ratio of the bacterial abundance in the incubations at the beginning of the experiment. With this correction, the lytic VP has additional relevance for an investigated environment. If you enter the parameters “bacterial abundance at the beginning of the VRA” and “viral and bacterial abundance”, their “secondary production” and the “burst size” in the original sample, as well as “carbon and nitrogen contents of bacterial cell”, then VIPCAL also calculates the percentage of lytically infected cells, lysis rate of bacteria, percentage of bacterial production lysed, proportion of bacterial loss per day, viral turnover time, and dissolved organic carbon and nitrogen release. When mousing over the calculated parameter, a pop-up window appears containing the respective equation.

If you enter more than one burst size, all the parameters are firstly calculated based on the first entered burst size. Pressing the “next burst size-button” calculates the values based on the second entered burst size and so on.

All entered parameters are saved in the input field (depending on the IP address of the computer). If you want to change a parameter, simply move back to the input field, change the specific value, and re-press “compute”. All results are saved as csv (comma separated values) and can easily be exported into an Excel file.

Although VIPCAL was developed to investigate lytic VP and lysogeny in heterotrophic bacteria, this program can, at least in principle, also be used to calculate viral parameters for infection of Cyanobacteria such as *Synechococcus* spp.

Conclusions

VIPCAL quantifies lytic and lysogenic VPs in a VRA and estimates the percentage of lysogenic cells. It can also calculate various viral parameters such as the percentage of lytically infected cells, lysis rate of bacteria, percentage of bacterial production lysed, proportion of bacterial loss per day, viral turnover times and dissolved organic carbon and nitrogen release. This helps characterize an environment based on the impact of lytic and lysogenic life cycles.

Using VIPCAL helps avoid differences between various studies or laboratories in calculating viral parameters, which facilitates the interpretation of results. Continuing methodological improvements such as the quantification of lytic and lysogenic viral pathways reveals more about the impact of viral infection on prokaryotes in aquatic ecosystems.

Acknowledgements

A grant (P17798) from the Austrian Science Fund (FWF) to P. P. supported this work.

We are grateful to H. Schwab for mathematical discussions and for computer programming.

Thanks are due to M. Weinbauer for discussions and to I. Kolar, M. Moeseneder and O. Zambiasi for help during sampling and incubations. Very helpful and valuable comments were provided by two anonymous reviewers on an early manuscript version.

References

- Bell, R.T. (1993) Estimating production of heterotrophic bacterioplankton via incorporation of tritiated thymidine. In *Handbook of Methods in Aquatic Microbial Ecology*. Kemp, P.F., Sherr, B.F., Sherr, E.B., and Cole, J.J. (eds). Boca Raton, FL, U.S.A.: Lewis Publishers, pp. 495-503.
- Cochran, P., and Paul, J. (1998) Seasonal abundance of lysogenic bacteria in a subtropical estuary. *Appl Environ Microbiol* **64**: 2308-2312.
- Fuhrman, J.A. (1999) Marine viruses and their biogeochemical and ecological effects. *Nature* **399**: 541-548.
- Fuhrman, J.A., and Azam, F. (1982) Thymidine incorporation as a measure of heterotrophic bacterioplankton production in marine surface waters: evaluation and field results. *Mar Biol* **66**: 109-120.
- Fuhrman, J.A., and Schwalbach, M. (2003) Viral influence on aquatic bacterial communities. *Biol Bull* **204**: 192-195.
- Fukuda, R., Ogawa, H., Nagata, T., and Koike, I. (1998) Direct determination of carbon and nitrogen contents of natural bacterial assemblage in marine environments. *Appl Environ Microbiol* **64**: 3352-3358.
- Gundersen, K., Heldal, M., Norland, S., Purdie, D., and Knap, A. (2002) Elemental C, N, and P cell content of individual bacteria collected at the Bermuda Atlantic time-series study (BATS) site. *Limnol Oceanogr* **47**: 1525-1530.
- Helton, R.R., Cottrell, M.T., Kirchman, D.L., and Wommack, K.E. (2005) Evaluation of incubation-based methods for estimating virioplankton production in estuaries. *Aquatic Microb Ecol* **41**: 209-219.
- Hennes, K.P., and Simon, M. (1995) Significance of bacteriophages for controlling bacterioplankton growth in a mesotrophic lake. *Appl Environ Microbiol* **61**: 333-340.
- Hewson, I., and Fuhrman, J.A. (2003) Viriobenthos production and virioplankton sorptive scavenging by suspended sediment particles in coastal and pelagic waters. *Microb Ecol* **46**: 337-347.
- Hewson, I., and Fuhrman, J. (2006) Viral impacts upon marine bacterioplankton assemblage structure. *J Mar Biol Ass U.K.* **86**: 577-589.
- Hewson, I., and Fuhrman, J. (2007a) Characterization of lysogens in bacterioplankton assemblages of the Southern California Borderland. *Microb Ecol* **53**: 631-638.

- Hewson, I., and Fuhrman, J. (2007b) Covariation of viral parameters with bacterial assemblage richness and diversity in the water column and sediments. *Deep-Sea Res I* **54**: 811-830.
- Jiang, S.C., and Paul, J.H. (1994) Seasonal and diel abundance of viruses and occurrence of lysogeny/bacteriocinogeny in the marine environment. *Mar Ecol Prog Ser* **104**: 163-172.
- Jiang, S.C., and Paul, J.H. (1996) Occurrence of lysogenic bacteria in marine microbial communities as determined by prophage induction. *Mar Ecol Prog Ser* **142**: 27-38.
- Lee, S., and Fuhrman, J.A. (1987) Relationships between biovolume and biomass of naturally derived marine bacterioplankton. *Appl Environ Microbiol* **53**: 1298-1303.
- Lenski, R.E. (1988) Dynamics of interactions between bacteria and virulent phage. In *Advances in Microbial Ecology*. Marshall, K.C. (ed): Plenum Publishing Corporation, pp. 1-44.
- McDaniel, L., Houchin, L.A., Williamson, S.J., and Paul, J.H. (2002) Lysogeny in marine *Synechococcus*. *Nature* **415**: 496.
- Mei, M.L., and Danovaro, R. (2004) Virus production and life strategies in aquatic sediments. *Limnol Oceanogr* **49**: 459-470.
- Noble, R.T., and Fuhrman, J.A. (1998) Use of SYBR Green I for rapid epifluorescence counts of marine viruses and bacteria. *Aquat Microb Ecol* **14**: 113-118.
- Noble, R.T., and Fuhrman, J.A. (2000) Rapid virus production and removal as measured with fluorescently labeled viruses as tracers. *Appl Environ Microbiol* **66**: 3790-3797.
- Ortmann, A., JE, L., and Suttle, C. (2002) Lysogeny and lytic viral production during a bloom of the cyanobacterium *Synechococcus* spp. *Microb Ecol* **43**: 225-231.
- Peduzzi, P., and Luef, B. (2008) Viruses, bacteria and suspended particles in a backwater and main channel site of the Danube (Austria). *Aquat Sci* **70**: 186-194.
- Proctor, L.M., and Fuhrman, J.A. (1990) Viral mortality of marine bacteria and cyanobacteria. *Nature* **343**: 60-62.
- Proctor, L.M., Okubo, A., and Fuhrman, J.A. (1993) Calibrating estimates of phage-induced mortality in marine bacteria: ultrastructural studies of marine bacteriophage development from one-step growth experiments. *Microb Ecol* **25**: 161-182.
- Schwalbach, M., Hewson, I., and Fuhrman, J. (2004) Viral effects on bacterial community composition in marine plankton microcosms. *Aquat Microb Ecol* **34**: 117-127.
- Simon, M., and Azam, F. (1989) Protein content and protein synthesis rates of planktonic marine bacteria. *Mar Ecol Prog Ser* **51**: 201-213.

- Tappe, M.A., and Hicks, R.E. (1998) Temperate viruses and lysogeny in Lake Superior bacterioplankton. *Limnol Oceanogr* **43**: 95-103.
- Weinbauer, M.G. (2004) Ecology of prokaryotic viruses. *FEMS Microbiol Rev* **28**: 127-181.
- Weinbauer, M.G., and Suttle, C.A. (1996) Potential significance of lysogeny to bacteriophage production and bacterial mortality in coastal waters of the Gulf of Mexico. *Applied and Environmental Microbiology* **62**: 4374-4380.
- Weinbauer, M.G., Fuks, D., and Peduzzi, P. (1993) Distribution of viruses and dissolved DNA along a coastal trophic gradient in the Northern Adriatic Sea. *Applied and Environmental Microbiology* **59**: 4074-4082.
- Weinbauer, M.G., Winter, C., and Höfle, M.G. (2002) Reconsidering transmission electron microscopy based estimates of viral infection of bacterioplankton using conversion factors derived from natural communities. *Aquatic Microbial Ecology* **27**: 103-110.
- Wilcox, R.M., and Fuhrman, J.A. (1994) Bacterial viruses in coastal seawater: lytic rather than lysogenic production. *Mar Ecol Prog Ser* **114**: 35-45.
- Wilhelm, S.W., Brigden, S.M., and Suttle, C.A. (2002) A dilution technique for the direct measurement of viral production: a comparison in stratified and tidally mixed coastal waters. *Microb Ecol* **43**: 168-173.
- Williamson, K., Schnitker, J., Radosevich, M., Smith, D., and Wommak, K. (2008) Cultivation-based assessment of lysogeny among soil bacteria. *Microb Ecol* **56**: 437-447.
- Williamson, S., Houchin, L., McDaniel, L., and Paul, J. (2002) Seasonal variation in lysogeny as depicted by prophage induction in Tampa Bay, Florida. *Appl Environ Microbiol* **68**: 4307-4314.
- Wilson, W.H., and Mann, N.H. (1997) Lysogenic and lytic viral production in marine microbial communities. *Aquat Microb Ecol* **13**: 95-100.
- Winget, D.M., Williamson, K.E., Helton, R.R., and Wommack, K.E. (2005) Tangential flow diafiltration: an improved technique for estimation of virioplankton production. *Aquat Microb Ecol* **41**: 221-232.
- Winter, C., Herndl, G.J., and Weinbauer, M.G. (2004) Diel cycles in viral infection of bacterioplankton in the North Sea. *Aquat Microb Ecol* **35**: 207-216.

Table 1: Computations used in the online tool *Viral Production Calculator (VIPCAL)*. Calculations of virus-related parameters based on a virus reduction approach (VRA) that can be performed with the program VIPCAL.

parameter	formula	reference
calculated parameters from the VRA		
lytic	$\text{mean } VP_{\text{lytic}} = \frac{[(VDC_{\text{max } 1} - VDC_{\text{min } 1}) / (t_{\text{max } 1} - t_{\text{min } 1}) + \dots + (VDC_{\text{max } n} - VDC_{\text{min } n}) / (t_{\text{max } n} - t_{\text{min } n})]}{n}$	this study
% of lytically infected cells	$100 \times [(VP_{\text{lytic } 1} / BS \times B_0) + \dots + 100 \times [(VP_{\text{lytic } n} / BS \times B_0)]$	Jiang and Paul, 1994 Weinbauer and Suttle, 1996 Weinbauer et al., 2002 Winter et al., 2004
lysogenic	$100 \times [(VP_{\text{lysogenic } 1} / BS \times B_0) + \dots + 100 \times [(VP_{\text{lysogenic } n} / BS \times B_0)]$	Jiang and Paul, 1994 Weinbauer and Suttle, 1996 Weinbauer et al., 2002 Tapper and Hicks, 1998
other ecologically relevant parameters		
lytic	$VP_{\text{lytic}} \times (B_{\text{os}} / B_0)$	Wilhelm et al., 2002
lytic rate of bacteria (cells $\text{mL}^{-1} \text{h}^{-1}$)	lytic VP_{os} / BS	Hewson and Fuhrman, 2007b
% of bacterial production lysed **	lysis rate of bacteria / BSP_{os}	Hewson and Fuhrman, 2007b
% of bacterial loss per day	lysis rate of bacteria $\times 100 / B_{\text{os}} \times 24$	Hewson and Fuhrman, 2007b
viral turnover time (h^{-1})	lytic $VP_{\text{os}} / V_{\text{os}}$	Wilhelm et al., 2002
DOC release (g C $\text{mL}^{-1} \text{h}^{-1}$) ***	lysis rate of bacteria \times elemental carbon content of a bacterium	
DON release (g N $\text{mL}^{-1} \text{h}^{-1}$) ***	lysis rate of bacteria \times elemental nitrogen content of a bacterium	

VP_{lytic} : lytic viral production from the experiment
 VDC_{max} , VDC_{min} : maximal (max) and minimal (min) viral direct counts in a time-period with a net-increase; index n denotes the number of peaks
 t_{max} , t_{min} : time-period with a net-increase in viral direct counts; index n denotes the number of peaks
 $VP_{lytic\ 1,...,n}$, $VP_{lytic\ n}$: lytic viral production from the experiment; index n denotes the number of peaks
 BS: burst size; it is assumed that the rate of viruses produced per cell is not affected by dilution
 B_0 : bacterial abundance at the beginning of the experiment
 * based on the assumption that the burst size is the same in lytic and lysogenic infected cells
 $VP_{lysogenic\ 1,...,n}$, $VP_{lysogenic\ n}$: lysogenic viral production from the experiment; index n denotes the number of peaks
 lytic VP_{os} : lytic viral production in the original sample
 B_{os} : bacterial abundance in the original sample
 ** also termed virus mediated mortality (VMM)
 BSP_{os} : bacterial secondary production in the original sample
 V_{os} : viral abundance in the original sample
 DOC: dissolved organic carbon
 DON: dissolved organic nitrogen
 *** release includes virus particles

Figure legends

Figure 1: *Changes of viral abundances over time in three independent virus reduction experiments.* The outcome of the virus reduction approaches (VRAs) exhibits different shapes of curves. Samples were taken from the Danube River on 05/23/2006 (A) and from an isolated subsystem known as Lobau on 05/29/2006 (B) and on 10/17/2005 (C).

Figure 2: *Screen shot of the online tool Viral Production Calculator (VIPCAL).* Input (A) and output (B) windows - data and graphic representation of curves (C) - of the applet VIPCAL. VIPCAL calculates and plots the development of viral abundances (with and without mitomycin C) during the time of incubation (in hours) of a viral reduction approach. Calculated lytic and lysogenic viral production and various other viral parameters for an environmental sample are presented.

The graph (C) shows the averages of the duplicate incubations. The error bars represent the range of the duplicate incubations. If the error bars are absent, they are smaller than the width of the symbol.

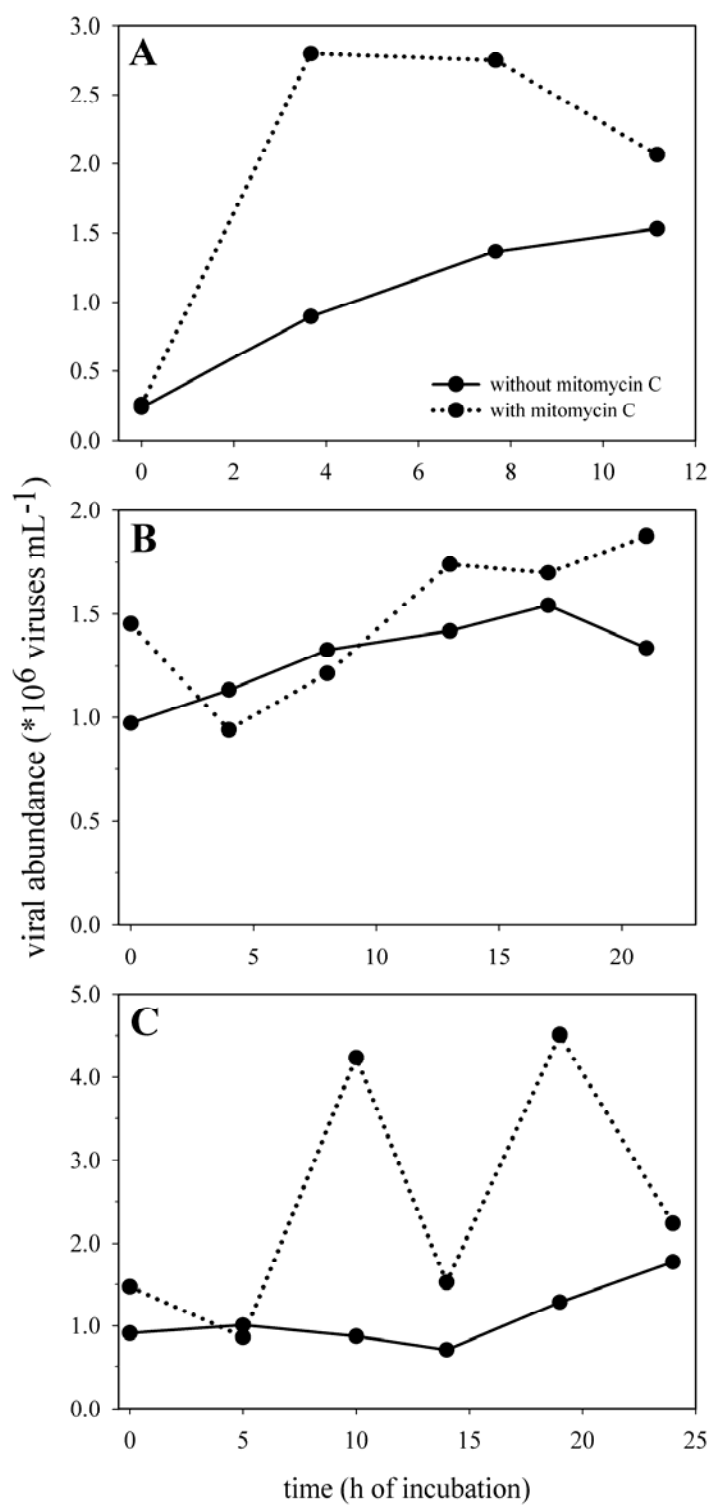


Figure 1

A

VIPCAL

Viral Production Calculator

« back

data from the viral reduction approach (VRA)

time
[h of incubation]

viral abundance
with mitomycin C
[$\times 10^6$ viruses mL^{-1}]
(use " ; " for multiple input)

viral abundance
without mitomycin C
[$\times 10^6$ viruses mL^{-1}]
(use " ; " for multiple input)

bacterial abundance at the
beginning of the experiment
[$\times 10^6$ cells mL^{-1}]
(use " ; " for multiple input)

data from the original sample

viral abundance
[$\times 10^6$ viruses mL^{-1}]

bacterial abundance
[$\times 10^6$ cells mL^{-1}]

bacterial secondary production
[$\times 10^6$ cells $\text{mL}^{-1}\text{h}^{-1}$]

burst size
(use " ; " for multiple input)

elemental C content of a
bacterium
[fg C cell^{-1}]

elemental N content of a
bacterium
[fg N cell^{-1}]

compute»

programmed by -h.e-

Figure 2a

B

VIPCAL

Viral Production Calculator

multiple burst size!
currently used burst size: **23.50**
next burst size: 13.17, 8.00 »

« back plot »

calculated parameters from the VRA

mean lytic viral production [x10 ⁶ viruses mL ⁻¹ h ⁻¹]	8.3528e-3
% of lytically infected cells	2.1600
% of lysogenic cells	1.7369

other ecologically relevant parameters

lytic viral production in the original sample	8.7730e-3
[x10 ⁶ viruses mL ⁻¹ h ⁻¹]	
lysis rate of bacteria: [x10 ⁶ cells mL ⁻¹ h ⁻¹]	3.7332e-4
% of bacterial production lysed	0.1383
% of bacterial loss per day	2.8800
viral turnover time [h ⁻¹]	4.0157e-4
DOC release [g C mL ⁻¹ h ⁻¹]	7.4663e-12
DON release [g N mL ⁻¹ h ⁻¹]	1.4933e-12

save results »

programmed by -h.c-

multiple burst size!
currently used burst size: **13.17**
next burst size: 8.00 »

plot »

calculated parameters from the VRA

mean lytic viral production [x10 ⁶ viruses mL ⁻¹ h ⁻¹]	8.3528e-3
% of lytically infected cells	3.8542
% of lysogenic cells	3.0992

other ecologically relevant parameters

lytic viral production in the original sample	8.7730e-3
[x10 ⁶ viruses mL ⁻¹ h ⁻¹]	
lysis rate of bacteria: [x10 ⁶ cells mL ⁻¹ h ⁻¹]	6.6613e-4
% of bacterial production lysed	0.2467
% of bacterial loss per day	5.1389
viral turnover time [h ⁻¹]	4.0157e-4
DOC release [g C mL ⁻¹ h ⁻¹]	1.3323e-11
DON release [g N mL ⁻¹ h ⁻¹]	2.6645e-12

save results »

programmed by -h.c-

mean lytic viral production

$$\frac{1}{n} \left[\frac{VDC_{max_1} - VDC_{min_1}}{t_{max_1} - t_{min_1}} + \dots + \frac{VDC_{max_n} - VDC_{min_n}}{t_{max_n} - t_{min_n}} \right]$$

VDC_{max₁}, ..., VDC_{max_n}: maximal viral direct counts in a time period with a net increase
VDC_{min₁}, ..., VDC_{min_n}: minimal viral direct counts in a time period with a net increase
t_{min₁}, ..., t_{max_n}: time period with a net increase in viral direct counts
index n denotes the number of peaks

currently used burst size: **8.00**

plot »

calculated parameters from the VRA

mean lytic viral production [x10 ⁶ viruses mL ⁻¹ h ⁻¹]	8.3528e-3
% of lytically infected cells	6.3450
% of lysogenic cells	5.1021

other ecologically relevant parameters

lytic viral production in the original sample	8.7730e-3
[x10 ⁶ viruses mL ⁻¹ h ⁻¹]	
lysis rate of bacteria: [x10 ⁶ cells mL ⁻¹ h ⁻¹]	1.0966e-3
% of bacterial production lysed	0.4062
% of bacterial loss per day	8.4599
viral turnover time [h ⁻¹]	4.0157e-4
DOC release [g C mL ⁻¹ h ⁻¹]	2.1932e-11
DON release [g N mL ⁻¹ h ⁻¹]	4.3865e-12

save results »

programmed by -h.c-

Figure 2b

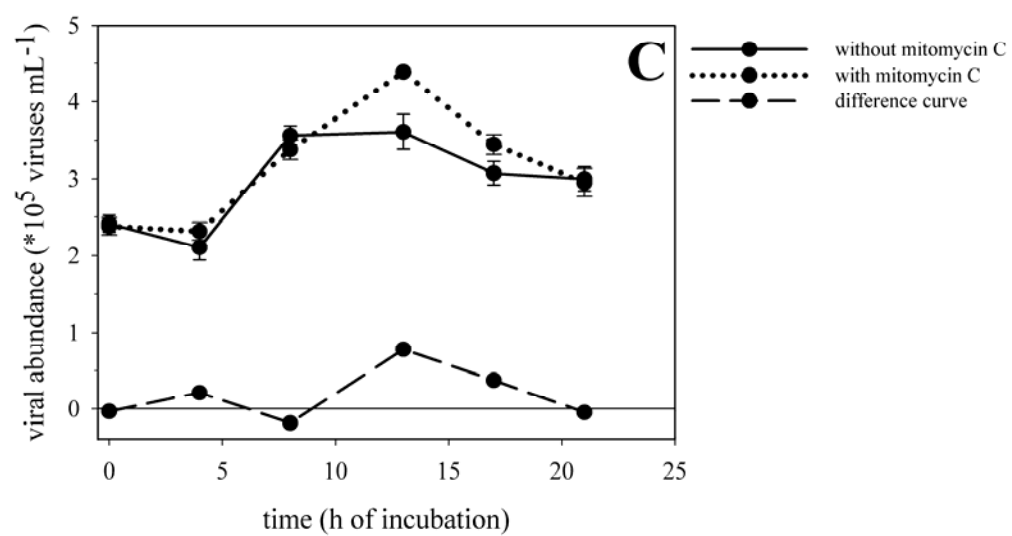


Figure 2c

Summary

Depending on the origin, riverine aggregates (suspended material) harbor a complex mixture of inorganic and organic components. The living organic components are characterized by nucleic acid-containing constituents such as algae, protozoa, fungi, bacteria and virus-like particles. The architecture and integrity of these aggregates are supplemented by the presence of extracellular polymeric substances (EPS) produced mainly by bacteria and algae.

A variety of Confocal Laser Scanning Microscopy (CLSM) strategies to examine aggregates, collected from the Danube and Elbe rivers, are presented. In order to collect multiple information, a variety of approaches is necessary. Firstly, advantage was taken of the autofluorescence of phototrophic organisms (algae, cyanobacteria) and of reflection imaging (mineral compounds, inorganic matrix, cellular reflection). Secondly, nucleic acid stains for visualization of viruses, bacteria, nuclei of eucaryotes as well as lectin-binding analysis for examination of the polymeric matrix (EPS-specific glycoconjugates) allowed us to obtain information on the aggregate architecture and on the spatial distribution of bacteria and viruses. The staining procedure included positive staining (polymeric matrix, cells, viruses) as well as negative-staining (volume of aggregates) and multi-channel recording. Furthermore, cryo-sectioning in combination with post-staining yields representative data on the internal distribution of constituents (viruses, bacteria, nuclei of eucaryotes, EPS glycoconjugates) across the whole aggregate. The CLSM data sets were then processed by using digital image analysis in order to extract quantitative information. For this purpose advanced software was used, which allows calculation of 3-dimensional (3-D) objects of various signal intensity and size classes. The two rivers, Danube and Elbe, appeared to harbor different aggregate qualities. Testing a panel of different lectins, only few lectins showed strong and clear binding to the specific glycoconjugates of the aggregates. The Danube and Elbe aggregates differed in their glycoconjugate composition when compared at the same season. Furthermore, the binding patterns of most lectins to the glycoconjugates of the riverine aggregates changed over time. Over an annual cycle, the relative contribution of the specific glycoconjugates and associated cellular nucleic acid signals (signals derive from bacteria, viruses, nuclei of eucaryotes) to the aggregate volume changed over time. Different spatial patterns of cellular nucleic acid signals inside of riverine aggregates were found, depending on the size of the aggregate and season. The spatial structure of cellular nucleic acid signals inside riverine aggregates was more complex in the Elbe than in the Danube.

Furthermore, CLSM was used in combination with different fluorochromes to obtain information on aggregate architecture and on the spatial distribution of viruses within fully hydrated aggregates. For example, aggregates from the Danube River harbored up to 5.39×10^9 viruses cm^3 .

Knowledge about the internal distribution of polymeric substances and cellular nucleic acid signals may be essential for understanding the relationship of structure, function and spatial dynamics of aquatic aggregates. 3-D visualization and 3-D quantification of the aggregate structures may provide a basis for modelling the aggregates' development.

An online program “**Viral Production Calculator**” (VIPCAL) that calculates lytic viral production and the percentage of lysogenic cells, based on data from a viral reduction approach (VRA), is presented. The main advantage of our method lies in its universal applicability also to different piecewise-linear curves. Therefore, the model is universally applicable to all possible data generated by a VRA. We demonstrate the application of our tool for the calculation of lytic viral production and the proportion of lysogenic bacteria in an environmental sample. Furthermore, the program can be used to calculate different parameters for estimating virus induced mortality. Differences in the calculation of viral production and diverse viral parameters between studies and laboratories can be avoided by using VIPCAL, which facilitates interpretation of the results.

Zusammenfassung

Schwebstoffe in Fließgewässern (suspendiertes partikuläres Material) setzen sich aus heterogenem, anorganischen und organischen Material zusammen. Die lebenden organischen Anteile wie Algen, Protozoa, Pilze, Bakterien und Viren sind durch nukleinsäurehaltige Bausteine charakterisiert. Die Architektur und der Zusammenhalt dieser Aggregate sind durch die Präsenz von extrazellulären polymeren Substanzen (EPS) gewährleistet, welche hauptsächlich von Bakterien und Algen erzeugt werden.

Um Schwebstoff-Aggregate aus den Flüssen Donau und Elbe zu analysieren, wurden eine Reihe von Konfokalen Laser Scanning Mikroskopie (CLSM) Techniken angewendet. All diese Methoden erlaubten vielfältige Informationen der untersuchten Aggregate zu erlangen. Zum einen wurden die Autofluoreszenz der phototrophen Organismen (Algen, Cyanobakterien) und die Reflektion mineralischer Substanzen (anorganische Matrix, zelluläre Reflektion) genutzt. Zum anderen erlaubte eine spezielle Nukleinsäurefärbung die Visualisierung von Viren, Bakterien und Zellkernen der Eukaryota. Die Analyse mittels Lektinen ermöglichte die Untersuchung der EPS-spezifischen Glycoconjugate. Daraus ergaben sich Informationen über die Architektur der Aggregate und die räumliche Verteilung von Bakterien und Viren. Die Färbe-Fluoreszenz-Techniken beinhalteten einerseits positives Färben (polymere Matrix, Zellen, Viren), andererseits negatives Färben (Aggregatvolumen) und die Anwendung von Multikanalaufnahmen am CLSM. Weiters ermöglichten Gefrierschnitte in Verbindung mit Nachfärbungen die Erhebung von repräsentativen Daten bezüglich der Verteilung von Bakterien und EPS-spezifischen Glycoconjugaten im Inneren von Aggregaten. Die CLSM Daten wurden anschließend mittels digitaler Bilderkennungsanalyse bearbeitet, um quantitative Aussagen zu gewinnen. Zu diesem Zweck wurden hochentwickelte Software Programme verwendet, welche die Berechnung von 3-dimensionalen (3-D) Objekten verschiedener Signalstärken und Größenklassen ermöglichten. Die beiden Flüsse Donau und Elbe besitzen Schwebstoff-Aggregate unterschiedlicher Qualität. Nur wenige der getesteten Lektine zeigten eine eindeutige Bindung mit den spezifischen Glycoconjugaten der Aggregate. Die Zusammensetzung der Glycoconjugate der Schwebstoff-Aggregate war beim Vergleich der beiden Flüsse zur selben Jahreszeit unterschiedlich. Außerdem änderte sich die Zusammensetzung der spezifischen Glycoconjugate der Aggregate innerhalb jedes Flusses im Laufe der verschiedenen Jahreszeiten. Zelluläre, nukleinsäurehaltige Signale (Signale stammen von Viren, Bakterien und Zellkernen der Eukaryota) zeigten Unterschiede in der räumlichen Anordnung innerhalb

der Aggregate, welche von der Größe der Schwebstoffflocken und von der Saison abhängig waren. Weiters zeigte die räumliche Struktur der zellulären nukleinsäurehaltigen Signale in der Elbe eine komplexere Anordnung als in der Donau.

Ferner wurde CLSM in Kombination mit verschiedenen Fluorochromen dazu verwendet, um die räumliche Anordnung von Virensignalen in der Struktur der Schwebstoff-Aggregate sichtbar zu machen. Aggregate der Donau beinhalten bis zu 5.39×10^9 Viren cm^3 .

Kenntnis über die räumliche Anordnung der polymeren Substanzen und zellulären nukleinsäurehaltigen Signalen in Aggregaten ist von enormer Wichtigkeit, um die Beziehung von Struktur, Funktion und räumlicher Dynamik besser verstehen zu können. 3-D Visualisierung und 3-D Quantifizierung der Aggregatstrukturen könnten eine Grundlage für die Modellierung der Entwicklung aquatischer Aggregate bilden.

Darüber hinaus präsentieren wir ein online Programm „VIPCAL“ (**v**iral **p**roduction **c**alculator) zur Berechnung lytischer viraler Produktion und des prozentualen Anteils lysogener Bakterien, basierend auf Daten eines Viren-Reduktionsansatzes (viral reduction approach, VRA). Die Berechnung der viralen Produktion basiert auf einem neuen Modell, welches beliebige Daten eines VRA durch stückweise stetige Kurven darstellt. Das Programm berechnet auch verschiedenste virale bzw. durch Virenaktivität beeinflusste Parameter. Durch die Benützung des Programms VIPCAL können unterschiedliche Berechnungsweisen diverser Parameter vermieden werden und Vergleiche verschiedener Studien in unterschiedlichen Laboratorien vereinfacht werden.

Danksagung

Diese Dissertation wäre sicher nicht zustande gekommen, ohne die große Unterstützung und Hilfe von vielen wunderbaren Personen. Ebenso sei all jenen ein großes Dankeschön ausgesprochen, die hier keine namentlich Erwähnung fanden, aber zum Gelingen dieser Arbeit beigetragen haben.

Im Besonderen möchte ich folgenden Personen danken:

Meinem Ehemann sei für die Geduld, unermüdliche Unterstützung, seine motivierenden Worte und seine Liebe während der Arbeit an meiner Dissertation gedankt. Seine moralische Unterstützung war von enormer Wichtigkeit. Ferner hat er mich tatkräftig bei der praktischen Durchführung meiner Arbeit unterstützt, indem er mehrmals Wasserproben von der Donau aus Wien zur Analyse nach Magdeburg brachte.

Meiner Familie danke ich für ihre fortwährende moralische Unterstützung, auch wenn sie die Hoffnung auf die Beendigung meiner Dissertation manchmal schon aufgegeben hatten.

Vielen Dank an meine Eltern und Schwiegereltern, die bei diversen Probennahmen mir ihre Zeit und ihr Auto selbstlos überließen.

Die Auswertung meiner Daten brachte meinen Computer an die Grenzen seiner Leistungsfähigkeit. In dieser Notlage sprang Harald Luef ein und gestattete mir die Benützung seines leistungsstarken Computers.

Ich danke herzlichst Professor Peter Peduzzi für die Betreuung meiner Dissertation und seiner Unterstützung während meiner Arbeit. Ein besonderes Dankeschön gebührt auch seiner Geduld. Seine wertvollen Anregungen und Ratschläge habe ich stets geschätzt. Weiters sorgte er dafür, dass ich meine wissenschaftlichen Erkenntnisse auf diversen internationalen Kongressen präsentierte und zu Manuskripten verarbeitete. Sein Interesse an meiner Arbeit und die zahlreichen Diskussionen waren stets unterstützend und befruchtend.

Dr. Thomas R. Neu danke ich für die großartige Möglichkeit einen großen Teil meiner Arbeit in seiner Arbeitsgruppe am Helmholtz Zentrum für Umweltforschung UFZ, Department Fließgewässerökologie in Magdeburg durchführen zu können. Die optimalen Arbeitsbedingungen in seiner Arbeitsgruppe, seine wissenschaftlichen Anregungen und sein

Interesse an meiner Arbeit waren von unschätzbarem Wert für die Beendigung meiner Dissertation.

Weiters sei Ute Kuhlicke gedankt für die großartige Hilfestellung im Labor und der erstklassigen fachlichen Betreuung am CLSM. An dieser Stelle möchte ich mich von ganzem Herzen bei Ute bedanken, denn sie war mir eine unschätzbare moralische Unterstützung und ohne sie, wäre meine Zeit in Magdeburg nicht von so vielen schönen Erinnerungen geprägt. Während meiner Arbeit hatte ich auch das Vergnügen die Bekanntschaft von Kerstin Garny und Marian Haesner zu machen, welche meinen Aufenthalt am UFZ so belebt haben und für die daraus entstandene Freundschaft.

Ferner bedanke ich mich bei Barabara Zippel und Christian Staudt für die fachlichen und kreativen Diskussionen.

Die Arbeit an dieser Dissertation fand an der Universität Wien statt, unter anderem in der Abteilung Cell Imaging und Ultrastrukturforschung. Mein spezieller Dank gilt Frau Prof. Waltraud Klepal und ihren beiden Mitarbeitern Daniela Gruber und Gerhard Spitzer für ihre professionelle Betreuung am TEM. Weiters danke ich Prof. Irene Lichtscheidl für die Unterstützung meiner Arbeit am CLSM in Wien.

Herrn Hubert Kraill danke ich für die Durchführung der chemischen Analysen. Überdies stand er mir stets mit kompetenten Ratschlägen zur Seite.

Harald Schwab sei gedankt für seine unendliche Geduld und großartige Hilfe beim Programmieren von VIPCAL.

Doris Bretterbauer und Thomas Klingenböck danke ich für ein stets offenes Ohr bei Fragen betreffend Bildbearbeitung.

Ein besonders Dankeschön gebührt Prof. Marc A. Rieffel für seinen Rat während einer lang andauernden Schreibblockade: „You are not getting paid for what you know, you are getting paid for what you communicate!“

Diese Dissertation hätte ohne die finanzielle Zuwendung von diversen Institutionen nicht beendet werden können: (1) Dem FWF für die Förderung diverser Projekte von Prof. Peduzzi, welche die Arbeit an dieser Dissertation erst ermöglichte. (2) Der Universität Wien für die Zuerkennung eines Forschungsstipendiums, welches unter anderem meinen ersten Aufenthalt

bei Dr. Neu erlaubte. (3) Der Europäischen Union für die Zuerkennung eines Marie Curie Fellowship - Training Sites an Dr. T. Neu, welches meinen zweiten Forschungsaufenthalt am UFZ ermöglichte.

Curriculum Vitae

Birgit Luef

maiden name Scharinger

Education

University of Vienna, May 2001. M.S. and final examination in ecology, limnology;
graduated with distinction
Department of Freshwater Ecology;
Advisor: Professor Peter Peduzzi
Thesis title: *Hydrological connectivity: An important factor influencing particles, bacteria and viruses in the River Danube floodplain system*

Professional Experience

- | | |
|---|---|
| Aug.06 – Dez.08 | Research Assistant
University of Vienna; Professor P. Peduzzi (PI)
Virioplankton in river floodplain systems
focus on transmission electron microscopy (TEM), lytic and lysogenic viral production |
| Aug.05 – March 06,
Oct.04 – March 05 | Research stays
Helmholtz Centre for Environmental Research - UFZ, Magdeburg, Germany; Dr. Thomas Neu

focus on lectins, confocal laser scanning microscopy (CLSM), image analysis |
| June 01 – May 04 | Research Assistant
University of Vienna; Professor P. Peduzzi (PI)
Impact of suspended matter on the ecology of viruses in a river-floodplain system of the Danube (Austria)
focus on TEM, CLSM |
| March 03 – Apr. 03 | Research stay
National Water Research Institute Canada, Centre for Inland Waters, Burlington; Professor Gary G. Leppard

focus on TEM |
| 2002, 2004, 2005,
2006, 2007, 2008 | Teaching assistant
University of Vienna;

Course in methods of aquatic microbial ecology (graduate course) |

Scholarships and Awards

2006	Ruttner Award for Limnology
2005	Research Fellowship, University of Vienna Performance grant, University of Vienna Marie Curie Fellowship (Training Sites; Aug. 05 – Jan. 06)
2004	Research Fellowship, University of Vienna National Park-Research Award for Master students Leonardo da Vinci Mobility (Oct. 04 – Apr. 05)
2001	Scholarship of excellence, University of Vienna
1998	Scholarship of excellence, University of Vienna

Publications, published abstracts, submitted papers

Luef B, Peduzzi P, Neu TR (submitted) Fluorescence lectin-binding analysis in riverine aggregates (river snow): a critical examination. FEMS Microbiology Ecology

Luef B, Neu TR, Peduzzi P (submitted) Imaging and quantifying virus fluorescence signals on aquatic aggregates: an unresolved problem? FEMS Microbiology Ecology

Luef B, Neu TR, Zweimüller I, Peduzzi P (submitted) The potential of Confocal Laser Scanning Microscopy in combination with statistical and image analysis to investigate volume, structure and composition of riverine aggregates. Limnology and Oceanography

Luef B, Luef F, Peduzzi P (under revision) Online program “VIPCAL” for calculating lytic viral production and lyogenic cells based on a viral reduction approach. Environmental Microbiology

Besemer K, Agis M, Eichberger B, **Luef B**, Preiner S, and Peduzzi P (under revision) Sources, composition and dynamics of organic matter in a river-floodplain system (Danube, Austria). Organic Geochemistry

Peduzzi P, **Luef B** (in press) Viruses. In: Likens GE (ed) Encyclopedia of Inland Waters. Elsevier, Oxford

Peduzzi P, **Luef B** (2008) Viruses, bacteria and suspended particles in a backwater and main channel site of the Danube (Austria). Aquatic Sciences 70:186-194

Peduzzi P, Aspetsberger F, Hein T, Huber F, Kargl Wagner S, **Luef B**, Tachkova Y (2008) Dissolved organic matter (DOM) and bacterial growth in floodplains of the River Danube under varying hydrological connectivity. Fundamental and Applied Limnology 171:49-61

Luef B, Aspetsberger F, Hein T, Huber F, Peduzzi P (2007) Impact of hydrology on free-living and particle-associated microorganisms in a river floodplain system (Danube, Austria). *Freshwater Biology* 52:1043 – 1057

Luef B, Neu TR, Peduzzi P (2005) Examination of glycoconjugate, bacterial and viral distribution in riverine aggregates by Confocal Laser Scanning Microscopy. *Geophysical Research Abstracts* 7: 6080

Agis M, **Luef B**, Peduzzi P (2004) Variability of virioplankton diversity in a river floodplain system. *European Geosciences Union* 6:4985

Aspetsberger F, Huber F, Kargl S, **Scharinger B**, Peduzzi P, Hein T (2002) Particulate organic matter dynamics in a river floodplain system: impact of hydrological connectivity. *Archiv für Hydrobiologie* 156:23-42

Conferences

2008

Online program (<http://www.univie.ac.at/nuhag-php/vipcal>) for calculating lytic viral production and lysogenic cells from a viral reduction approach (VRA)

Luef B, Luef F, Peduzzi P

The 12th International Symposium on Microbial Ecology - ISME-12. Cairns (Australia); August 17 – 22, 2008.

2006

Laser Scanning Microscopy: A structural approach to investigate mobile biofilms

Luef B, Peduzzi P, Neu TR

BIOFILMS II, Attachment and Detachment in Pure and Mixed Cultures; Leipzig (Germany); March 23 - 24, 2006.

Dense aggregates and thick biofilms – look beyond the limits!

Zippel B, Garny K, Hille A, **Luef B**

BIOFILMS II, Attachment and Detachment in Pure and Mixed Cultures; Leipzig (Germany); March 23 - 24, 2006.

Structure of riverine aggregates, bacterial and viral colonization by laser scanning microscopy

Luef B, Peduzzi P, Neu TR

The 11th International Symposium on Microbial Ecology – ISME-11. The hidden powers – Microbial Communities in Action; Vienna (Austria); August 20 – 25, 2006.

2005

Imaging of viruses on aquatic aggregates: a non-solvable problem?

Luef B, Neu TR and Peduzzi P

1st European Workshop on Aquatic Phage Ecology (EWAPE-1), Thonon-les Bains (France), February 2 – 4, 2005.

Examination of glycoconjugate, bacterial and viral distribution in riverine aggregates by Confocal Laser Scanning Microscopy

Luef B, Neu TR and Peduzzi P

European Geosciences Union, Vienna (Austria), April 24 - 29, 2005.

Intrinsic properties and extrinsic probes useful for 3-D characterization of aquatic bio-aggregates

Luef B, Kuhlicke U, Peduzzi P, Neu TR

9th Symposium on Aquatic Microbial Ecology, SAME-9, Helsinki (Finland), August 21 – 26, 2005.

2004

The importance of microorganisms and particles in the Danube River floodplains: an experimental approach

Kernegger L, **Luef B**, Peduzzi P

Student Conference on Conservation Science, University of Cambridge (England), March 24 – 26, 2004.

Variability of virioplankton diversity in a river floodplain system

Agis M, **Luef B**, Peduzzi P

European Geosciences Union, Nice (France), April 25 – 30, 2004.

2003

How much is plentiful? Counting bacteria and viruses with conventional epifluorescence and confocal laser scanning microscopy

Agis M, **Luef B**, Peduzzi P

FEMS Workshop: Assessing the variability in aquatic microbial populations: Facts and fiction, Mondsee (Austria), February 16 – 20, 2003.

2002

Riverine particles: Hotspots for microbial life?

Luef B, Agis M, Peduzzi P

8th Symposium on Aquatic Microbial Ecology, Taormina (Italy), October 25 – 30, 2002.

2001:

The microplankton dynamics in a large river floodplain system: significance of hydrological connectivity.

Hein T, Huber F, Kargl S, Keckeis S, Riedler P, **Scharinger B** & Schiemer F
ASLO Meeting in Albuquerque (USA), February 12 – 16, 2001.

2000

Hydrological connectivity: An important factor on particles, bacteria and viruses in a river floodplain system

Scharinger B, Aspetsberger F, Hein T, Huber F, Kargl S, Peduzzi P

7th European Marine Microbiology Symposium, Noordwijkerhout (Netherlands), September 17 – 22, 2000.

Isotopic and elemental characterization of particulate organic matter in a river floodplain system.

Aspetsberger F, Huber F, Kargl S, Peduzzi P, **Scharinger B** & Hein T
International Symposium on Nuclear Techniques in Integrated Plant Nutrient, Water and Soil Management, Vienna (Austria), October 16 – 20, 2000.